AN ABSTRACT OF THE THESIS OF

Lawrence A. Krissek for the degree of Doctor of Philosophy in Oceanography presented on 13 April 1982

TITLE: Sources, Dispersal, and Contributions of Fine-grained Terrigenous Sediments on the Oregon and Washington Continental Slope

Abstract approved. Redacted for Privacy

Kenneth F. Scheidegger

Holocene hemipelagic deposition of terrigenous silts and clays dominates sedimentation on most of the Oregon and Washington continental slope. The sources of these sediments, the mechanisms causing sediment dispersal, and the relative contributions of the various continental sources to the marine deposits have been investigated using quantitative mineral and geochemical data for the 2-20 μm and the <2 μm size fractions.

In the 2-20 μm size fraction, material derived from the Klamath Mountains and the California and Washington Coast Ranges contains chlorite and illite, but only Klamath material contains hornblende. Columbia River material lacks chlorite, and the Oregon Coast Range source is dominated by smectite. In the <2 μm fraction, source area compositions are less distinctive due to the ubiquity of smectite, but the northern and southern sources again contain both chlorite and illite. Regional and local mineralogic and textural variations in the fluvial sediments reflect geologic and geographic changes between drainage basins. Amorphous material is a minor component in the 2-20 μm fraction of the fluvial sediments, but may form 25-50% of the <2 μm fraction in some source areas.

Sediments derived from all source areas are transported north and northwestward across the margin, either by a poleward-flowing undercurrent along the slope, by wind-driven surface currents on the shelf and associated turbid layers on the slope, or by a combination of the two processes. Columbia River <2 μm material may also be carried southward along the shelf and upper slope by summer surface currents. The poleward undercurrent (an eastern boundary undercurrent) appears to have limited sedimentological significance when compared to the role of the western boundary undercurrent in sediment transport and deposition on the continental slope and rise of the eastern United States.

Linear programming has been applied successfully to estimate source area contributions to the 2-20 μm marine sediments. The influence of each source is largest in proximal environments, and the contribution estimates indicate that material derived from each source area is transported northward along the margin. Similar estimates for the <2 μm material are considered unreliable because of internal inconsistencies and the uniform nature of the <2 μm compositions used in the modelling. The contributions have been used to calculate a sediment budget for the 2-20 μm fraction. This budget indicates that the mass accumulating on the entire slope within the study area contains 47% Columbia River, 32% Klamath Mountain, and 21% California Coast Range material in the 2-20 μm fraction, and demonstrates the importance of multiple sediment sources and sediment mixing in the formation of hemipelagic sediments on the continental margin.

SOURCES, DISPERSAL, AND CONTRIBUTIONS OF FINE-GRAINED TERRIGENOUS SEDIMENTS ON THE OREGON AND WASHINGTON CONTINENTAL SLOPE

by

Lawrence A. Krissek

A THESIS

submitted to

Oregon State University

in partial fulfillment of
the requirements for the
degree of
Doctor of Philosophy

Completed 13 April 1982
Commencement June 1982

APPROVED

Redacted for Privacy

Associate Professor of Oceanography in charge of major

Redacted for Privacy

Dean of The School of Oceanography

Redacted for Privacy

Dean of The Graduate School

Date thesis is presented 13 April 1982

Typed by Rebecca Simpkins for Lawrence A. Krissek

ACKNOWLEDGEMENTS

Countless people have contributed in one way or another to the completion of this work, and I thank them all. Ken Scheidegger served as my advisor and provided gentle yet firm guidance and encouragement through my term as a graduate student. I leave with pleasant memories of my work here, and only hope that I will treat my future students as fairly and kindly as he has treated me. Jack Dymond, Ross Heath, and Vern Kulm served on my committee and provided valuable support and enlightenment during the past five years, for which I am grateful. Julius Dasch served as minor professor and Roman Schmitt served as Graduate School representative; I thank them for their interest and time. Keith Oles kindly consented on short notice to serve as a substitute at the thesis defense.

Mark Hower assisted with sample collection and analysis, and Milo Clauson kept the XRD in operation through numerous crises. Andy Ungerer was a patient and constant source of information, and Chi Meredith and Nick Pisias aided in the computer calculations. Al Federman, Pete Kalk, and students from the Clatsop (OR.) Community College ocean technician program were instrumental in obtaining the slope cores used in this study. Becky Simpkins typed the thesis and Melissa Seward and Sally Kulm drafted the illustrations.

I have benefitted, both socially and intellectually, from time spent with my fellow students: Will Schweller, Bill Busch, Bob Karlin, Dave Murray, Anne Matherne, Todd Thornburg, Heidi Powell, Karen Weliky, Al Federman, Kathy Fischer, and all the rest, both past and present. Mark, Andy, and Bobbi also have shared many activities apart from

school and research. I thank Michelle for reminding me of the joy and innocence of youth. The noontime Langton runners and the Saturday Waremart group played critical roles in keeping me sane; although their humor was often questionnable, their friendship and support were not. Fred Hasle and Chester deserve special thanks for many peaceful mornings in McDonald Forest. Many thanks to Maureen for her support and companionship during my undergraduate and graduate careers. I only wish that the price had not been so high. Cindy provided much-needed encouragement during the writing of this thesis.

Finally, I thank my parents, who provided an early environment in which education and effort were encouraged, and who always supported me in my quest for this degree. Without their help, the journey would have been much longer and lonelier.

TABLE OF CONTENTS

TABLE OF CONTENTS (cont.)

LIST OF FIGURES

LIST OF FIGURES (cont.)

LIST OF TABLES

LIST OF TABLES (cont.)

SOURCES, DISPERSAL, AND CONTRIBUTIONS OF FINE-GRAINED TERRIGENOUS SEDIMENTS ON THE OREGON AND WASHINGTON CONTINENTAL SLOPE

INTRODUCTION

A common approach to the study of fine-grained terrigenous sediment dispersal in the marine environment has been to examine spatial variations in semiquantitative clay mineral abundances (smectite, chlorite, illite, kaolinite) away from a continental source region (Griffin and Goldberg, 1963; Biscaye, 1965; Griffin et al., 1968; Kolla and Biscaye, 1973; Kolla et al., 1976; Griggs and Hein, 1980). From the offshore abundance patterns, the composition of material derived from the continental source, its dispersal mechanisms in the marine environment, and the relative contribution from that source to the marine sediments are then inferred. This approach is generally limited by the following: 1.) the mineral data used are semiquantitative; 2.) they apply to only the <2 μm fraction; 3.) no samples are obtained directly from the continental source as a check on the inferred source area composition; 4.) no process-oriented measurements or samples (current meter measurements, sediment trap and/or water samples) are collected to identify the processes and timing of sediment dispersal; and 5.) contributions to the marine sediments are inferred in only a qualitative manner for a single source area.

Studies of the geology and processes of sedimentation on the Oregon and Washington continental margin and adjacent deep-sea environments (Maloney, 1965; Carlson, 1968; Chambers, 1968; Duncan and Kulm, 1970; Duncan et al., 1970; Griggs and Kulm, 1970; White, 1970; Scheidegger et al., 1971; Harlett, 1972; Sternberg and McManus, 1972; Baker, 1973; Kulm et al., 1975; Stokke et al., 1977) have investigated the continental shelf and deep-sea canyon, channel, fan and abyssal

plain systems. Only work by Spigai (1971) on the southern Oregon margin and by Karlin (1980) on the entire Oregon margin have considered sedimentation on the continental slope, but both of these studies were based on semiquantitative clay mineral data from limited sample suites. These studies (Spigai, 1971; Karlin, 1980) conclude that sediments are transported northward on the Oregon margin. Spigai (1971) concluded that material was carried northward by wind-driven winter surface currents on the continental shelf, with subsequent downslope transport in turbid layers. Karlin (1980) emphasized the role of a poleward undercurrent along the slope in the northward transport of sediments. Because of the types of samples and data used for these studies, however, both are subject to the limitations discussed above.

Previous studies of the sand fraction mineralogy from beaches and the continental shelf (Kulm et al., 1968; Scheidegger et al., 1971) and a fluvial suspended sediment discharge budget constructed by Karlin (1980) indicate that several major continental source areas can be delineated in the Pacific Northwest. From south to north, these are the California Coast Range, Klamath Mountains, Oregon Coast Range, Columbia River, and Washington Coast Range. None of these studies, however, determined either the composition of the fine-grained material derived from each source or the effects of mixing sediment from several sources in the formation of any type of sediment on the continental margin.

With these previous studies providing a framework of dispersal models, the study described in this thesis was designed to more

completely investigate the patterns and processes of hemipelagic sediment formation on the Oregon-Washington continental slope using quantitative chemical and mineral data. The study focused on the 2-20 μm and the <2 μm fractions because these two size classes form an average of approximately 81% of the slope sediments. A suite of samples was collected from 52 of the major streams entering the Pacific Ocean in northern California, Oregon, and Washington and was used to characterize the material derived from each source area. The mineral compositions of these samples indicate that the five source areas have distinctive signatures in the 2-20 μm fraction, but that the <2 μm mineralogies are less distinctive tracers of sediment source-area. Changes in source area composition do reflect the regional and local geology.

By knowing the source-area compositions directly, it is then possible to closely examine the relation of mineral abundances in marine samples to the continental sources and identify sediment sources and dispersal patterns. Surface samples from 78 cores taken in open continental slope environments were analyzed using quantitative chemical and mineral techniques. Biostratigraphic data indicated that these sediments were deposited in the late Holocene; their chemical and mineral compositions were used to establish recent dispersal patterns and to evaluate the role of the poleward-flowing, eastern boundary undercurrent (Karlin, 1980) in sediment dispersal along the continental margin. While these data do indicate northward transport of material on most of the slope, they do not uniquely identify the process (poleward undercurrent and/or wind-driven winter surface circulation followed by turbid layer transport) causing such dispersal.

Consequently, it appears that the eastern boundary undercurrent within this study area plays a less dominant role in sedimentation than the western boundary undercurrent does on the eastern United States continental slope and rise.

The fluvial and mineral data sets were used in linear programming to estimate source area contributions to the slope sediments. Chemical data sets from deep-sea samples have been successfully modelled by Dymond and Eklund (1978), Dymond et al. (1980), Dymond (1981), and Heath and Dymond (1981), but this study describes the first application of such modelling to continental margin sediments. Because this study dealt with recent sediments in high sedimentation rate margin environments, diagenetic modifications of the material appear to be minor. Modelling of the 2-20 μm fraction was successful, and these results demonstrate the importance of multiple sediment sources and sediment mixing in the formation of hemipelagic sediments on the continental margin. In the <2 μm fraction, however, the modelling was not successful because of uniform slope sediment and source area compositions. The chemical results may provide more reasonable estimates than the mineral analysis, but the calculated contributions for the <2 μm data could not be taken with any confidence.

The use of 1.) quantitative mineral and chemical data in the <2 and 2-20 μm size fractions, 2.) fluvial samples taken directly from the source areas of interest, and 3.) linear programming to estimate source area contributions in this study, removes four of the five limitations on sediment dispersal studies listed above. This study was initially designed to include process-oriented water-column

measurements so that the question of poleward undercurrent vs. surface current and turbid-layer transport could be directly addressed. However, this portion of the study was eliminated due to financial constraints, and the actual process or processes active in the northward transport of material remain unknown. The acquisition of such process-oriented data is the next logical step in the study of hemipelagic sediment formation on the Oregon-Washington continental slope.

CHAPTER I

COMPOSITION OF FINE-GRAINED FLUVIAL SEDIMENTS OF THE PACIFIC NORTHWEST

ABSTRACT

Samples of bank and suspended material from 52 of the major streams entering the Pacific Ocean along the Pacific Northwest coast have been used to characterize the mineral composition of 2-20 μm and <2 μm material derived from major continental source areas using quantitative and semi-quantitative x-ray diffraction techniques. In the 2-20 μm fraction, the southerly sources (Klamath Mountains and the California Coast Range) and the Washington Coast Range contain chlorite and illite, but only the Klamath source contains hornblende. Columbia River material lacks chlorite, and the Oregon Coast Range source is dominated by smectite. Plagioclase feldspar compositions are distinctive for the northern and southern source areas, but all chlorites appear to be type IIb polytypes. In the <2 μm fraction, source area compositions are less distinctive due to the ubiquity of smectite. However, the northern and southern sources again contain both chlorite and illite, while the Columbia lacks chlorite and the Oregon Coast Range contains neither phase.

These regional differences, as well as local variability within the Washington Coast Range and Klamath Mountain sources, can be explained by regional and local changes in drainage lithologies. Differences in the grain size of material derived from the various source areas reflect geographic and geologic changes between basins. Repeated sampling of fluvial material over time indicates that mineral abundances within a given grain size vary by less than a factor of 2. Amorphous material is a minor component in the 2-20 μm fraction, but may form as much as 25-50% of the <2 μm fraction in some source areas.

INTRODUCTION

One of the classical approaches to the study of fine-grained sediment dispersal in the marine environment has been to examine areal patterns in semi-quantitative clay mineral abundances away from known or inferred continental sediment sources. Such studies are numerous, ranging from world or ocean-wide (Griffin and Goldberg, 1963; Biscaye, 1965; Griffin et al., 1968; Kolla and Biscaye, 1973; Kolla et al., 1976) to local or regional scales (Russell, 1967; Duncan et al., 1970; Spigai, 1971; Olmstead, 1972; Baker, 1973; Pinet and Morgan, 1979; Griggs and Hein, 1980; Karlin, 1980; Rosato and Kulm, 1981). Most of these investigations contain little or no data on samples of the fluvial material within each continental source area. As a result, the postulated source area compositions are tentative, and relationships to the onshore geology are general in nature. Equally troublesome is the possibility that, because different clay mineral groups have different grain-size distributions (Gibbs, 1967a; Arcaro, 1978), lateral variations in clay mineral abundances may reflect distance-of-transport effects more than source area influences (Arcaro, 1978). Such situations can only be recognized by actually determining the composition and grain-size distributions of material derived from each continental source region.

Previous work on the Oregon and Washington margins (Russell, 1967; Duncan et al., 1970; Spigai, 1971; Olmstead, 1972; Baker, 1973; Karlin, 1980) has identified five major continental areas which act as sediment sources. From north to south, these are: the Washington Coast Range, the Columbia River, the Oregon Coast Range, the Klamath Mountains, and

the Northern California Coast Range (Fig. 1, Karlin, 1980). Of these, only the fine-grained sediments carried by the Columbia River have been investigated in any detail (Knebel et al., 1968; Whetten et al., 1969; Glenn, 1973). Single samples have been analyzed from the Rogue and Umpqua rivers of Oregon (Griffin et al., 1968; Duncan et al., 1970; Spigai, 1971) and the Eel, Mad, Klamath, and Smith rivers and Redwood Creek of the California Coast Range (Griffin et al., 1968). Nearly all of these data are semi-quantitative in nature, and therefore, can be used in only a qualitative manner (Heath and Pisias, 1979; Krissek and Scheidegger, 1982a).

I have attempted to obtain basic quantitative compositional data for Pacific Northwest fluvial sediments through an extensive sampling and analysis program. The results of this project, concentrated on the 2-20 μm and <2 μm size fractions, are presented here. The basic questions addressed by this study include: 1.) Can key mineral signatures be recognized that are distinctive for each source area? If so, these signatures can act as sediment tracers in offshore areas. 2.) Do these signatures (i.e., mineral compositions) change significantly with sediment grain size? If so, then the signature for each source area in each grain-size fraction of interest must be known before contributions to offshore deposits can be estimated. In addition, some grain sizes may prove to be easier to trace than others. 3.) Does the mineral signature which characterizes a source area change with time? Such temporal variability may reflect seasonal responses to climate within portions of a drainage basin and limit the usefulness of the mineral signature as a long-term sediment tracer. Large

Figure I-1. Major streams of the American Pacific Northwest, showing approximate channel locations, and boundaries of the major drainages (dotted). Inset shows the Columbia River Basin (from Karlin, 1980). A full listing of the streams sampled, sample types, and source areas is given in Table I-1.

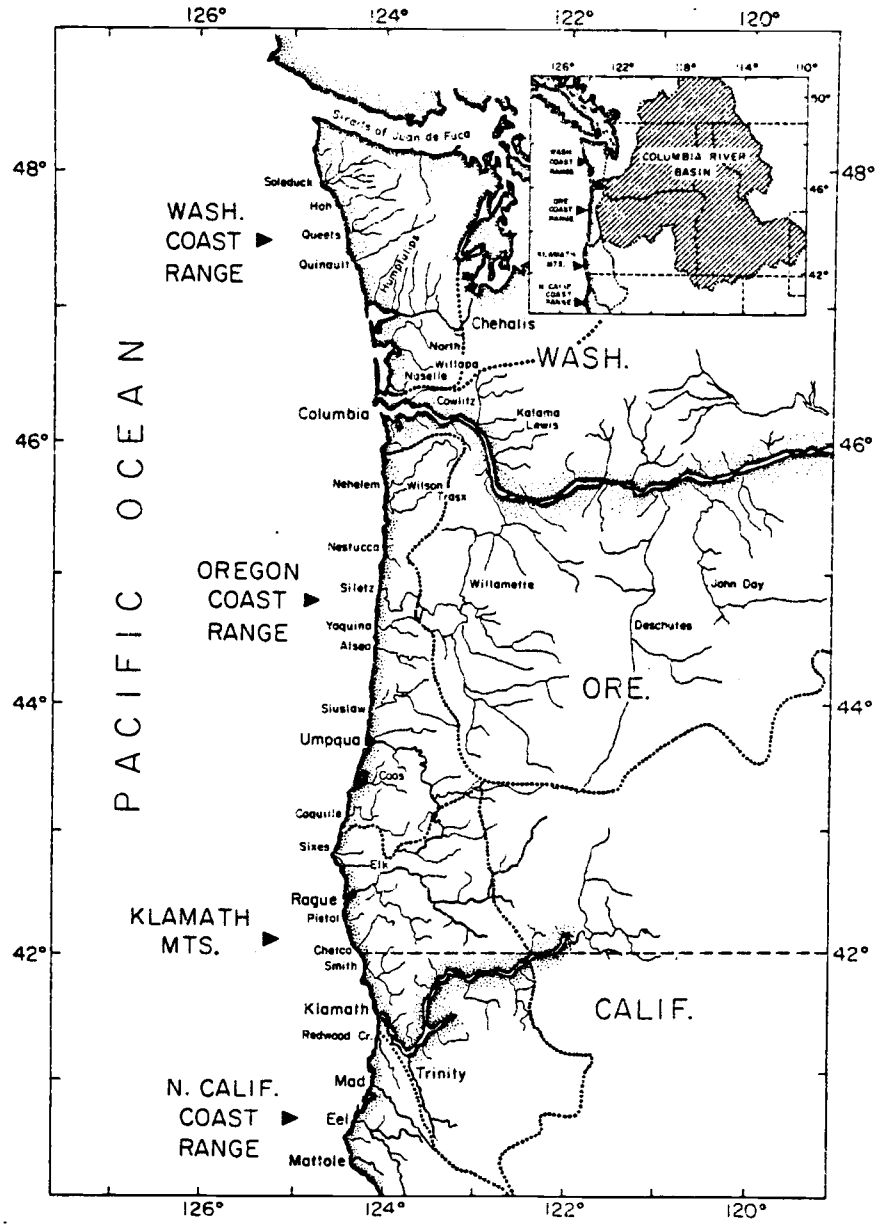
126°
124°
122°
120°
48°
46°
44°
42°
PACIFIC OCEAN
WASH. COAST RANGE
OREGON COAST RANGE
KLAMATH MTS.
N. CALIF. COAST RANGE
WASH.
ORE.
CALIF.
COLUMBIA RIVER BASIN
Strait of Juan de Fuca
Soleduck
Hoh
Queets
Quinault
Humptulips
Chehalis
North
Willapa
Naselle
Cowlitz
Columbia
Kalama
Lewis
Nehalem
Wilson
Trask
Nestucca
Siletz
Yaquina
Alsea
Siuslaw
Umpqua
Coos
Coquille
Sixes
Elk
Rogue
Pistol
Chetco
Smith
Klamath
Redwood Cr.
Mad
Eel
Mattole
Trinity
Willamette
John Day
Deschutes

Figure I-1

drainages, where sub-sections of the basin can be influenced by different climatic regimes, may be more susceptible to such temporal variation than small drainages. 4.) What is the grain-size distribution of material derived from each source area? Since such information is commonly not available, an assumption of uniform grain size for all source areas is generally made. However, the grain size of fluvial sediments can reflect the rock type and weathering regime within a source area so that, for example, material derived from one source area is rich in clay-sized sediments, while material from another source is silt rich. Such differences can strongly influence the mechanisms and directions of transport for the fluvially-derived material in the marine environment. In addition to the basic knowledge of fluvial sediments which results from this study, the sediment compositions have been used for a detailed and quantitative examination of fine-grained terrigenous sediment dispersal and deposition on the Oregon and Washington continental slope (Krissek, 1982a; Krissek and Scheidegger, 1982b).

SAMPLING AND ANALYTICAL TECHNIQUES

Samples were obtained from 52 of the major rivers and streams which drain into the Pacific Ocean between 41°30'N and 48°00'N. The rivers which were sampled, the types of samples taken, and the source area each drains are listed in Table 1. Drainages of the major rivers are shown in Figure 1. The four samples from the Chehalis River in Washington were collected during January and February, 1978, by Jim Phipps of Grays Harbor Community College. The two Columbia River samples were obtained by Tom Beasley of Oregon State University. All other samples were collected in February and March, 1980, during high discharge events. Samples were taken at distances of 5-10 miles inland from the coast to avoid marine material which may be brought into the estuaries. In addition, work by Peterson et al. (1982) in several of these estuaries has shown that fluvially-transported fine-grained material passes directly through the estuaries, especially during high discharge events; as a result, I am confident that the samples are representative of the fine-grained material which enters the Pacific Ocean from each drainage basin. Bank material samples were taken by hand at waterline at each site and stored in sealed plastic bags. Suspended material was obtained by collecting a 50 ℓ water sample, allowing it to settle for 8-12 hours, and decanting the overlying water. Sufficient suspended material for all analyses was obtained only from the Chehalis, Umpqua, Rogue, Klamath, Mad, and Eel rivers.

In the laboratory, the samples were disaggregated with 30% H_2O_2 (neutralized to pH 7.0), wet sieved at 63 μm, and the fine fraction was separated into 20-63 μm, 2-20 μm, and <2 μm components by repeated

Table I-1. Samples and sample types (B = bank material, S = suspended material) used in this study. Source areas as distinguished by Karlin (1980), with WCR = Washington Coast Range, CR = Columbia River, OCR = Oregon Coast Range, KM = Klamath Mountains, CCR = Northern California Coastal Range. Samples are arranged from north to south.

Number	River Name	Samples Taken	Source Area
1	Soleduck River	B + S	WCR
2	Bogachiel River	B + S	WCR
3	Hoh River	B + S	WCR
4	Queets River	B + S	WCR
5	Quinault River	B + S	WCR
6	Humptulips River	B + S	WCR
7	Chehalis River	4S	WCR
8	North River	B + S	WCR
9	Willapa River	B + S	WCR
10	Columbia River	2B	CR
11	Necanicum River	B + S	OCR
12	Nehalem River	B + S	OCR
13	Miami River	B + S	OCR
14	Kilchis River	B + S	OCR
15	Wilson River	B + S	OCR
16	Trask River	B + S	OCR
17	Tillamook River	B + S	OCR
18	Nestucca River	B + S	OCR
19	Little Nestucca River	B + S	OCR
20	Neskowin Creek	B + S	OCR
21	Salmon River	B + S	OCR
22	Siletz River	B + S	OCR
23	Yaquina River	B + S	OCR
24	Alsea River	B + S	OCR
25	Yachats River	B + S	OCR
26	Big Creek	B	OCR
27	Cape Creek	B	OCR
28	Siuslaw River	B + S	OCR
29	Siltcoos River	B + S	OCR
30	Smith (OR) River	B + S	OCR
31	Umpqua River	B + S	OCR
32	Coos River	B + S	OCR
33	Millicoma River	B + S	OCR
34	Coos River (below Coos/ Millicoma junction)	B + S	OCR
35	Coquille River	B + S	OCR
36	Fourmile Creek	B + S	
37	Floras Creek	B + S	

continued

Table I-1, continued

Number	River Name	Samples Taken	Source Area
38	Sixes River	B + S	KM
39	Elk River	B + S	KM
40	Brush Creek	B	KM
41	Euchre Creek	B	KM
42	Rogue River	B + S	KM
43	Hunter Creek	B + S	KM
44	Pistol River	B + S	KM
45	Chetco River	B + S	KM
46	Winchuck River	B + S	KM
47	Smith (CA) River	B + S	KM
48	Klamath River	B + S	KM
49	Redwood Creek	B + S	CCR
50	Little River	B + S	CCR
51	Mad River	B + S	CCR
52	Eel River	B + S	CCR

settling and decantation. Oriented X-ray diffraction slides of the <2 μm material were prepared on pre-pressed Ag backings placed over gentle suction (Karlin, 1980; Krissek and Scheidegger, 1982a). The remaining <2 μm material and the 2-20 μm material were then freeze-dried.

Random X-ray diffraction mounts were constructed for the 2-20 μm and <2 μm fraction using 10% by weight boehmite (AlOOH) as an internal standard according to the technique described in Krissek and Scheidegger (1982a). The use of an internal standard and the generation of calibration curves from known mineral standards allow the calculation of quantitative mineral abundances for both phyllosilicate and non-phyllosilicate minerals (Gibbs, 1967b; Scheidegger and Krissek, 1982).

All slides were solvated with warm ethylene-glycol vapor for 8-12 hours immediately preceding analysis on a Norelco diffractometer. Slides were scanned at a step size of 0.02° 2θ per step and scan time of 3 seconds per step with monochromatic Cu Kα radiation. The raw data were smoothed with a 17-point Gaussian algorithm and then plotted on a strip chart recorder. The 15-18 Å smectite (001), 10 Å illite (001), and 7 Å chlorite (002) + kaolinite (001) peak areas were measured for all samples using a polar planimeter. In addition, the hornblende 9.03 Å (020), boehmite 6.11 Å (020), quartz 4.26 Å (100), and plagioclase feldspar 4.02 Å (201) peak areas were measured on diffractograms from the random mounts. Since I found no evidence for the kaolinite (002) peak, the entire 7 Å peak was assumed to represent the chlorite component on all mounts.

Calibration curves were constructed by using known mixtures of standard minerals and glass-rich pumice (a non-diffracting material with mass absorption coefficients similar to those of naturally-occurring aluminosilicates) with 10% boehmite by weight added. These curves then allow calculation of mineral abundances from the mineral/boehmite peak-area ratios. Standard minerals used to produce the calibration curves were: smectite, naturally-occurring material isolated from the Kilchis River and Cape Creek samples; chlorite, Source Clay Minerals Repository, CMS-CCa-1; illite, Wards 46W0315; hornblende, naturally-occurring material isolated from the Klamath River sample; quartz, Wards 46W6560; and plagioclase feldspar, Wards oligoclase 46W5800. The chlorite, illite, quartz, and plagioclase standards all produced diffraction patterns similar to those of the naturally-occurring phases.

The semi-quantitative method proposed by Biscaye (1965) was used to calculate clay mineral abundances from the peak areas of the oriented mounts. In spite of the errors and limitations inherent in this type of estimate (Heath and Pisias, 1979; Krissek and Scheidegger, 1982a), I performed these analyses to compare my results to previous work done in the study area using the same technique (Griffin et al., 1968; Duncan et al., 1970; Spigai, 1971; Baker, 1973; Griggs and Hein, 1980; Karlin, 1980).

For the quantitative determinations, accuracy is estimated from calculations of known abundances to be ±5% for smectite, ±2% for chlorite and illite, and ±1% for quartz and plagioclase feldspar (Krissek and Scheidegger, 1982a; Scheidegger and Krissek, 1982). Precision is estimated from replicate slides and analyses to be ±15%

for smectite, ±9% for illite, ±3% for chlorite, quartz, and plagioclase, and ±1.5% for hornblende. Detection levels are estimated from the calibration curve determinations to be approximately 15% for smectite, 2% for chlorite, illite, and plagioclase, 1% for quartz, and 0.5% for hornblende. The semi-quantitative analyses are more precise (Karlin, 1980) but less accurate (Krissek and Scheidegger, 1982a) because of the assumptions made in the semi-quantitative calculations.

DATA AND RESULTS

Mineralogy of the Bank vs. Suspended Samples

Because of insufficient material in the suspended samples from all rivers but the Chehalis, Umpqua, Rogue, Klamath, Mad, and Eel, I was forced to assess the use of bank material to represent the sediments carried by these rivers. For the latter five rivers listed above (no bank sample was available from the Chehalis), mineral abundance data were obtained for the bank and suspended material in both the 2-20μ m and the <2 μm fraction. The results for all minerals from all samples are plotted in Figure 2, and the regression line has the equation $y = 1.00x + 0.49$, with $r^2 = 0.78$. This slope value of 1.00 indicates that the mineral abundances within a size fraction are approximately equal for the bank and suspended material. The <2 μm data points with suspended sample abundances >10% and bank sample abundances <10% are illite and smectite measurements. The quantification of these minerals has relatively poor precision and accuracy at low abundances (close to their detection limits), which may explain the lack of agreement between the measured values. While mineral abundances may be different for the bulk bank and suspended samples (owing to differences in their size composition), I feel justified in using the bank material to represent the fluvially transported sediments within restricted size fractions (i.e., 2-20 μm and <2 μm intervals).

Figure I-2. Plot of mineral abundances in corresponding bank and suspended fluvial samples in the 2-20 μm and <2 μm-size fractions from five rivers. Dots are 2-20 μm data points; stars are <2 μm data points. Regression line has equation $y = 1.00x + 0.49$, $r^2 = 0.78$, indicating that mineral abundances within each size fraction are approximately equal for the bank and suspended sediments.

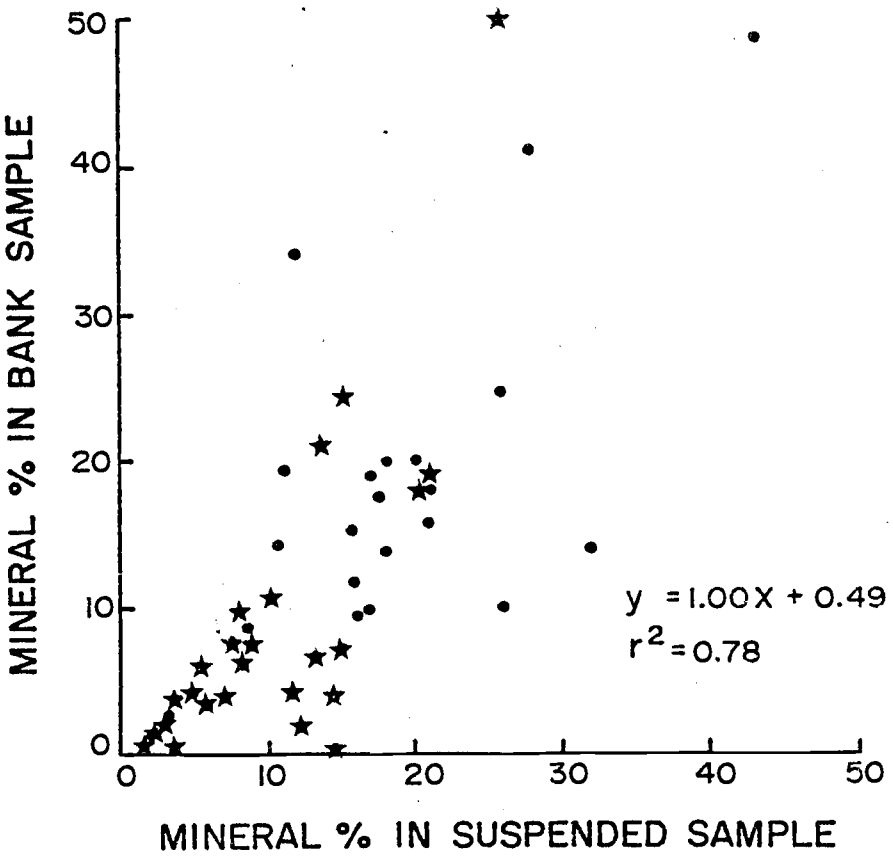
MINERAL % IN BANK SAMPLE
MINERAL % IN SUSPENDED SAMPLE
y = 1.00X + 0.49
r² = 0.78
0
10
20
30
40
50

Figure I-2

Continental Provenance and Within-Source Variability

The mineral compositions of material derived from each of the five major continental source areas shown in Figure 1 are summarized in Figures 3, 4, 5, and 6 and in Tables 2, 3, and 4. I will first consider the 2-20 μm fraction data, then the <2 μm fraction quantitative data, and finally, the <2 μm fraction semi-quantitative data.

Figure 3a is a graphical representation of the mean values listed in Table 2. The range about each mean value is also given in Table 2. Figure 3b shows the discharge-weighted source area abundance of each mineral, calculated as:

$$\%M_T = \sum_{n} \frac{(\%M)_n \cdot (Q)_n}{Q_T}$$

where

$\%M_T$ = mineral abundance for source area (Fig. 3b and Table 2),

$\%M_n$ = mineral abundance in sample from river n,

Q_n = average annual suspended sediment discharge from river n,

Q_T = total average annual suspended sediment discharge from the source area of interest,

n = number of rivers in the source area of interest.

Values for Q_n and Q_T were taken from Karlin (1980, Table 3). Thus, in the discharge-weighted average, the rivers with highest suspended sediment discharges are most important, while all samples are weighted equally in the mean values. The individual data points (recalculated so that % smectite + quartz + plagioclase + chlorite + illite = 100%) are shown in Figure 4; hornblende contents are not included because

Table I-2. Summary of mineral composition of the 2-20 μm size fraction derived from the five major source areas of the Pacific Northwest. Discharge-weighted province average calculated as described in the text.

Source Area	Smectite (%)	Chlorite (%)	Illite (%)	Hornblende (%)	Quartz (%)	Feldspar (%)
Washington Coast Range 2-20 μm						
Mean	9.7	6.2	16.0	0	18.4	26.7
Range	0-57.2	1.3-14.6	5.3-42.1	0	9.6-35.6	17.8-47.4
Discharge-Weighted Average	9.6	9.3	27.4	0	25.5	30.9
Columbia River 2-20 μm						
Mean	0	1.9	24.2	1.0	15.5	33.5
Range	0	1.6-2.2	23.1-25.3	0.7-1.3	15.0-16.8	31.1-36.5
Discharge-Weighted Average	0	1.9	24.2	1.0	15.5	33.5
Oregon Coast Range 2-20 μm						
Mean	72.1	1.8	6.9	0.2	14.1	16.2
Range	18.8-137.0	0-5.2	0-26.0	0-1.3	5.6-26.0	7.7-28.2
Discharge-Weighted Average	63.5	2.5	8.2	1.3	18.9	17.4
Klamath Mountains 2-20 μm						
Mean	19.7	18.4	23.0	6.5	18.0	18.9
Range	0-84.2	6.3-41.2	0.4-69.8	0-18.5	10.7-31.3	11.2-37.0
Discharge-Weighted Average	1.6	15.3	26.3	9.3	21.5	26.0
California Coast Range 2-20 μm						
Mean	0	19.0	26.8	0	18.1	21.6
Range	0	9.8-32.0	10.0-68.2	0	11.7-21.7	12.8-25.0
Discharge-Weighted Average	0	17.3	20.3	0	17.6	32.1

Figure I-3. Mineral abundances in the 2-20 μm material derived from the five major source areas of the Pacific Northwest. Note chlorite presence to north and south, hornblende in Klamath Mountain source, smectite in Oregon Coast Range, and chlorite absence in Columbia River.

a) Mean values (each stream given equal weight).

b) Discharge-weighted values (see text for calculation procedures).

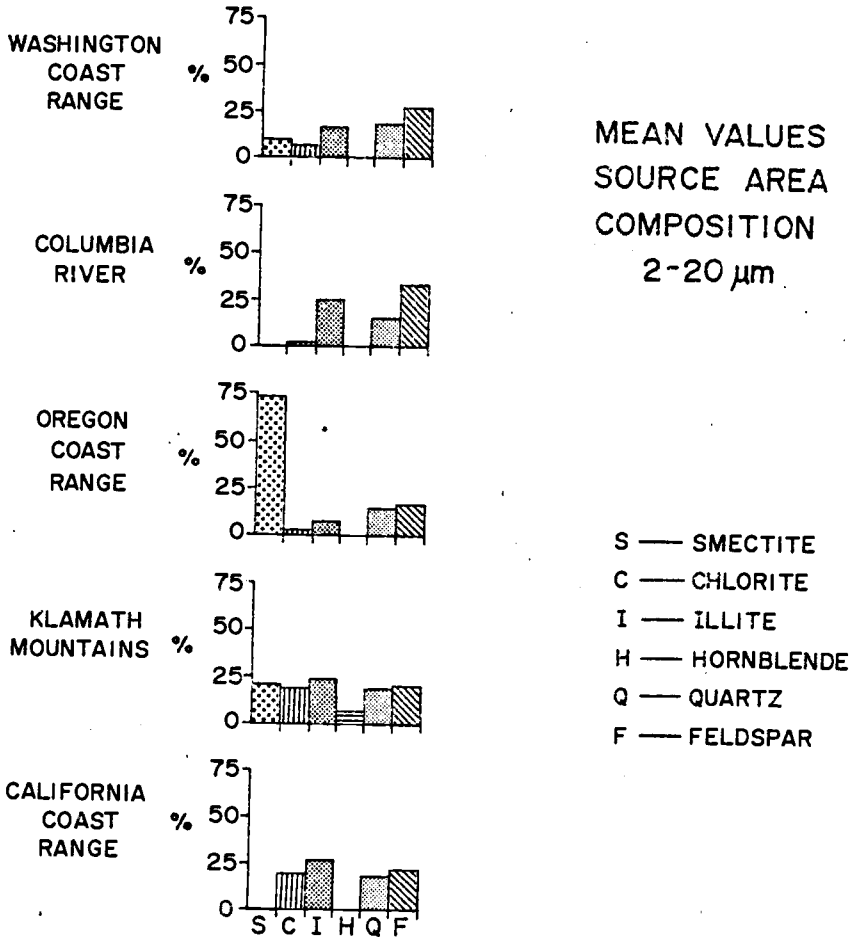
WASHINGTON COAST RANGE
COLUMBIA RIVER
OREGON COAST RANGE
KLAMATH MOUNTAINS
CALIFORNIA COAST RANGE
%
75
50
25
0
S C I H Q F
MEAN VALUES
SOURCE AREA
COMPOSITION
2-20 μm
S — SMECTITE
C — CHLORITE
I — ILLITE
H — HORNBLENDE
Q — QUARTZ
F — FELDSPAR

Figure I-3a

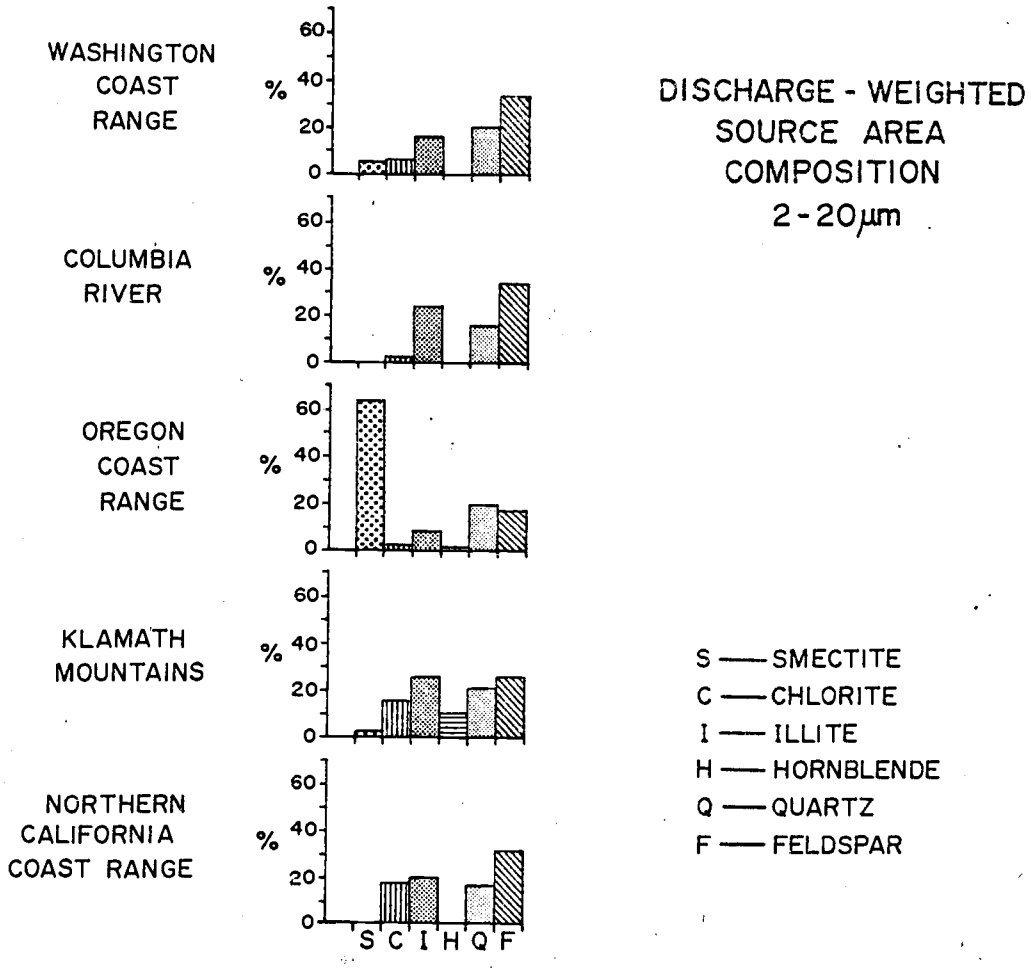
WASHINGTON COAST RANGE
COLUMBIA RIVER
OREGON COAST RANGE
KLAMATH MOUNTAINS
NORTHERN CALIFORNIA COAST RANGE
%
60
40
20
0
S C I H Q F
DISCHARGE - WEIGHTED SOURCE AREA COMPOSITION 2-20μm
S — SMECTITE
C — CHLORITE
I — ILLITE
H — HORNBLENDE
Q — QUARTZ
F — FELDSPAR

Figure I-3b

Figure I-4. Mineral compositions of Pacific Northwest fluvial sediments, recalculated so that % smectite + (quartz + plagioclase) + (chlorite + illite) = 100%.

A.) Composition of Washington Coast Range and Columbia River samples. Columbia River samples are relatively uniform while Washington Coast Range samples form three sub-groups in the 2-20 μm and two sub-groups in the <2 μm fractions. Labels for individual data fields (e.g., WCR I) are used in the text.

B.) Composition of Oregon Coast Range samples, showing broad but continuous ranges in composition with low abundances of chlorite and illite.

C.) Composition of Klamath Mountain samples, showing two sub-groups in both size fractions. Compositions vary from smectite-rich to quartz + plagioclase/chlorite + illite rich.

D.) Composition of California Coast Range samples. The 2-20 μm fraction is compositionally uniform while the <2 μm fraction ranges between smectite-rich and chlorite + illite rich.

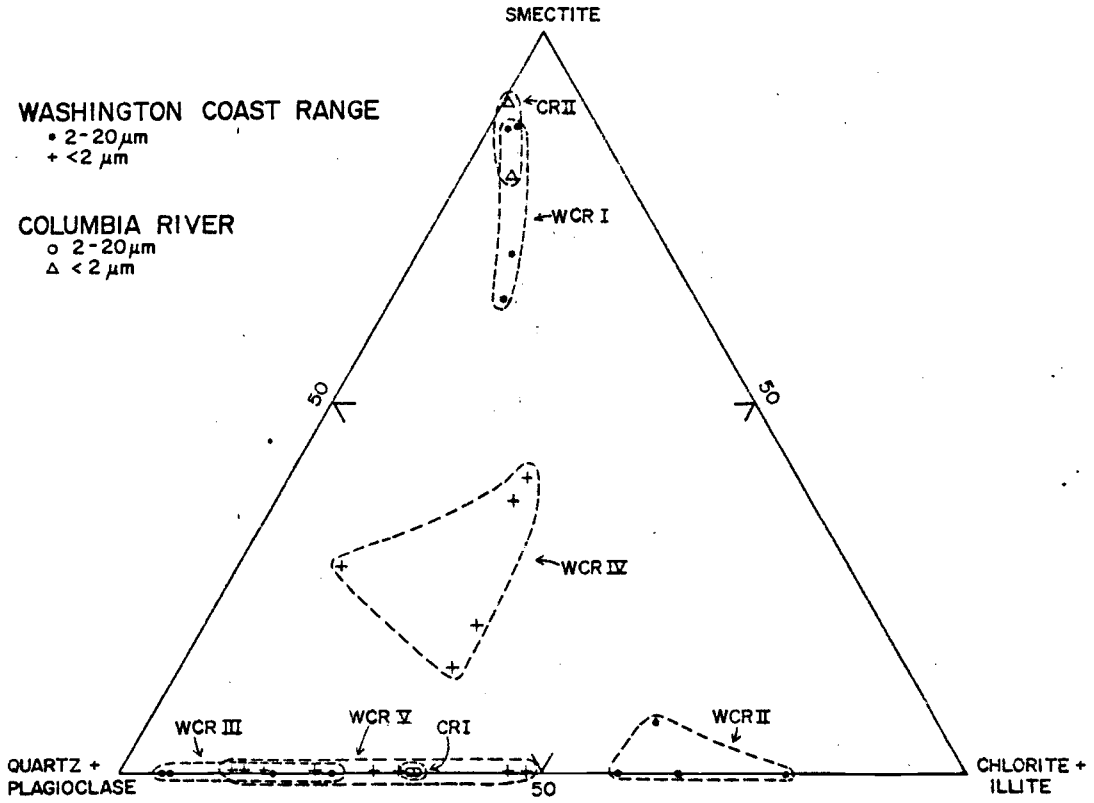
SMECTITE
WASHINGTON COAST RANGE
• 2-20μm
+ <2 μm
COLUMBIA RIVER
o 2-20μm
Δ <2 μm
CRII
WCR I
50
50
WCR IV
WCR III
WCR V
CRI
WCR II
QUARTZ + PLAGIOCLASE
50
CHLORITE + ILLITE

Figure I-4a

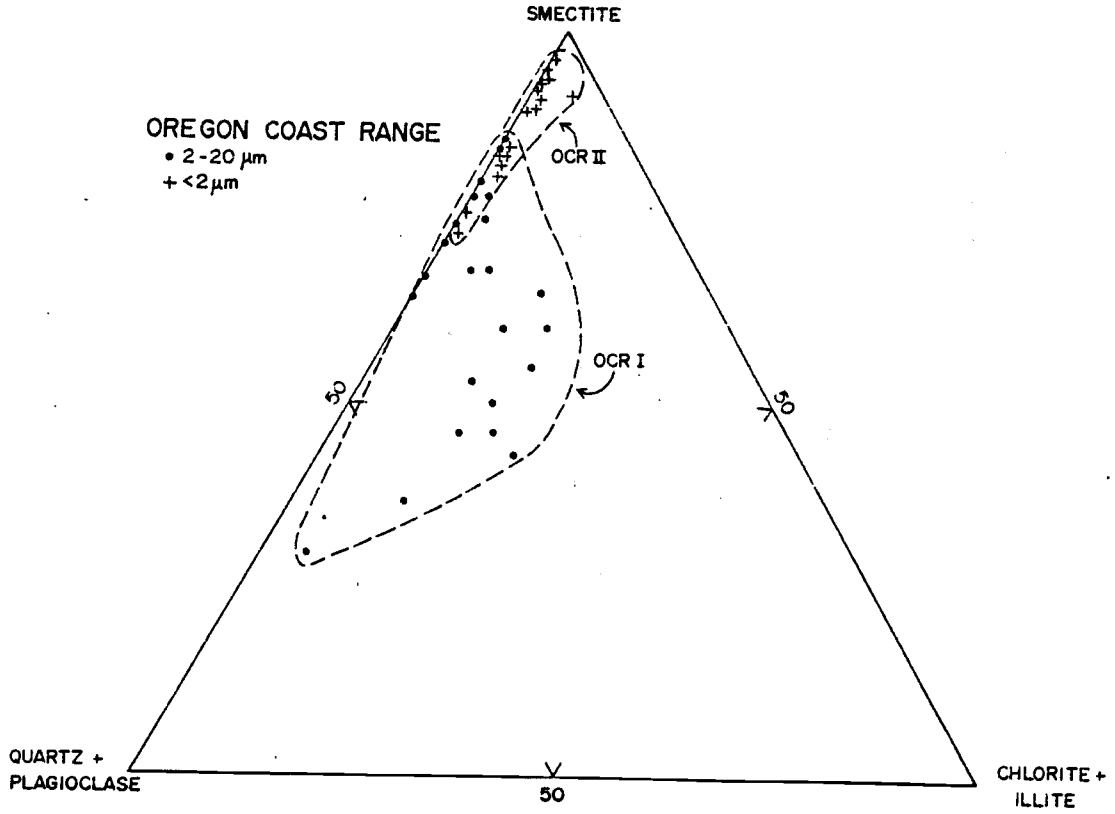
SMECTITE
OREGON COAST RANGE
• 2-20 μm
+ <2μm
OCR II
OCR I
50
50
QUARTZ +
PLAGIOCLASE
50
CHLORITE +
ILLITE

Figure I-4b

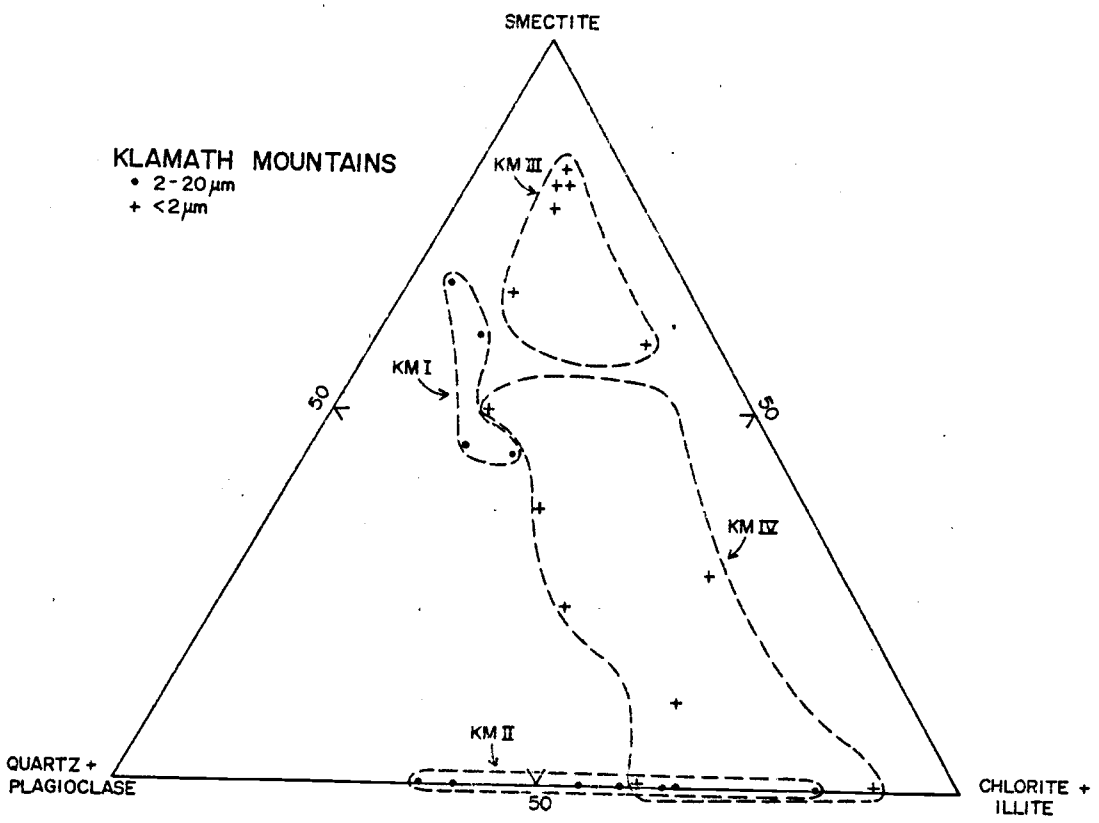
SMECTITE
KLAMATH MOUNTAINS
• 2-20μm
+ <2μm
KM III
KM I
KM IV
KM II
50
50
50
QUARTZ + PLAGIOCLASE
CHLORITE + ILLITE

Figure I-4c

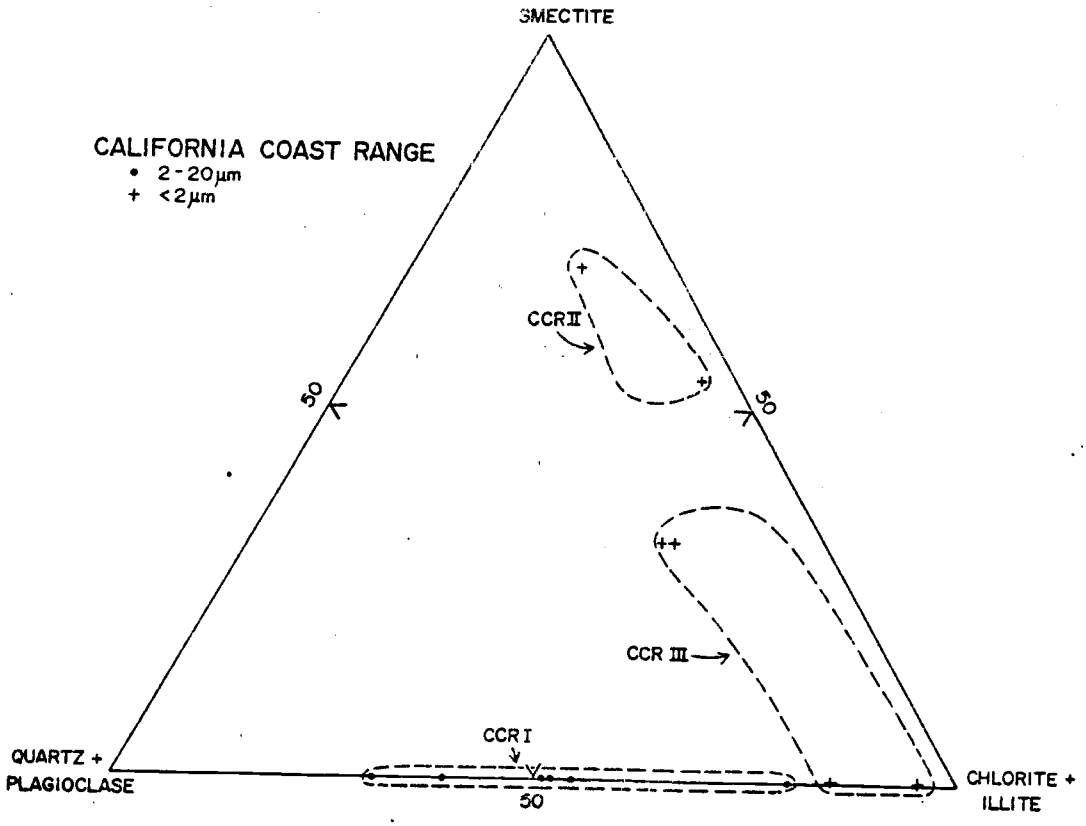
SMECTITE
CALIFORNIA COAST RANGE
• 2-20μm
+ <2μm
CCR II
50
50
CCR III
CCR I
QUARTZ +
PLAGIOCLASE
50
CHLORITE +
ILLITE

Figure I-4d

hornblende is only a distinctive tracer of the Klamath Mountain 2-20 μm material (Fig. 3).

A comparison of Figure 3a and Figure 3b shows that the mean and discharge-weighted values agree quite well except when intra-source variability becomes large, as indicated in Figure 4 and by large ranges in Table 2. These results show that 2-20 μm material derived from:

1) the Washington Coast Range is illite-, quartz-, and plagioclase-rich, and three subgroups can be identified (Fig. 4a; WCRI is smectite-rich, WCRII is chlorite- and illite-rich, and WCRIII is quartz- and plagioclase-rich).
2) the Columbia River is illite- and plagioclase-rich, with lesser quartz, and the two Columbia River samples have uniform compositions (Fig. 4a; CRI)
3) the Oregon Coast Range is smectite-rich with lesser quartz and plagioclase. Though the Oregon Coast Range material has a wide compositional range (Fig. 4b; OCRI), the samples form a continuum instead of distinct groups.
4) the Klamath Mountains is illite-, quartz-, and plagioclase-rich, with lesser chlorite and a significant hornblende component. Two groups of Klamath Mountain samples (Fig. 4c; KMI and KMII) can be distinguished; one is smectite-rich, the other lies on the quartz + plagioclase and chlorite + illite join.

and, 5) the California Coast Range is enriched in plagioclase, with lesser but equal chlorite, illite, and quartz abundances.

These samples form a continuous series (Fig. 4d; CCRI) on the quartz + plagioclase and chlorite + illite join.

In summary, the major changes in mineral abundances within the 2-20 μm fraction are chlorite enrichment in the south relative to the north, hornblende enrichment in the Klamath Mountain source, and smectite enrichment in the Oregon Coast Range source.

The quantitative mineral data for the <2 μm fraction are summarized in Figure 4 and Figure 5 and Table 3. Quartz and plagioclase contents are lower in the <2 μm fraction than in the 2-20 μm fraction (compare Figures 3 and 5), and hornblende is absent. Smectite is present in all source areas, however, and dominates the material derived from the Columbia River and the Oregon Coast Range (Figure 4a; CRII; Figure 4b; OCRII; Figure 5). The compositional ranges of the Washington Coast Range (Figure 4a, WCR IV, WCR V), Klamath Mountain (Figure 4c, KM III, KM IV), and California Coast Range (Figure 4d, CCR II, CCR III) sediments overlap with each other and with the Columbia River and Oregon Coast Range sediments. As a result, the material derived from these five source areas is not as distinctive in the <2 μm fraction as it was in the 2-20 μm fraction. At best, it appears that three sources may be distinguished -- California Coast Range and Klamath Mountains (southern chlorite- and illite-rich), Oregon Coast Range and Columbia River (central smectite-rich), and the Washington Coast Range (northern chlorite- and illite-rich).

The semiquantitative clay mineral abundances (Figures 6a, 6b, and Table 4) are included here to allow a comparison of these results to

Table I-3. Summary of mineral composition of <2 μm size fraction of material derived from the five major source areas of the Pacific Northwest. Abundances calculated using a quantitative X-ray diffraction technique. Discharge-weighted province average calculated as described in text.

Source Area	Smectite	Chlorite	Illite	Quartz	Feldspar
Washington Coast Range					
Quantitative <2 μm					
Mean (Range)	18.1(0-100.5)	4.3(0-11.1)	8.7(0-33.4)	6.0(5.0-9.7)	8.2(0.9-13.1)
Discharge-Weighted Average	23.2	4.3	15.4	5.9	5.3
Columbia River					
Quantitative <2 μm					
Mean (Range)	60.4(52.1-68.8)	0(0)	2.1(0-4.2)	4.2(3.8-4.5)	3.5(3.0-4.0)
Discharge-Weighted Average	60.4	0	2.1	4.2	3.5
Oregon Coast Range					
Quantitative <2 μm					
Mean (Range)	66.3(20.7-131.5)	0.3(0-5.7)	0.4(0-2.2)	4.8(2.6-8.9)	4.1(0.6-12.6)
Discharge-Weighted Average	74.8	0.3	0	3.9	1.9
Klamath Mountains					
Quantitative <2 μm					
Mean (Range)	28.4(0-65.1)	6.0(1.4-14.4)	10.5(0-33.9)	5.8(3.5-9.8)	3.9(0.8-4.3)
Discharge-Weighted Average	18.0	8.6	14.5	8.7	10.9
California Coast Range					
Quantitative <2 μm					
Mean (Range)	21.8(0-49.7)	10.0(5.5-13.8)	23.2(7.1-64.1)	4.5(3.3-7.0)	2.2(0-4.4)
Discharge-Weighted Average	20.0	12.9	19.2	6.4	4.0

Figure I-5. Quantitative mineral abundances in the <2 μm material derived from the five major source areas of the Pacific Northwest. Note that smectite occurs in all sources, chlorite is present in the northern and southern sources, and smectite is predominant in the Columbia River and Oregon Coast Range.

a) Mean values.

b) Discharge-weighted values.

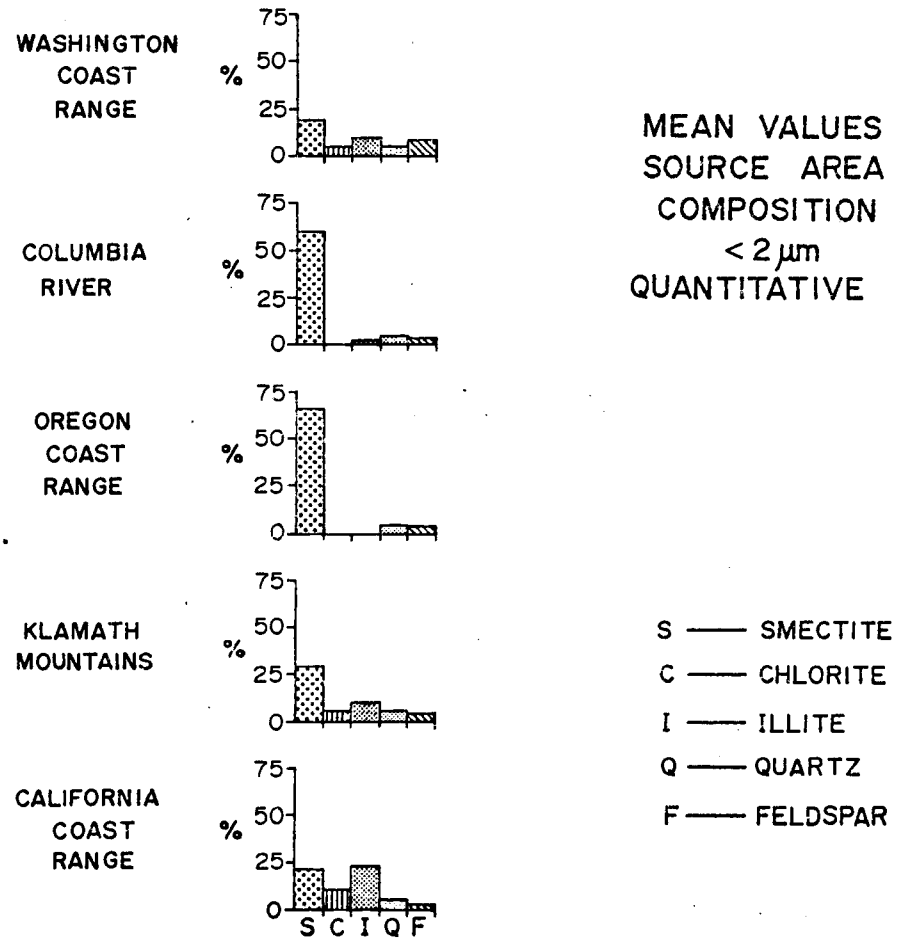
WASHINGTON COAST RANGE
COLUMBIA RIVER
OREGON COAST RANGE
KLAMATH MOUNTAINS
CALIFORNIA COAST RANGE
%
75
50
25
0
S C I Q F
MEAN VALUES
SOURCE AREA
COMPOSITION
< 2 µm
QUANTITATIVE
S —— SMECTITE
C —— CHLORITE
I —— ILLITE
Q —— QUARTZ
F —— FELDSPAR

Figure I-5a

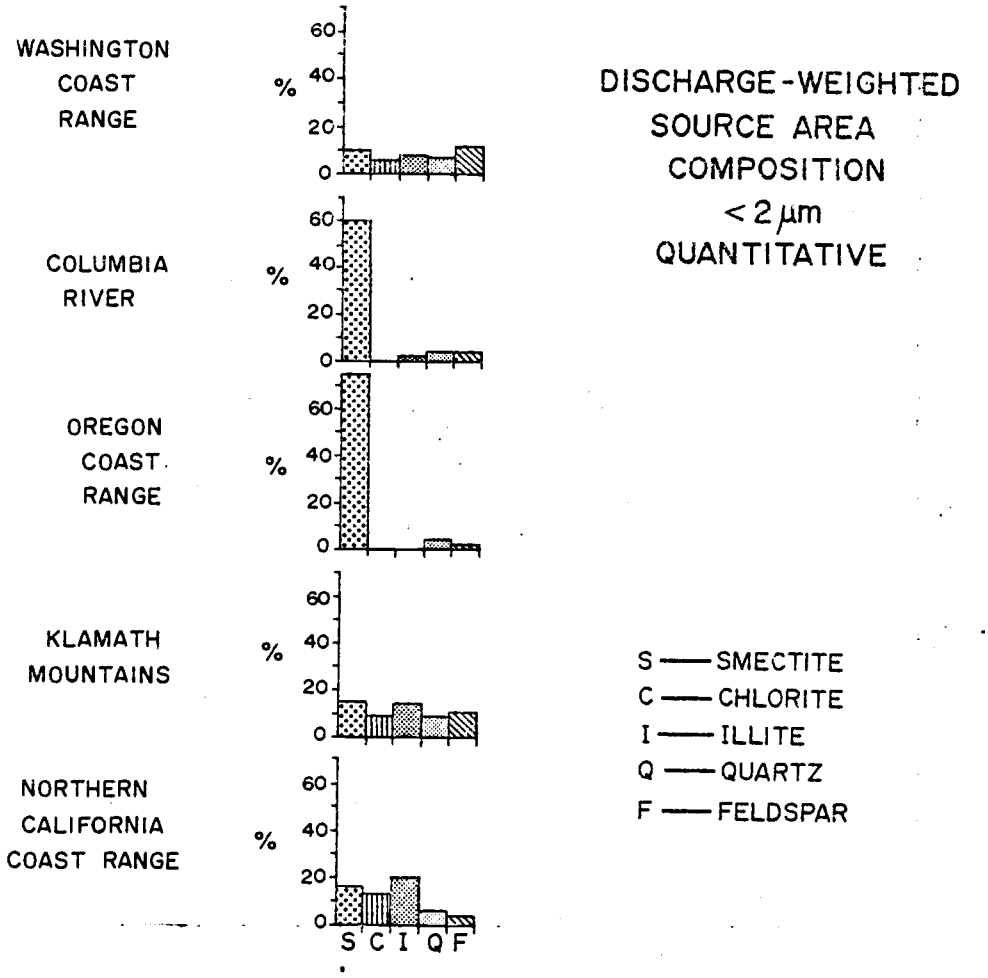
WASHINGTON COAST RANGE
COLUMBIA RIVER
OREGON COAST RANGE
KLAMATH MOUNTAINS
NORTHERN CALIFORNIA COAST RANGE
%
60
40
20
0
S C I Q F
DISCHARGE-WEIGHTED SOURCE AREA COMPOSITION
< 2 μm
QUANTITATIVE
S — SMECTITE
C — CHLORITE
I — ILLITE
Q — QUARTZ
F — FELDSPAR

Figure I-5b

Table I-4. Summary of semiquantitatively-determined mineral composition of the <2 μm size fraction of material derived from the five major source areas of the Pacific Northwest. Discharge-weighted province average calculated as described in the text.

Source Area	Smectite (%)	Chlorite (%)	Illite (%)
Washington Coast Range			
<2 μm Semiquantitative			
Mean (Range)	16.7 (0-88.1)	54.7 (5.3-62.0)	28.5 (6.5-53.4)
Discharge-Weighted Average	21.6	39.6	35.0
Columbia River			
<2 μm Semiquantitative			
Mean (Range)	52.8 (42.8-62.7)	22.0 (18.0-26.0)	25.2 (19.3-31.1)
Discharge-Weighted Average	52.8	22.0	25.2
Oregon Coast Range			
<2 μm Semiquantitative			
Mean (Range)	68.8 (31.9-100)	19.4 (0-48.8)	11.7 (0-23.6)
Discharge-Weighted average	71.3	20.6	7.8
Klamath Mountains			
<2 μm Semiquantitative			
Mean (Range)	15.0 (0-35.2)	51.9 (26.8-64.5)	33.1 (14.3-52.3)
Discharge-Weighted Average	9.2	47.0	43.5
California Coast Range			
<2 μm Semiquantitative			
Mean (Range)	6.9 (0-12.0)	49.5 (41.0-57.1)	43.7 (38.6-58.9)
Discharge-Weighted Average	10.5	49.5	39.9

Figure I-6. Semiquantitative clay mineral abundances in the <2 μm material derived from five major source areas of the Pacific Northwest. Abundances calculated according to the method of Biscaye (1965). Note chlorite presence in northern and southern source areas, smectite abundance in Columbia River and Oregon Coast Range.

a) Mean values.

b) Discharge-weighted values.

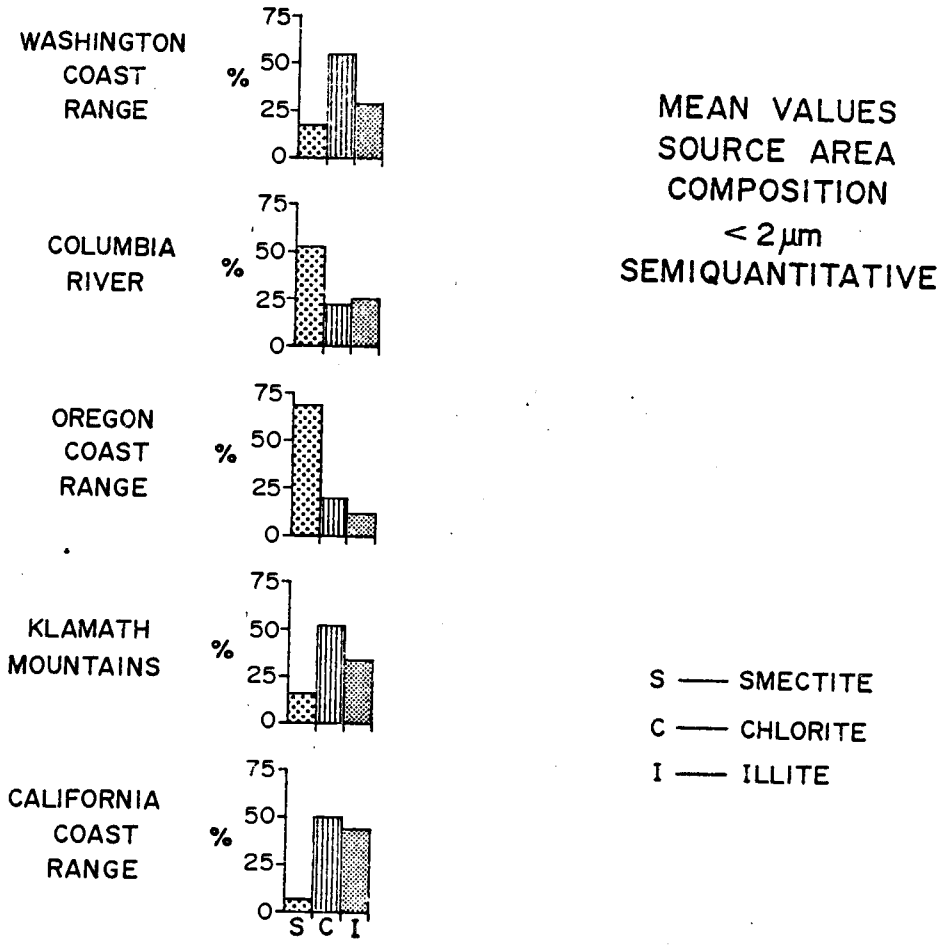
WASHINGTON COAST RANGE
COLUMBIA RIVER
OREGON COAST RANGE
KLAMATH MOUNTAINS
CALIFORNIA COAST RANGE
%
75
50
25
0
S C I
MEAN VALUES
SOURCE AREA
COMPOSITION
< 2 μm
SEMIQUANTITATIVE
S — SMECTITE
C — CHLORITE
I — ILLITE

Figure I-6a

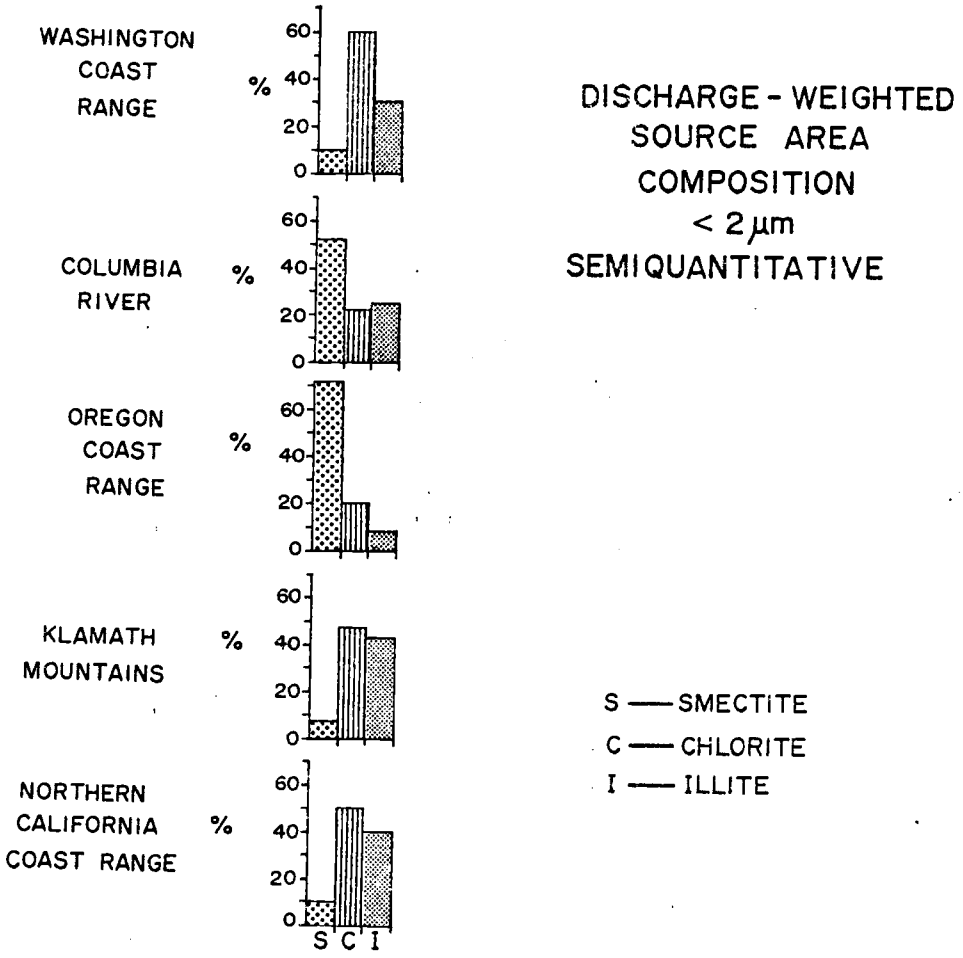
WASHINGTON COAST RANGE
COLUMBIA RIVER
OREGON COAST RANGE
KLAMATH MOUNTAINS
NORTHERN CALIFORNIA COAST RANGE
%
60
40
20
0
S C I
DISCHARGE - WEIGHTED SOURCE AREA COMPOSITION
< 2 μm
SEMIQUANTITATIVE
S — SMECTITE
C — CHLORITE
I — ILLITE

Figure I-6b

data published from previous studies of fluvial and marine sediments within the study area. Although the abundance values are different, both sets of data for the <2 μm fraction show chlorite and illite enrichment in the Washington Coast Range, Klamath Mountains, and California Coast Range, while the Columbia River and Oregon Coast Range are smectite-rich. In neither case is the mineralogy as distinctive between source areas as it was in the 2-20 μm fraction.

These semiquantitative data agree well with the few analyses of Pacific Northwest fluvial material found in the literature. Samples from the Columbia River were analyzed previously by Griffin et al. (1968), Knebel et al. (1968), Baker (1973), and Glenn (1973). Knebel et al. (1968) and Glenn (1973) report relative values from bottom samples of 50-60% montmorillonite, 10-25% chlorite, and 20-35% illite. Griffin et al. (1968) and Baker (1973) list suspended material relative compositions of 30-40% smectite, 15-30% chlorite, and 40-50% illite. Data from this study (Table 4) give abundances of 53%, 22%, and 25% for smectite, chlorite, and illite, respectively, in the Columbia River samples, in close agreement with the bottom sample data and slightly more smectite-rich and illite-poor than the suspended material. Such variations may reflect seasonal and grain size differences (Knebel et al., 1968; Baker, 1973) in the samples which were analyzed. Samples from the Rogue (Duncan et al., 1970), Umpqua (Spigai, 1971), and the Umpqua, Rogue, Smith (CA), Klamath, Mad, and Eel Rivers and Redwood Creek (Griffin et al., 1968) have also been analyzed previously. These earlier results agree well with data obtained during this study,

showing high smectite content for the Umpqua, less smectite and more chlorite and illite for the Rogue, and low smectite (<20%)/high chlorite + illite for the Klamath Mountain and California Coast Range streams. The analyses performed during this study provide quantitative mineral abundances for the 2-20 μm and <2 μm fraction which complement the regional provenance framework described by previous workers in the study area. In addition, these data add detailed information on variability within each source area.

Temporal Variability within a Source

To investigate temporal variations in fluvial sediment composition four samples of suspended material were obtained from the Chehalis River in January and February, 1978. Each was taken following a major storm. The quantitative mineral data and semiquantitative clay mineral abundances are plotted in Figure 7. These samples appear to contain no smectite. In all three sample sets, the mineral abundances are constant to within a factor of 2; variations for the less-abundant components are commonly within the analytical uncertainty. Feldspar abundances are subject to the largest variation over time. While the causes for these changes are unknown, they may include local conditions which control contributions from various areas within the drainage basin (localized heavy rains, localized mass wasting, etc.). As a result, it appears that the temporal variability in the composition of fluvial material is small (changes by less than a factor of 2), at least during high flow events. Since high flow transports a significant fraction of the total annual sediment load (Karlin, 1980), such constancy over time implies similar annual constancy.

Figure I-7. Time series of mineral abundances in the 2-20 μm and <2 μm fraction of four samples from the Chehalis River. All abundances remain constant within a factor of 2 or less.

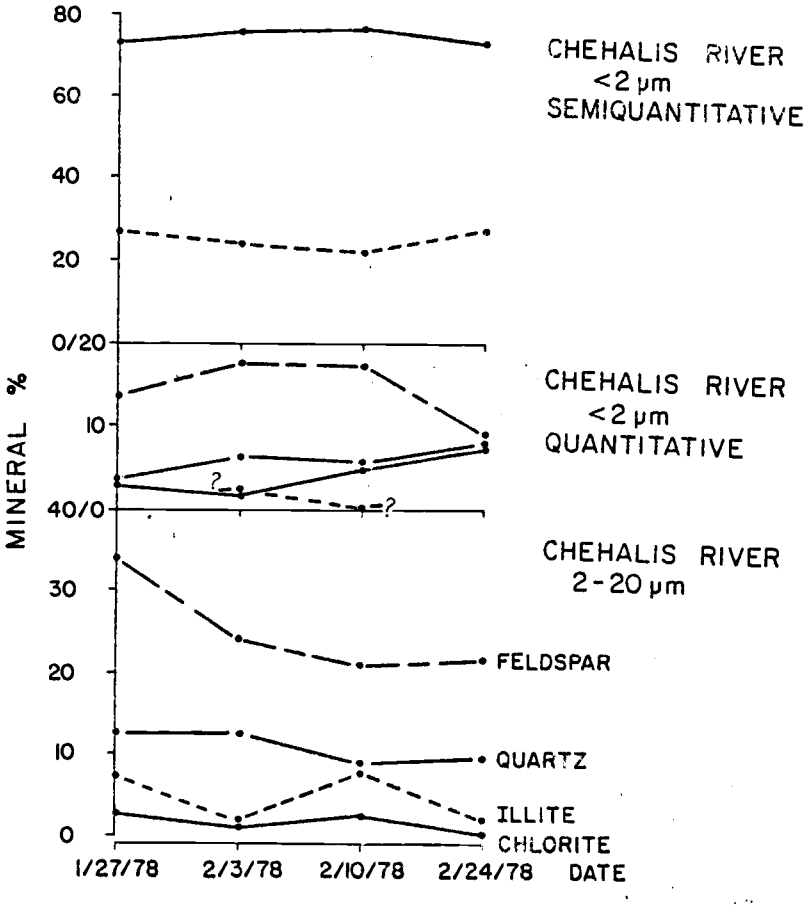
80
60
40
20
0/20
10
40/0
30
20
10
0
MINERAL %
CHEHALIS RIVER
<2 μm
SEMIQUANTITATIVE
CHEHALIS RIVER
<2 μm
QUANTITATIVE
?
?
CHEHALIS RIVER
2-20 μm
FELDSPAR
QUARTZ
ILLITE
CHLORITE
1/27/78
2/3/78
2/10/78
2/24/78
DATE

Figure I-7

Less detailed results of semiquantitative analyses of suspended material from the Columbia River (Baker, 1973; J. L. Glenn, unpublished data) also suggest that the composition varies by less than a factor of 2 on a seasonal to annual basis. Baker (1973) reported that the mean relative smectite content changed from 27% in summer to 39% in winter, while relative chlorite abundance varied from 19% to 16% in the same period. Samples taken at Astoria from October through December, 1969 (J. L. Glenn, unpublished data) have essentially constant relative smectite content (40-50%). On the basis of these data and the Chehalis River results, I conclude that a single fluvial sample can adequately represent the material carried within a given size fraction (i.e., 2-20 μm, <2 μm) over a longer time period (annually or longer), especially when the sample is taken during high flow conditions. Schneider and Angino (1980) and Ongley et al. (1981) reached similar conclusions from year-long studies of suspended materials in streams of eastern Kansas and of Ontario.

Textural Variability Between Source Areas

In addition to carrying a distinctive mineralogic signature within each size fraction, the grain size of suspended material derived from a source area may yield insights into the relative amounts of different size fractions available for transport and the weathering and erosion regimes active within that region. Textural controls also determine the distance that the fluvially derived material can be transported away from its source. To investigate such variability within the study area, we have compiled the available textural data

for suspended fluvial material sampled from Pacific Northwest streams during high flow events. These data are listed in Table 5. Detailed analyses are only available for four rivers, and these are graphed in Figure 8. Material derived from the Klamath Mountains (Klamath and Rogue River samples) is the coarsest found in the study area in terms of both percent fines (<62 μm) and the entire size distribution <62 μm (Fig. 8). The Eel River, the major stream draining the California Coast Range, is most enriched in the finest (<2 μm) fraction, but has intermediate abundances of material in the 14 μm-62 μm size range. Redwood Creek, another large stream in the California Coast Range, has intermediate abundances for all grain sizes. The Columbia River material appears as an inverse of the Eel River sample, with intermediate abundances of the finer components (<14 μm) and relatively enriched in the medium to coarse silts. In terms of the fraction of material <62 μm in these and all other samples for which data are available, the areas rank as follows: Washington Coast Range, 89%; Columbia River, 86%; California Coast Range, 79%; Oregon Coast Range, 78%; and Klamath Mountains, 67%.

Table I-5. Grain-size distribution of fluvial suspended material. Values listed are mean and range of data. Columbia River values are unpublished U.S.G.S. data provided by D. W. Hubbell. All other values are from the U.S.G.S. Water Quality Reports for California, Oregon, and Washington, 1977-1980.

River	Weight % Finer Than: 2 μm	4 μm	8 μm	16 μm	31 μm	62 μm
Chehalis River @ Porter						89
Columbia River @ Astoria	24 (1-45)	34 (9-55)	48 (8-76)	64 (13-92)	79 (19-99)	86 (24-100)
Nehalem River @ Foss						82
Alsea River @ Tidewater						68
Siuslaw River @ Mapleton						71
Umpqua River @ Elkton						82
Rogue River @ Agness						73
Klamath River @ Klamath	17 (14-23)	25 (24-29)	34 (32-37)	44 (43-47)	54 (52-57)	63 (32-77)
Redwood Creek @ Orick	25 (19-38)	33 (20-38)	45 (30-49)	58 (39-64)	70 (49-79)	79 (57-88)
Eel River @ Scotia	31 (21-37)	40 (30-46)	52 (41-62)	62 (54-74)	71 (63-80)	80 (46-85)

Figure I-8. Grain-size frequency distributions for the <62 μm fraction of suspended samples from four major Pacific Northwest streams, showing coarse nature of Klamath River sample. Textural data are listed in Table I-5.

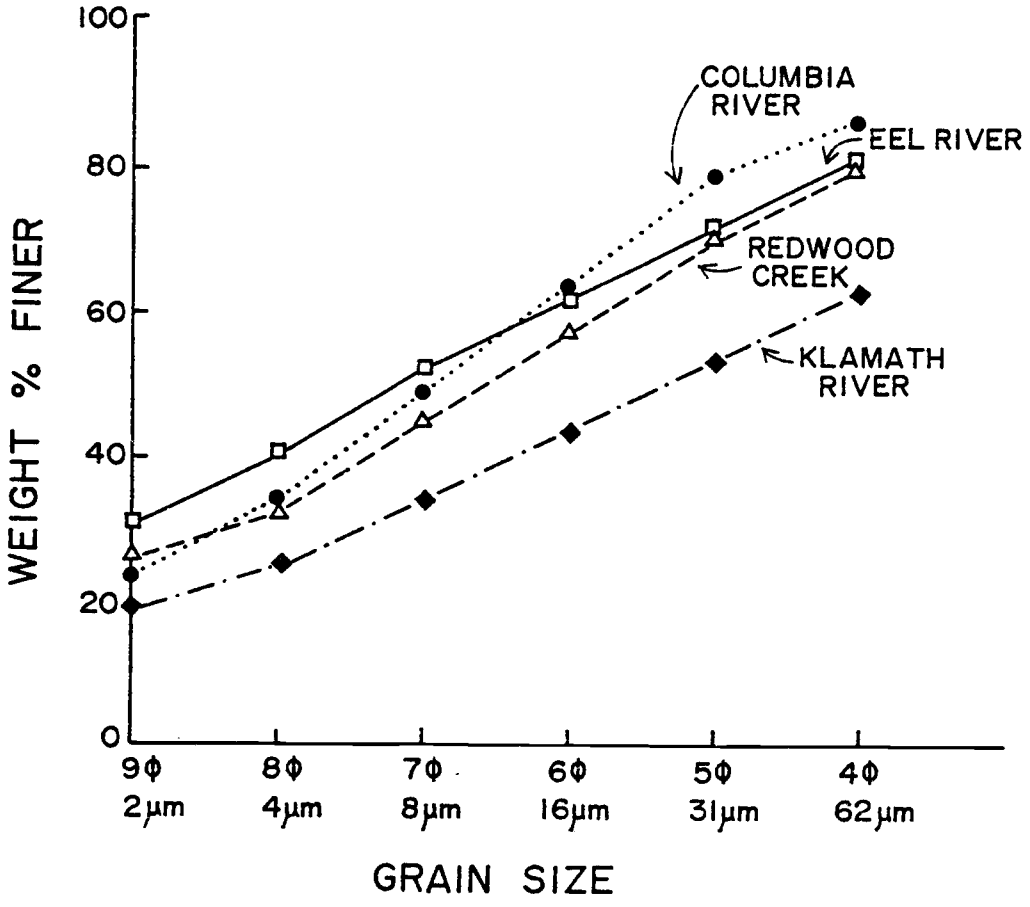
100
80
60
40
20
0
WEIGHT % FINER
COLUMBIA RIVER
EEL RIVER
REDWOOD CREEK
KLAMATH RIVER
9φ 2μm
8φ 4μm
7φ 8μm
6φ 16μm
5φ 31μm
4φ 62μm
GRAIN SIZE

Figure I-8

DISCUSSION

From the data presented above, combinations of single bank material samples have been shown to represent the material derived from a continental source area over time; however, some of the fluvial sediments (i.e., from the Washington Coast Range and Klamath Mountains) have significant within-source variability. The factors which cause variations in the bulk mineral composition and texture of the transported material can be identified by examining the geology, physiography, and climate of the continental source areas. Such relations have been discussed by Kulm et al. (1968) and Scheidegger et al. (1971) for the sand-sized heavy mineral suites derived from the drainages of the northern California and Oregon coast.

The Washington Coast Range fluvial sediments contain abundant plagioclase, quartz, and illite in the 2-20 μm fraction (Figure 3b) and relatively high abundances of non-smectite phases in the <2 μm size range (Figure 5). The 2-20 μm fraction can be subdivided into 3 groups (Figure 4), one each with abundant smectite, chlorite + illite, and quartz + plagioclase, while two groups with intermediate composition are distinguishable from the <2 μm data. According to the geologic map of Washington (Weissenborn, 1969), the smectite-rich streams all drain Miocene or pre-Miocene volcanic rocks; smectites are known to be alteration products of volcanic material (Griffin et al., 1968), so their presence in rivers draining such terranes is reasonable. Illite, on the other hand, is thought to be derived by physical erosion or a mica or feldspar component in the source area (Griffin et al., 1968). The illite-rich streams drain both pre-Pleistocene sedimentary

units and adjacent Cretaceous and Paleocene continental sedimentary deposits, while the illite- and smectite-poor drainages lie predominantly on the former. Therefore, the illite enrichment may be caused by recycling of an illite or mica component within the Cretaceous and Paleocene rocks.

Material carried by the Columbia River in the 2-20 μm fraction is distinguishable by its high plagioclase and illite contents, with abundant associated quartz and little or no chlorite (Figure 3). Provenance characteristics within the Columbia River have been discussed in detail by Kulm et al. (1968), Knebel et al. (1968), Whetten et al. (1969), and Scheidegger et al. (1971). These studies conclude that a wide variety of rock types contribute to its fluvial load -- sedimentary, granitic, and and coarse-grained metamorphic rocks in its upper reaches, and basaltic to andesitic volcanic and sedimentary rocks in its lower reaches. Whetten et al. (1969) found that the ratio of quartz to "unstable" constituents in bottom sediments decreased downstream, indicating that much of the sediment has undergone relatively little chemical weathering. Thus, the quartz and illite in the 2-20 μm fraction may have been derived by physical and/or chemical weathering in the acidic terranes of the upper Columbia, while the plagioclase feldspar is supplied by physical erosion of the more mafic rocks of the lower Columbia. In the finest (<2 μm) fraction, the Columbia river sediment is dominated by smectite (Figures 3 and 5), indicating the importance of volcanic material throughout the Columbia basin, especially its lower reaches. Because smectite-rich tributaries of the lower Columbia obtain their water directly from winter rains, the relative smectite content of suspended sediment in the Columbia is higher in the winter than the summer (Baker, 1973).

Material derived from the Oregon Coast Range is dominated by smectite in both the 2-20 μm and the <2 μm fractions (Figures 3, 4, and 5), reflecting the dominant influence of basic igneous source rocks in the river drainages. Studies of the heavy mineral suites of the sands transported by these streams (Kulm et al., 1968; Scheidegger et al., 1971) have distinguished several sub-groups within the Oregon Coast Range, with the northern rivers containing relatively simple, basic-igneous-dominated suites. Southern rivers, especially the Umpqua, also drain portions of the metamorphic Klamath Mountains and the volcanic Cascade Mountains, and the heavy minerology of their sand-sized fraction reflects this more diverse provenance. Such a difference is not seen in the data for either the 2-20 μm or <2 μm size fraction of these fluvial sediments; instead, the fine-grained material examined here reflects the predominance of volcanic material throughout the entire Oregon Coast Range. Only a Columbia River/Oregon Coast Range distinction can be made in the 2-20 μm size fraction, and even that distinction is difficult in the <2 μm fraction due to the predominance of smectites.

Material derived from the Klamath Mountains in the 2-20 μm fraction is distinguished by its hornblende component and by the relatively equal abundances of the other minerals examined here (Figure 3). This material can be subdivided into two groups (Figure 4c, KMI and KMII), one which is smectite-rich and one which lies along the quartz + plagioclase/chlorite + illite join. In the <2 μm fraction, Klamath Mountain material contains subequal amounts of smectite, chlorite,

illite, quartz, and plagioclase (Figure 5), again with variation from smectite-rich samples to those dominated by chlorite and illite (Figure 4c, KMIII and KMIV).

Rock types in the Klamath Mountains include Paleozoic and Mesozoic metasedimentary, matavolcanic, and sedimentary rocks intruded by granitoid and untramatic bodies (Baldwin, 1964); heavy-mineral assemblages of these streams are dominated by high-rank metamorphic minerals (Kulm et al., 1968; Scheidegger et al., 1971). The high chlorite and illite abundances of the samples in groups KMII and KMIV (Figure 4c), along with the high hornblende content in the 2-20 μm size fraction, also indicate the strong metamorphic influence. The samples of groups KMI and KMIII were obtained from relatively short streams which drain the south end of the Cenozoic sedimentary and minor volcanic rocks of the Oregon Coast Range (Walker and King, 1969), so that the metamorphic influence is reduced and smectite, the volcanic alteration product, dominates the fluvial sediments.

Material derived from the California Coast Range contains subequal (20-30%) amounts of chlorite, illite, quartz, and plagioclase in the 2-20 μm fraction (Figure 3), and covers a limited range of compositions (Figure 4d, CCRI). In the <2 μm fraction, sediments contain more phyllosilicate minerals (smectite, chlorite, and illite) than quartz and plagioclase (Figure 5), and can be subdivided into smectite-rich (Figure 4d, CCRII) and smectite-poor (Figure 4c, CCRIII) groups. Illite and chlorite are abundant in the Franciscan shales of northern California (Griggs and Hein, 1980), providing a ready source of these minerals, while smectite may originate from weathering of localized volcanic terranes.

In addition to the distinctive mineral abundances described above, the composition of the plagioclase feldspar derived from each source area also provides a tool for distinguishing between the northern (Columbia River + Oregon Coast Range) and southern (Klamath Mountain + California Coast Range) sources. The composition of these plagioclases are summarized in Table 6. The data show that samples from the Oregon Coast Range and the Columbia River contain plagioclase with >30% anorthite, while plagioclase derived from the Klamath Mountains and the California Coast Range is relatively albite-rich, reflecting the importance of volcanic terranes to the north and metamorphic source rocks to the south. The (002) plagioclase diffraction (3.18 Å) also changes along the margin, from a single sharp, well-defined peak for the southern samples to a broader doublet peak for Columbia River sediments. This change provides an easily-recognized qualitative means of distinguishing between the northern and southern source areas.

Both regional and local variations in fluvial sediment composition can be explained in terms of changes in provenance and weathering regime. However, the total mineral abundance accounted for by the quantitative XRD technique does not always sum to 100%, and the difference between the total and 100% may provide information on the relative amounts of crystalline and amorphous material derived from each source area. Total mineral abundances for each source area are summarized in Table 7. Values significantly >100% (such as the Oregon Coast Range 2-20 μm and <2 μm and Klamath Mountain 2-20 μm maximum totals) indicate some difficulty with the quantification calculation; in the case of the Oregon Coast Range samples, smectite abundances alone are extremely high (>100%), due to better crystallinity of the

Table I-6. Composition of plagioclase feldspars in river samples calculated from X-ray diffraction lattice parameters (after Smith, 1956). Plagioclase composition is distinctive for northern and southern sources within the study area.

Sample	$2\theta(111) - 2\theta(1\bar{1}1)$ (degrees 2θ)	Approximate Plagioclase Composition %(An/Ab+An)
Columbia River	0.78	>30
Nehalem River	0.80	>30
Nestucca River	0.80	>30
Siletz River	0.76	>30
Alsea River	0.81	>30
Umpqua River	0.70	30
Rogue River	0.60	18
Klamath River	0.61	19
Mad River	0.56	13
Eel River	0.57	14

Table I-7. A summary of the total mineral abundances calculated by quantitative XRD. Mean values less than 100% indicate that a portion of the sediments was not quantified and may represent an amorphous or poorly crystalline phase.

Source Area and Size Fraction	Mean Total	Standard Deviation	Max.	Min.
Washington Coast Range 2-20 μm	73.5	28.3	122.7	32.9
Washington Coast Range <2 μm	43.7	32.4	114.7	19.7
Columbia River 2-20 μm	76.1	4.4	79.2	73.0
Columbia River <2 μm	70.2	7.6	75.6	64.8
Oregon Coast Range 2-20 μm	110.4	19.5	162.1	63.2
Oregon Coast Range <2 μm	74.4	29.4	141.7	28.8
Klamath Mountains 2-20 μm	104.1	29.2	150.6	53.3
Klamath Mountains <2 μm	55.1	17.3	82.1	25.6
California Coast Range 2-20 μm	85.5	16.2	114.7	64.8
California Coast Range <2 μm	61.7	23.3	85.8	23.3

smectites in these samples than of the mineral used to generate the smectite calibration curve. The Klamath Mountain maximum of 150% is from a sample with an anomalously high illite abundance which also reflects a difference in crystallinity between the natural mineral and the standard used to generate our calibration curves (Gibbs, 1967b). These examples illustrate the difficulty of selecting proper standard minerals for the generation of calibration curves, since local mineral variability (which is impossible to avoid) can increase the errors associated with mineral abundance determinations. However, the calculated smectite and illite abundances are reasonable for all other samples, indicating that, with caution, these calibration curves can be applied to regional studies.

Mean total abundances of the minerals quantified in the 2-20 μm fraction range from 73.5% to 110.4%, indicating that, within the analytical uncertainty, essentially all of these sediments are accounted for by the mineral determinations. Therefore, I conclude that amorphous material forms a minor component of the 2-20 μm size fraction. In the <2 μm fraction, however, the mean values range from 43.7% to 74.4%, indicating that amorphous material may form a significant portion (25-50% or more) of the sediments derived from some of these source areas. Such material may be especially important in the Washington and California Coast Ranges and Klamath Mountains, where high rainfall, relatively steep slopes, and acidic soils could combine to leach Fe and Al rapidly from the soil and leave amorphous or poorly-crystalline SiO_2 frameworks behind (Leeper, 1952) for subsequent erosion and transportation in the fluvial load.

The data compiled in Table 5 indicate that suspended fluvial sediments from each source area have a characteristic grain-size distribution; such between-source variability implies that source-area contributions to offshore sediments can be size dependent. The textural variations are also interrelated with the mineral compositions discussed above. For example, Klamath Mountain sediments are both coarser-grained (Table 5) and enriched in quartz + plagioclase ± hornblende (Figs. 3 and 5) relative to California Coast Range material. These compositional characteristics may reflect the cycling of coarse-grained non-phyllosilicate phases from the Klamath Mountain marine sedimentary, metamorphic, and granitic rocks which are not present in the Franciscan shales of the California Coast Range (Griggs and Hein, 1980). The data compiled in Table 5 can also be combined with annual total suspended sediment discharges (Karlin, 1980) to calculate contributions from each source area to the total regional discharge of fine-grained sediments. These results are listed in Table 8 and show that the input of California Coast Range material is more important, in a regional sense, in the <2 μm fraction than in the coarser grain size. Subtle differences such as these are important in the calculation of sediment budgets for adjacent marine environments.

It should be stressed that, with decreasing grain size, source areas cannot be distinguished very well. As discussed above in relation to the Oregon Coast Range, studies of the sand-sized heavy mineral suites have outlined two (Scheidegger et al., 1971) or three (Kulm et al., 1968) subgroups which cannot be identified in either the 2-20 μm or the <2 μm size fractions of the fluvial sediments. This

Table I-8. Contributions from the Columbia River, Klamath Mountains, and California Coast Range to the annual discharge of suspended material in the <2, 2-20, and 20-63 μm-size fractions. Note that the "% of total" value for each source area varies with grain size. Average suspended sediment discharge values from Karlin (1980).

	Source Area		
	Columbia River	Klamath Mountains	California Coast Range
Average suspended sediment discharge (10^3 tonnes/year)	14282	16901	30753 61936
% <2 μm	23.8	19.0	28.2
Discharge <2 μm (10^3 tonnes/year)	3400	3210	8670 15280
% 2-20 μm	44.0	27.0	34.0
Discharge 2-20 μm (10^3 tonnes/year)	6280	4560	10460 21300
% 20-63 μm	18.1	16.8	17.3
Discharge 20-63 μm (10^3 tonnes/year)	2580	2840	5320 10740
% of total discharge	23.0	27.2	49.6
% of <2 μm discharge	22.0	21.0	56.7
% of 2-20 μm discharge	29.5	21.4	49.1
% of 20-63 μm discharge	24.0	26.4	49.5

loss of sensitivity is a result of the decreasing number of identifiable minerals in the finer grain sizes, and it presents a real problem in the <2 μm fraction where distinctions are difficult to make between even the Columbia River and Oregon Coast Range source areas. In addition, it is impossible to distinguish between sediments derived from the Washington Coast Range, Klamath Mountains, and California Coast Range sources in the <2 μm fraction because of their similar (smectite-poor) compositions. Hayes (1973) identified the chlorites derived from the Klamath Mountains as the IIb polytype, but our data indicate that chlorites derived from the California and Washington Coast Ranges are also IIb polytypes. Therefore, the polytype signature is not a distinctive tracer for chlorites derived from these source areas. As a result, coarser-grained fractions contain the most distinctive signatures, but these tracers are limited by the areal distribution of the sands. Fine-grained sediments, on the other hand, carry less distinctive signatures but have greater areal distributions; any fine-grained tracers which can be developed, therefore, have the potential of describing sediment dispersal over much larger areas. This large-scale applicability provides a major justification for the extensive analyses needed to develop fine-grained sediment tracers.

In summary, this study has defined the distinctive mineral composition of material in the 2-20 μm and <2 μm size fractions derived from the major continental source areas of northern California, Oregon, and Washington, and has showed that single river-bank samples can adequately represent the mineral composition of material carried over a longer time in a given size fraction. Both regional and local changes in mineralogy can be related to changes in drainage basin lithology, and

the grain size characteristics of material derived from each source area can be explained in terms of geologic and geographic factors active in each setting. The grain size of the fluvial material carried in suspension varies with source area so that source area contributions are not constant over the entire size range. Amorphous material is a minor component in the 2-20 μm fraction, but it may comprise 25-50% of the <2 μm material derived from the Washington Coast Range, Klamath Mountains, and California Coast Range. The ability to discriminate between sediment sources on the basis of mineralogy appears to decrease in finer grain sizes as a result of increased compositional homogeneity of the finer sediments. Any source area distinctions which can be made, however, have broad areal applicability due to the regional extent of fine-grained sediment dispersal. Such detailed knowledge of source area composition and variability is necessary before quantitative estimates of source area contributions to offshore sediments and, therefore, sediment budgets, can be made.

PROJECT ACKNOWLEDGEMENTS

The author wishes to thank Mark E. Hower for valuable assistance in sample collection and analysis during this study. Jim Phipps of Grays Harbor (WA.) Community College and Tom Beasley of Oregon State University provided Chehalis River and Columbia River sediment samples, respectively, and D. W. Hubbell and J. L. Glenn of the U.S.G.S. provided unpublished mineral and textural data for Columbia River suspended sediments. Their contributions are gratefully acknowledged. Ken Scheidegger reviewed the manuscript and made valuable suggestions regarding its form and content. This work was funded by the National Science Foundation under grant OCE-7819825 and by the NSF/Ocean Margin Drilling Program under JOI Subcontract 26-81.

CHAPTER II

SEDIMENTOLOGICAL SIGNATURE OF AN EASTERN BOUNDARY UNDERCURRENT AND ITS ROLE IN CONTINENTAL MARGIN SEDIMENTATION

ABSTRACT

Surface sediment samples from 78 cores taken in open slope environments on the Oregon and Washington continental slopes have been analyzed for sediment texture and quantitative mineralogy of the 2-20 μm and <2 μm size fractions. These data have been used to infer dispersal pathways and mechanisms and to compare the role of eastern and western boundary undercurrents in sediment dispersal.

Material derived from all sources within the study area are transported north and northwestward across the margin. Two mechanisms may be active in this dispersal: transport within a weak (<10 cm/sec.) poleward flow along the continental slope and transport to the northwest across the shelf by wind-driven winter currents followed by turbid-layer and fine-grained suspensate transport down the slope. Available data do not allow a distinction between the two processes to be made, and some combination of the two may actually be occurring. Columbia River material in the <2 μm fraction may also be transported southward along the shelf and upper slope by summer surface currents.

The continental slope off Oregon and Washington is subject to large sediment contributions from several proximal sources and the eastern boundary undercurrent is sluggish and variable. Characteristic mineral signatures can only be traced for several hundred kilometers, mean silt grain size does not record current activity, and the relative importance of down-slope and along-slope processes is difficult to assess from bottom sediment data. In contrast, the continental slope and rise of the eastern United States are effectively shielded from

from proximal sediment sources and subject to the vigorous and persistent circulation of the western boundary undercurrent. As a result, along-margin processes dominate sedimentation, characteristic mineral assemblages can be traced for thousands of kilometers, and the mean silt grain size is a sensitive indicator of current velocity. Process-oriented studies within the water column are needed to adequately evaluate the relative roles of along-slope and down-slope transport in sediment dispersal in eastern and western boundary undercurrent systems.

INTRODUCTION

Detailed studies of recent fine-grained terrigenous sediment deposition have not been performed on the Oregon and Washington continental slopes. Previous investigations in the region have concentrated on the continental shelf (Maloney, 1965; Chambers, 1968; White, 1970; Scheidegger et al., 1971; Harlett, 1972; Sternberg and McManus, 1972; Kulm et al., 1975) and deep-sea canyon, channel, fan and abyssal plain systems (Royse, 1964; Russell, 1967; Carlson, 1968; Duncan and Kulm, 1970; Duncan et al., 1970; Griggs and Kulm, 1970; Baker, 1973; Stokke et al., 1977). Each of these studies emphasized either nearshore (continental shelf) deposition or the processes, especially active in submarine canyons, which allow material to bypass the continental slope. While the dominant process within a canyon may be depositional over a long time interval (Kulm and Scheidegger, 1979), these features occupy only a small portion of the slope. Therefore, in order to understand the processes of transport and deposition which influence most of the continental slope, detailed sedimentological studies of open slope environments are needed.

A preliminary study of sedimentation on the Oregon margin, including the continental slope, has been presented by Karlin (1980). The portion of that study which addressed slope sedimentation was based on semiquantitative clay mineral abundances in 37 cores taken at 42.5°, 44°, and 45° to 47° N. He identified five major continental source areas (Washington Coast Range, Columbia River, Oregon Coast Range, Klamath Mountains, and California Coast Range; Figure

Figure II-1. Bathymetry of the Oregon-Washington continental slope and location of the cores used in this study. Contours are in meters. The five major source areas identified by Karlin (1980) are indicated along the coast.

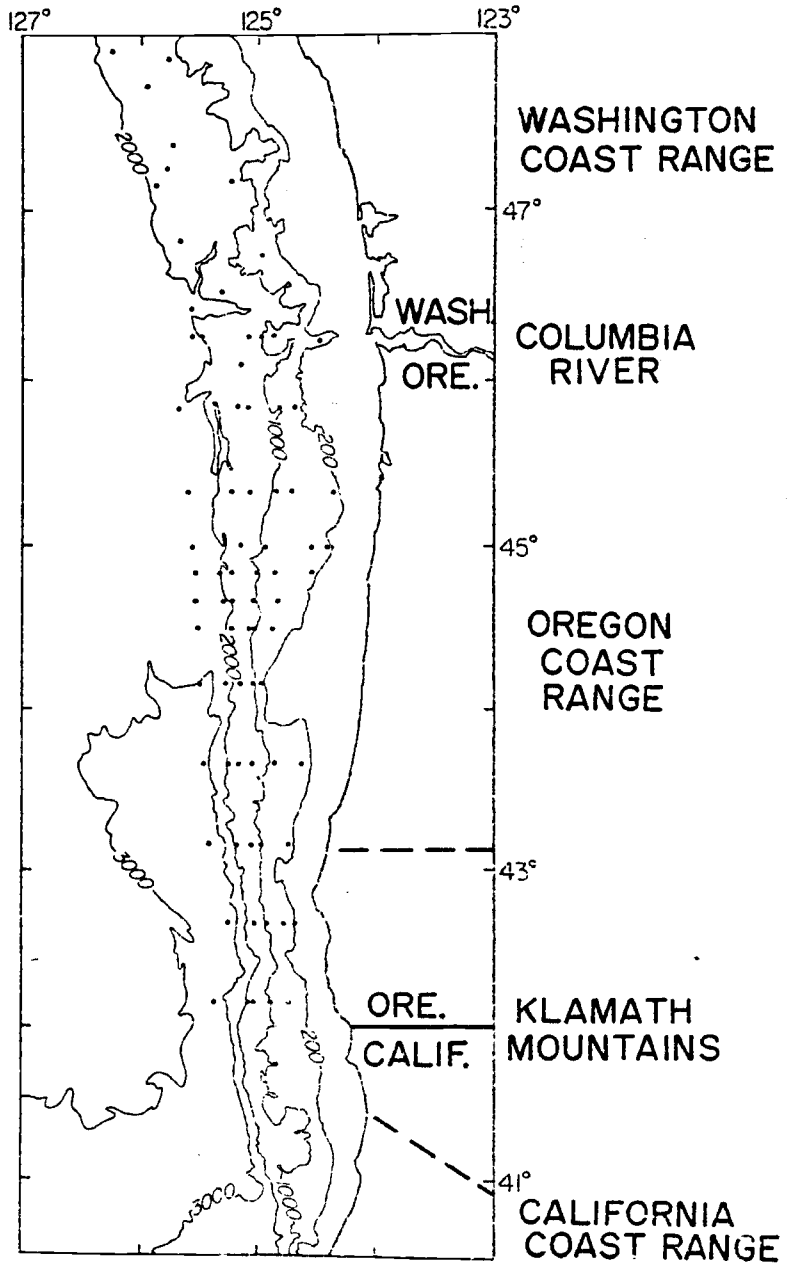
127°
125°
123°
WASHINGTON
COAST RANGE
47°
WASH.
ORE.
COLUMBIA
RIVER
45°
OREGON
COAST
RANGE
43°
ORE.
CALIF.
KLAMATH
MOUNTAINS
41°
CALIFORNIA
COAST RANGE
2000
1000
200
2000
3000
200
3000
1000

Figure II-1

1), and concluded that material derived from the California Coast Range and the Klamath Mountains is carried northward as far as the Washington continental slope. He proposed the California Undercurrent system (Hickey, 1979) as the agent for such transport and suggested that much of the continental slope is influenced by the undercurrent flow. While along-margin transport for long distances has been shown to dominate sedimentary processes under western boundary undercurrents (WBUC; Heezen et al., 1966; Hollister and Heezen, 1972; Zimmerman, 1971, 1972; Tucholke et al., 1973; Tucholke, 1975; Johnson and Damuth, 1979; Camden-Smith et al., 1981), the role of relatively weaker eastern boundary undercurrents in sediment dispersal and deposition has not been demonstrated.

In the present study Karlin's (1980) preliminary model of poleward transport by an eastern boundary undercurrent is tested by examining textural and quantitative mineral abundance data from a set of 78 additional slope cores (Figure 1). Relations between the mineralogy of slope sediments and adjacent continental source areas are rigorously examined to establish the transport patterns and mechanisms effective on the Oregon-Washington continental slope. These data provide evidence for the poleward transport of silts and clays along the margin, but available current and sediment grain size data do not indicate the existence of a well-developed core in the eastern boundary undercurrent. This study demonstrates that the relative importance of a poleward undercurrent along the Oregon-Washington continental slope is also significantly minimized by surface current and downslope processes and by dilution from

several prominent continental sediment sources. This study presents greater insight into the relative importance of eastern and western boundary undercurrents in the transport and deposition of fine-grained sediments along continental margins.

SAMPLING AND METHODS

Sixty large-diameter gravity cores and six piston cores were taken in 12 transects across the Oregon continental slope and these were supplemented with 12 cores taken previously on the Washington slope by University of Washington personnel (Figure 1). All cores were specifically chosen to avoid known submarine canyons and channels. The samples used in this study are from the core tops (0-5 cm.), thereby providing the most recent material available at each site. Following disaggregation in 30% H_2O_2 (buffered to pH 7.0 to preserve carbonates), textural analyses were performed by sieving and pipette techniques (Folk, 1980). The <63 μm fraction of each sample was then separated into <2, 2-20, and 20-63 μm components by repeated settling and decantation. Oriented mounts of the <2 μm fraction were made on pre-pressed Ag backings placed over a gentle suction (Karlin, 1980; Krissek and Scheidegger, 1982a), and the 2-20 μm and the remainder of the <2 μm material were then freeze-dried.

Random powder X-ray diffraction mounts were prepared for the 2-20 μm and <2 μm fraction of each sample using 10% boehmite (AlOOH) as an internal standard according to the technique described in Krissek and Scheidegger (1982a). By using an internal standard and generating calibration curves from known mineral standards, it is possible to calculate quantitative mineral abundances for both phyllosilicate and non-phyllosilicate minerals in any size fraction (Gibbs, 1967b). All slides were solvated with warm ethylene glycol

vapor for 8-12 hours immediately preceding analysis on a Norelco diffractometer. Slides were scanned at a step size of 0.02° 2θ per step and scan time of 3 seconds per step with monochromatic $Cu_{\alpha}K$ radiation. The raw data were smoothed with a 17 point Gaussian algorithm and then plotted on a strip chart recorder. Peak areas were measured with a polar planimeter. For the random mounts, abundances of smectite, chlorite, illite, hornblende, quartz and plagioclase feldspar were quantified using the techniques discussed in Krissek (1982b). Relative abundances of clay minerals were calculated for the oriented mounts by the method of Biscaye (1965), and confirmed that our samples had the same relative composition as those analyzed by previous workers.

For the quantitative determinations, accuracy is estimated to be $\pm$ 5% for smectite, $\pm$ 2% for chlorite and illite, and $\pm$ 1% for quartz and plagioclase feldspar (Krissek and Scheidegger, 1982a; Scheidegger and Krissek, 1982). Precision is estimated to be $\pm$ 15% for smectite, $\pm$ 9% for illite, $\pm$ 3% for chlorite, quartz, and plagioclase, and $\pm$ 1.5% for hornblende. Detection levels are approximately 15% for smectite, 2% for chlorite, illite, and plagioclase, 1% for quartz, and 0.5% for hornblende.

The composition of the plagioclase feldspar was also investigated as a potential sediment tracer using the lattice parameters discussed by Smith (1956). This technique relates the separation (in °2θ) of the (111) and $(\bar{1}\bar{1}1)$ plagioclase peaks to the anorthite/anorthite + albite content of the feldspar for low temperature forms. Although the plagioclase derived from the Columbia River

and the Oregon and Washington Coast Ranges may be slightly less ordered than that from the southern two source areas, this easy and direct analysis provides an additional indicator of plagioclase composition throughout the entire study area.

The <2 μm fraction was examined using Mg and K saturation and differential thermal techniques (Brindley, 1961; Carroll, 1970) to discriminate between smectite, chlorite, and smectite-chlorite intergrades. Representative results are shown in Figure 2; sample 122G is a lower slope core at 45° 20' N and water depth of 1651 m. The similarity of diffractograms from the original and the Mg-saturated samples indicate that the original untreated smectites expand uniformly in the presence of ethylene glycol. The absence of the 17 Å peak in the K-saturated, 105° C. pattern indicates collapse of the smectites under conditions of gentle heating, implying that these components contain little or no chlorite interlayering (Brindley, 1961; Harward, 1969; Carroll, 1970). There is little change in the patterns at higher temperatures (Figure 2), reinforcing the interpretation that the material represented by the 17 Å peak in the untreated samples is a smectite form with little or no chlorite interlayering. In addition, the low intensity of the chlorite (001) peak (14Å) relative to the chlorite (002) peak (7Å) in the K-saturated 105° and 300° C. patterns indicates that chlorites throughout the study area are Fe-rich forms (Brindley, 1961; Carroll, 1970).

Figure II-2. Diffractograms of the 3-13^{o} 2θ range of Mg and K-saturated and heat-treated samples from core 122G. Smectites collapse at 105^{o} C., indicating a relatively pure smectite structure with limited intergraded chlorite.

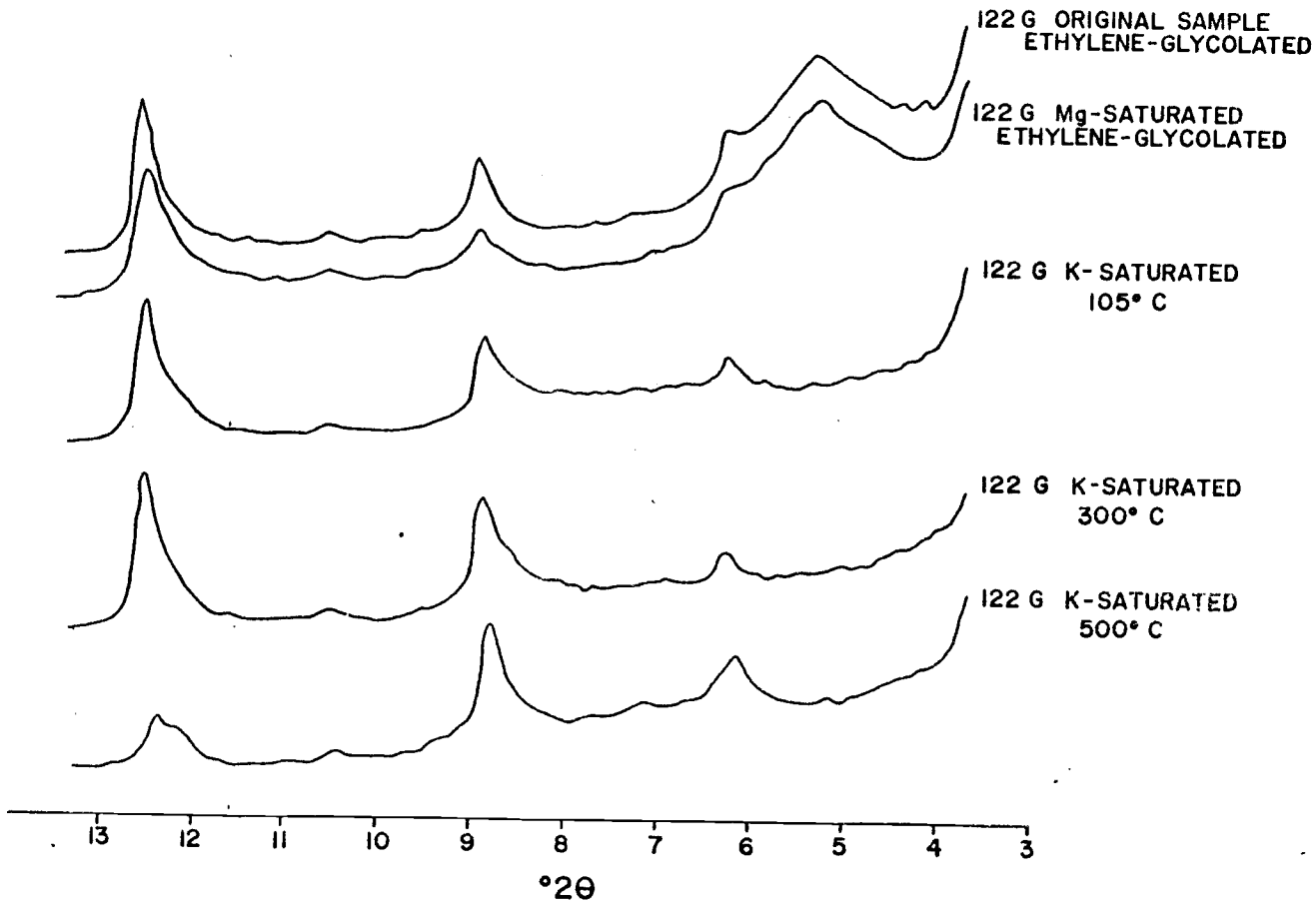
122 G ORIGINAL SAMPLE
ETHYLENE-GLYCOLATED
122 G Mg-SATURATED
ETHYLENE-GLYCOLATED
122 G K-SATURATED
105° C
122 G K-SATURATED
300° C
122 G K-SATURATED
500° C
13
12
11
10
9
8
7
6
5
4
3
°2θ

Figure II-2

DATA AND RESULTS

Sediment Age and Distribution

Despite the fact that all samples used in this study were from core tops, it is still possible that Pleistocene or older deposits were exposed at the surface. To verify that most of the samples are late Holocene in age, the relative abundances of radiolaria and planktonic foraminifera in the <63 μm fraction were used as a biostratigraphic indicator (Duncan, 1968; Barnard, 1978). For deep-sea environments off Oregon, Duncan (1968) established that a change from a foraminifera-rich to a radiolaria-rich assemblage occurred at stratigraphic levels approximately 12,500 ybp in age. The same transition occurred between 11,500 and 5,000 ybp on the Washington slope below 1500 m. (Barnard, 1978). Spigai (1971) investigated the microfossil composition of a suite of cores taken on the southern Oregon slope, and found that radiolaria-rich assemblages occurred in most of the surface sediments. Radiocarbon dating and tephrachronology of these sediments indicated that they were deposited at or after approximately 6600 ybp.

With only three exceptions (all just north of the Columbia River mouth), the samples used in this study have radiolaria/radiolaria + planktonic foraminifera ratios of 0.8 or greater, and 67% of the samples had ratios larger than 0.9. No areally-consistent changes in the ratio occur in either the along-slope or the down-slope directions. Thus, with three exceptions, the assumption that these samples represent middle to late Holocene (i.e., recent) deposits is reasonable.

The combination of numerous structural benches, hills, ridges, and steep escarpments on the Oregon continental slope with along-margin

changes in sediment supply and dispersal result in non-uniform sediment accumulation along the slope of this active margin (Kulm and Scheidegger, 1979). Kulm and Scheidegger (1979) described three types of morphotectonic settings on the slope. The first, which extends from the California border to the Umpqua River, consists of marginal plateaus, benches, and intervening escarpments, and show thin sediment cover on the upper slope and minor sediment ponds behind topographic highs on the lower slope. The second setting, from the Umpqua River to Cascade Head (45°00' N), is a region of steep escarpments and small equidimensional hills and basins with thick, ponded sediments on the upper slope and thin cover on the lower slope. The third setting contains a large structural bench on the upper slope and a series of linear, N-NW trending ridges and intervening basins which form the lower slope from Cascade Head to the southern Washington margin. Sediments in this setting form a thick cover on the broad upper slope with minor ponds deposited in the lower slope basins. Examples of the characteristic topographies and deposits from these three regions are shown in Kulm and Scheidegger (1979).

Sediment Mineralogy

Major patterns of the quantitative mineral abundances in the <2 μm slope sediments are summarized in Figure 3. Smectite abundances >90% are found off the mouth of the Columbia River and extend southward along the upper continental slope (Figure 3a). Major continental smectite sources, the Columbia River and the Oregon Coast Range, only contain 60-75% smectite; therefore, some process or processes must be acting to

Figure II-3. Quantitative mineral abundances in the $<2\,\mu m$ fraction of the slope sediments. Boundaries of the continental source areas are shown, and the values given along the coast are mineral abundances in material derived from each source area (after Krissek, 1982a). The California Coast Range source lies entirely south of 42^{o} N.

a.) Smectite abundance; major source is apparently the Columbia River, with subsequent southward transport during the summer.

b.) Chlorite abundance; major sources are to the south (Klamath Mountains and California Coast Range), with subsequent transport northward.

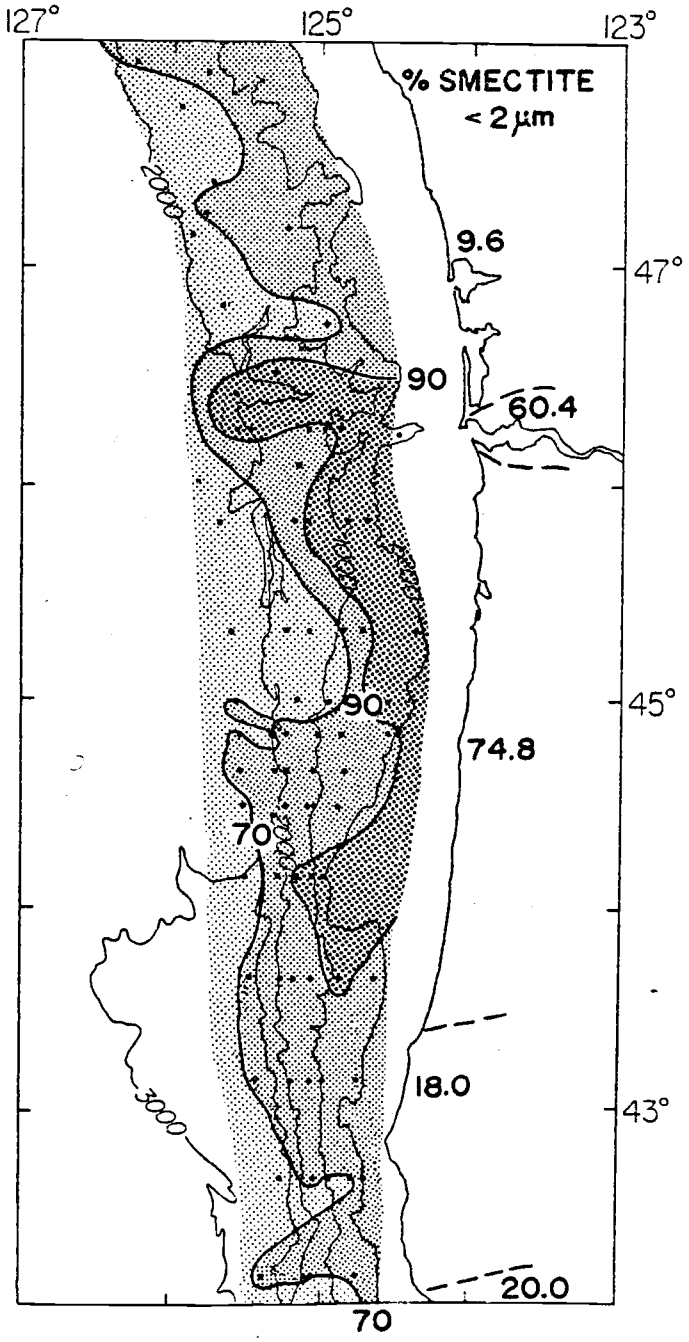
127°
125°
123°
% SMECTITE
< 2 μm
2000
9.6
47°
90
60.4
90
45°
74.8
70
2000
18.0
43°
3000
20.0
70

Figure II-3a.

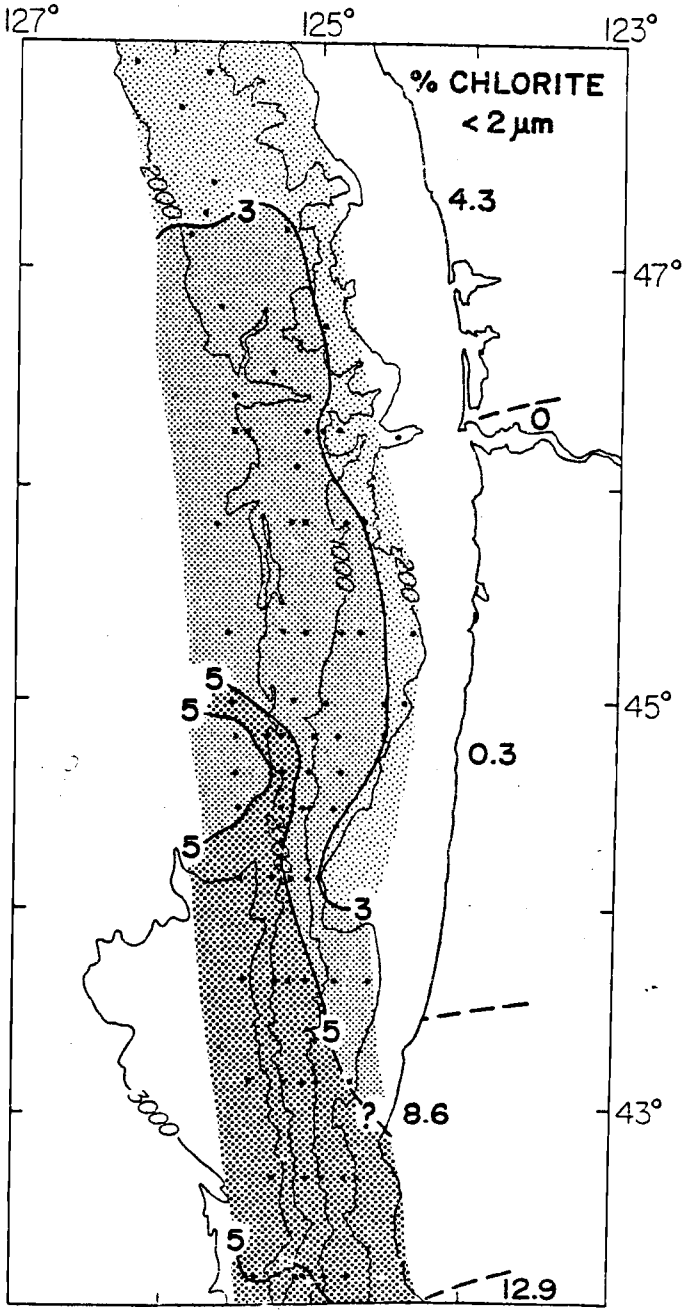
127°
125°
123°
% CHLORITE
< 2 µm
4.3
47°
0
2000
3
2000
2000
5
5
45°
0.3
5
3
5
?
8.6
43°
3000
5
12.9

Figure II-3b.

further enrich the marine sediments in smectite. One possible explanation is that fluvially-derived smectite particles (aggregates) coarser than <2 μm are disaggregated by oceanic water motions, diluting the original <2 μm fluvial material with a pure smectite signal. Because the 2-20 μm sediments derived from the Oregon Coast Range are smectite-rich (Krissek, 1982b), this mechanism appears reasonable for our study area. A second cause of the smectite enrichment may be size-selective transport of the fluvial material (Gibbs, 1967a). However, smectites are concentrated in the finest portion of the sediments (Gibbs, 1967a; Arcaro, 1978) so that they should be transported farthest from their source. Instead, smectite maxima occur near the sources and concentrations decrease offshore, making this mechanism appear unlikely. Finally, local variations in smectite composition can cause errors in the abundances calculated using a single calibration curve (Krissek and Scheidegger, 1982a). Such errors are extremely difficult to eliminate, undoubtedly influence our results to an unknown extent, and may be the major source of uncertainty in the smectite quantification.

While magnitudes differ because of analytical techniques, Karlin's (1980; Figure 3) montmorillonite (smectite) data indicate highest abundances on the entire Washington margin and the Oregon margin north of 44°N and shallower than 500 m. His zone on the Oregon margin corresponds to the smectite-rich region shown by our data (Figure 3a), but our data indicate no corresponding smectite enrichment off Washington. Karlin (1980) analyzed no samples from the Washington continental shelf and his Washington slope samples were located both in and between canyons.

In contrast, our data are limited to non-canyon samples (Figure 1). Both Baker (1973) and Karlin (1980) demonstrated that Washington upper canyon samples are enriched in montmorillonite relative to the rest of the slope. Therefore, Karlin's (1980) montmorillonite-rich zone on the Washington margin may reflect the combined influences of sample location, analytical technique, and extrapolation of slope results onto the Washington continental shelf.

The abundance pattern shown in Figure 3a indicates that smectite dominates the <2 μm mineral assemblage over the entire study area, forming >40% of the finest sediment fraction. Both semiquantitative (Karlin, 1980) and quantitative data indicate zones of smectite enrichment along the upper continental slope north of 44°N and extending downslope directly offshore from the Columbia River. This material may be derived either from the Columbia and transported southward or from the Oregon Coast Range and transported northward and offshore. Neither data set by itself allows a distinction between the two possibilities. The smectite abundance decreases downslope (Figure 3a), perhaps reflecting dilution by material transported northward along the middle to lower slope from the southern source areas as proposed by Karlin (1980). However, our smectite data provide no direct evidence in support of his model.

Chlorite abundances in the <2 μm fraction of the slope sediments (Figure 3b) decrease from south (>5%) to north (<3%); the highest continental chlorite values are found in the Klamath Mountain and California Coast Range source areas. Hays (1973) identified chlorites found offshore from the Klamath Mountains as type IIb polytypes; our data indicate

that the chlorites found on the continental slope throughout the entire study area are type IIb polytypes, similar to material derived from the Klamath Mountains and the California and Washington Coast Ranges (Krissek, 1982b). Although the chlorite abundances shown in Figure 3b seem suspiciously low and the smectite abundances in Figure 3a appear quite high, the results of Mg and K saturation and differential thermal analyses of the <2 μm fraction indicate that the diffraction peaks used for the quantitative mineral estimates do represent only chlorite and smectite components (Figure 2). Chlorite-smectite intergrades do not appear to form a significant portion of the <2 μm fraction.

Because we have no samples at water depths less than 200 m, there is no data control on the location of the 5% contour south of 43° N. Karlin (1980) shows semiquantitative chlorite abundances >50% for the entire margin south of 43°20'N, but five of his nine shelf samples from this region had contents below 50%. Therefore, the exact relationship of the offshore chlorite high to the continental source areas remain unknown. Northward transport of material by some mechanism does appear to influence most of the Oregon continental slope and the Washington slope south of 47°N and deeper than 500-1000 m.

The major features of the mineral abundance patterns for the 2-20 μm fraction are summarized in Figure 4. Smectite was not detected in the 2-20 μm fraction of the marine sediments (though Oregon Coast Range rivers did contain smectite in their 2-20 μm fraction; Krissek, 1982b), the quartz abundance pattern is similar to that exhibited by plagioclase feldspar (Figure 4a), and illite abundances show limited along-margin structure.

Figure II-4. Mineral data in the 2-20 μm fraction of the slope sediments. Source area boundaries are shown and values given along the coast are mineral data for material derived from each source area (after Krissek, 1982a). The California Coast Range source lies entirely south of 42^{o} N.

a.) Feldspar abundances; the major source appears to be the Columbia River, with transport to the northwest.

b.) Separation of the plagioclase (111) and ($1\bar{1}1$) diffraction peaks ($^{o}2\theta$), which is related to the relative albite/anorthite content of the feldspar (Smith, 1956). Plagioclase composition indicates northward transport of material along the margin.

c.) Hornblende abundance; the major source is the Klamath Mountain area, with both downslope and along-margin transport.

d.) Chlorite abundance; the major sources are the Klamath Mountains and the California Coast Range, with subsequent northward transport.

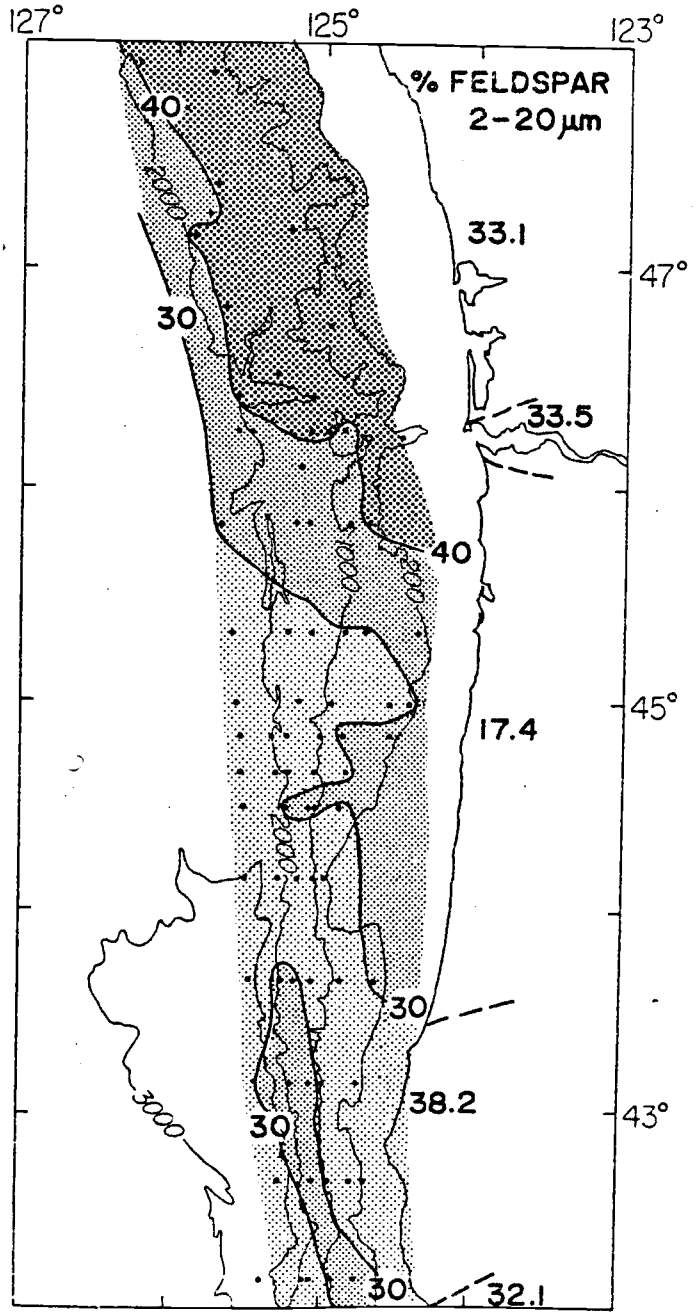
127°
125°
123°
% FELDSPAR
2-20μm
40
1000
30
33.1
47°
33.5
40
2000
1000
45°
17.4
2000
30
38.2
3000
30
43°
30
32.1

Figure II-4a

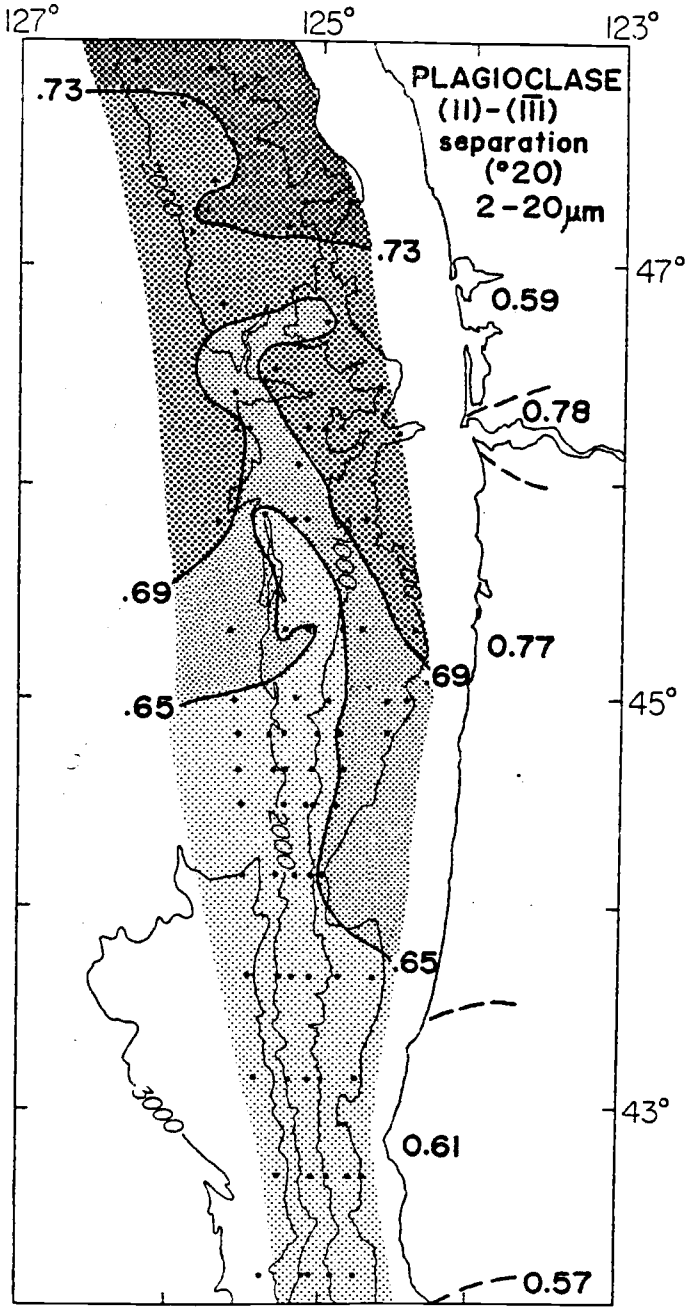
127°
125°
123°
47°
45°
43°
PLAGIOCLASE
(11)-(1̄11)
separation
(°20)
2-20μm
.73
.73
0.59
0.78
.69
0.77
.69
.65
.65
0.61
0.57
1000
2000
3000

Figure II-4b.

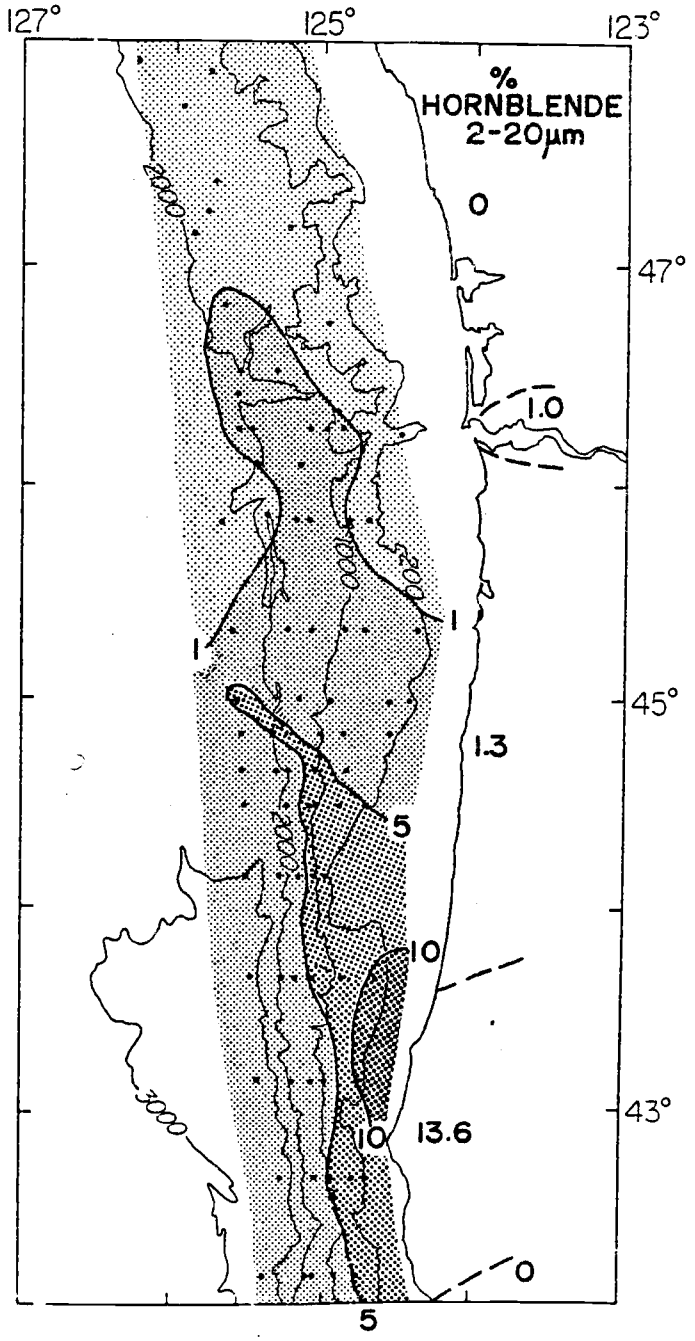
127°
125°
123°
% HORNBLENDE 2-20μm
47°
45°
43°
2000
3000
0
1.0
1
1.3
5
10
13.6
0
5

Figure II-4c.

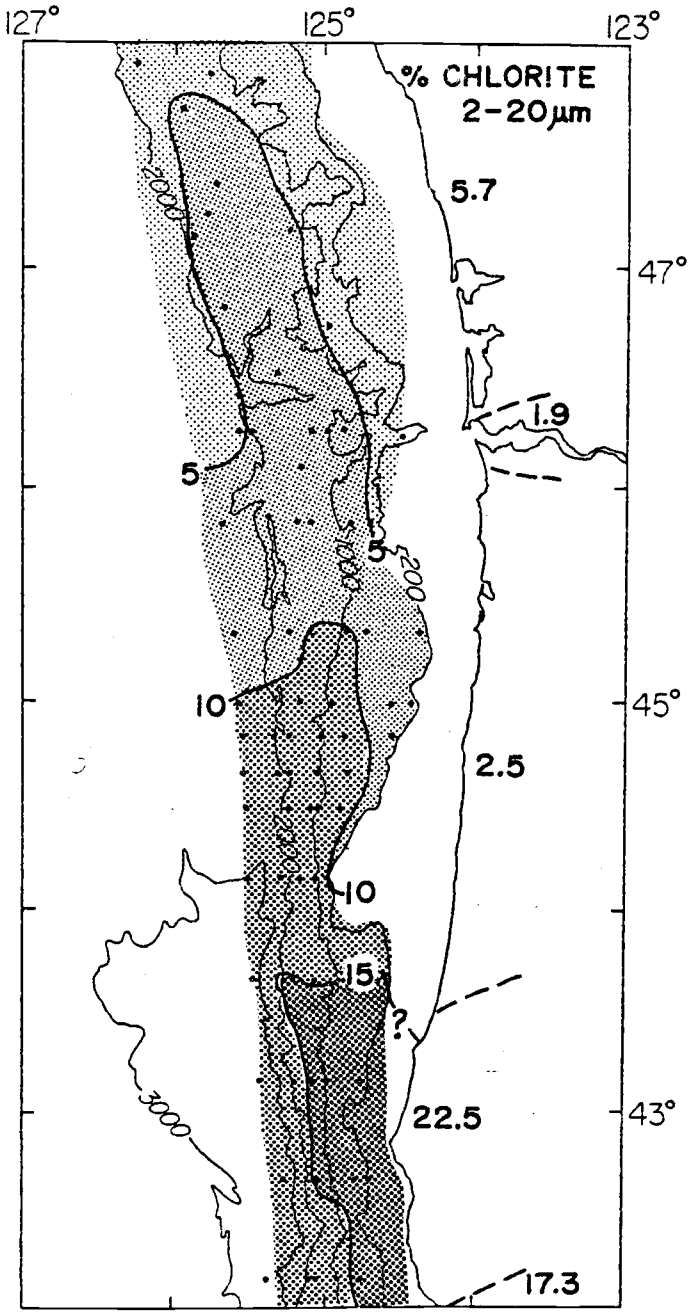
127°
125°
123°
% CHLORITE
2-20μm
5.7
47°
1.9
5
5
2000
1000
200
10
45°
2.5
10
15
?
22.5
43°
3000
17.3

Figure II-4d.

Feldspar contents of the 2-20 μm fraction (Figure 4a) are highest (>40%) on the Washington margin to the north-northwest away from the Columbia River. Slightly lower values (30-40%) occur southward and seaward of this zone, and extend furthest southward along the uppermost continental slope. A zone with contents >30% also trends northward and downslope from the southern boundary of the study area. The plagioclase (111)-($1\bar{1}1$) peak separation increases from south to north (Figure 4b), paralleling a similar trend which occurs in the composition of the continentally-derived plagioclase. This change indicates a shift from relatively albite-rich to relatively more anorthite-rich feldspars from south to north (Smith, 1956). Maximum relative northward transport appears to occur on the middle to lower slope (1500-2000 m), with moderate transport below 2000 m and weakest transport on the upper continental slope. The apparently weak northward transport on the upper slope, however, may reflect dilution either by Columbia River material which is transported southward on the continental shelf and upper slope or by Oregon Coast Range material which is transported offshore and to the northwest. While some northward component of transport does appear to occur on most of the slope, the actual process involved cannot be determined from our sediment data.

Hornblende abundances (Figure 4c) have a maximum (10-15%) in the upper slope samples at 43°-44°N, and decrease both downslope and alongslope to the north. Hornblende-poor samples seaward of this maximum are thought to be strongly diluted by material derived from the California Coast Range (Krissek, 1982a). In agreement with the plagioclase compositional data (Figure 4b), maximum northward transport appears

to occur below approximately 1000 m, but the hornblende distribution pattern also indicates a significant westerly (downslope) component of dispersal, especially close to the Klamath Mountain source area. Chlorite abundances decrease from south to north in the 2-20 μm fraction (Figure 4d) as they do in the <2 μm fraction (Figure 3b), with the southern source areas (Klamath Mountains and California Coast Range) containing relatively high chlorite abundances in their fluvial sediments. All chlorites are type IIb polytypes. As before, however, while northward transport of material appears to influence most of the continental slope, no direct evidence indicates the connection between source area and site of deposition. The dispersal mechanism, therefore, remains open to question, especially in view of the downslope transport which occurs proximal to the continental source areas (Figures 3b, 4c, and 4d).

Sediment Texture

The textural composition, both bulk and fine (<62 μm) fraction, of the slope sediments is summarized in Figure 5. The slope has been divided into four depth ranges, and results from two transects each from the northern (46°20' and 45°50'N.), central (44°40' and 44°30'N.), and southern (43°10' and 42°40'N.) Oregon slope have been averaged within these depth ranges. The data show a general trend of grain size decreasing downslope by a drop in sand content, increase in weight percent in the >9 ϕ (<2 μm) size fraction, and shift of the silt size distribution toward smaller grain size. In an along-margin sense, the sediments become fine-grained from south to north at all depth intervals

Figure II-5. Grain-size frequency distributions of the < 63 μm fraction of slope samples from four water depth ranges. The north, central, and south profiles are averages of data from two transects each. Sand contents are also listed. Sediments become finer-grained both downslope and alongslope from south to north.

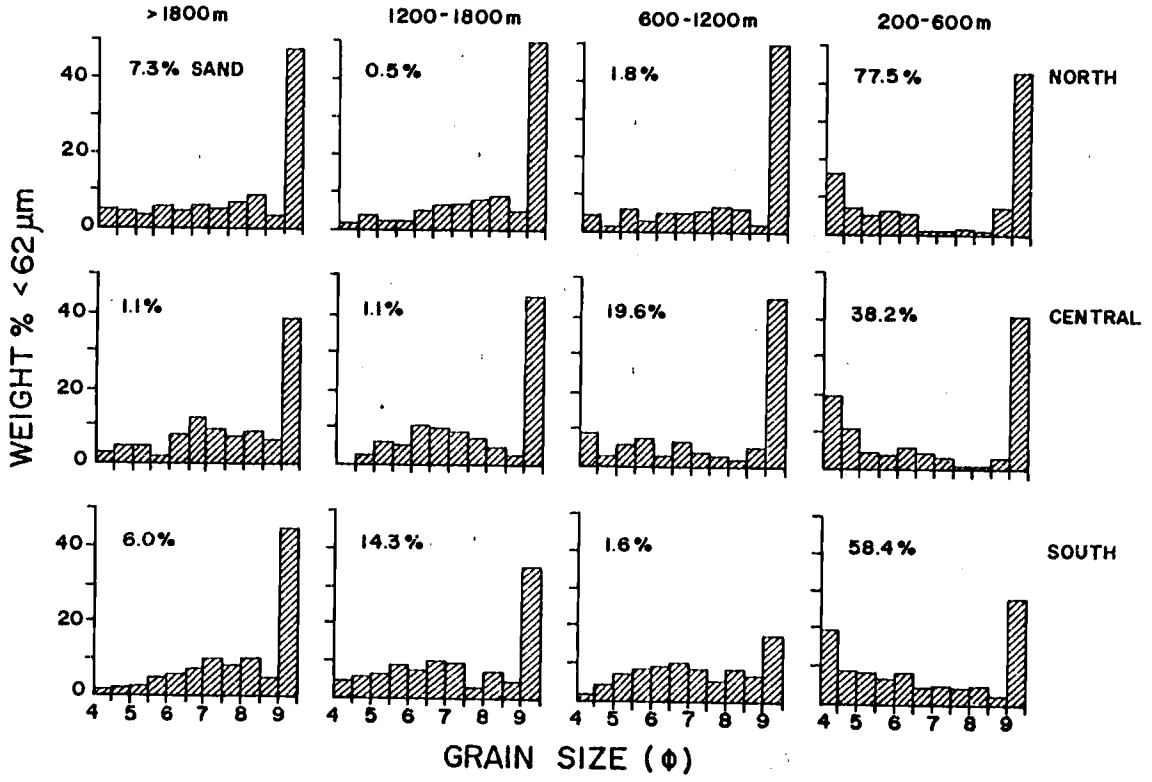
>1800m
1200-1800m
600-1200m
200-600m
7.3% SAND
0.5%
1.8%
77.5%
NORTH
1.1%
1.1%
19.6%
38.2%
CENTRAL
6.0%
14.3%
1.6%
58.4%
SOUTH
WEIGHT % < 62 µm
GRAIN SIZE (Φ)

Figure II-5.

as evidenced by increasing weight percent in the <2 μm (>9 ϕ) fraction and subtle shifts in the silt size distribution toward smaller grain size. The presence of a channel on lower Astoria Fan near the deepest northern samples may indicate that downslope processes dominate deposition in this region and explain the relatively coarse nature of these samples. The regional pattern of decreasing grain size from south to north is overlain with much local variability. No distinctive textural signature appears consistently along the slope at any depth to indicate the presence or effects of an eastern boundary undercurrent. Instead, the local and regional variations may reflect the input of relatively silt-rich material from the southern source areas and the clay-rich nature of Columbia River sediments (Krissek, 1982b), combined with the localized influence of the other continental sources. In addition, the relatively weak nature of an eastern boundary undercurrent may limit its capacity to distinctly modify sediments derived from many proximal source areas.

DISCUSSION

Sediment Dispersal and the Poleward Undercurrent

The data presented herein indicate that northward transport of material does occur along the Oregon and Washington continental margin. However, no evidence directly indicates the processes involved in such transport. One mechanism, proposed by Karlin (1980), is that a northward-flowing undercurrent influences sedimentation on most of the continental slope, carrying material into the system from the southerly (Klamath Mountain and California Coast Range) source areas. Another mechanism, proposed by Spigai (1971) from a study limited to the continental margin off southern Oregon, emphasizes the importance of more direct downslope transport of silts and clays during winter in low-density turbid layers and fine-particle suspensate. These bottom turbid layers are thought to be generated predominantly by long-period swell on the continental shelf, and then move north and west across the shelf, past the shelf break, and down the slope in both canyon and open slope environments. In order to assess the importance of these two mechanisms to slope sediment dispersal and deposition, the data presented above must be examined in light of present knowledge of the physical oceanography and seasonality of sediment input on the Oregon-Washington continental margin.

Maximum discharge from the Columbia River occurs during the late spring and early summer (33-50% of the total annual discharge is released in April, May, and June; Whetten et al., 1969) because

the discharge is derived from mountain snowmelt. Peak discharges of streams in the other source areas occur as a result of winter storms, and are concentrated in December, January, and February. However, because of the influence of storm runoff on tributaries of the lower Columbia, its winter sediment discharge is not negligible.

The oceanographic conditions of the region also vary seasonally. In spring (March to June), currents flow southward across the entire continental shelf at all depths, but speeds at the surface are about twice those near the bottom (Huyer et al., 1975). From July to October, surface flow is southward and deep flow is northward; a southward coastal jet occurs 12-18 km offshore while the deep northward velocity increases with distance offshore. Mean monthly surface speeds are on the order of 20-40 cm/sec. (Huyer et al., 1975). In fall and winter (October to March), the current is to the north at all points across the shelf and speeds are relatively independent of depth, with maxima of approximately 20 cm/sec. (Huyer et al., 1975).

Calculations using dynamic topographies and the geostrophic assumption indicate northward subsurface flow, termed the California Undercurrent (Hickey, 1979), over the continental slope in May and November (Ingraham, 1967), September (Reed and Halpern, 1973), September and October (Reed and Halpern, 1976), and July (Halpern et al., 1978). The calculated velocities are generally less than 10 cm/sec., and the strongest flow is commonly located inshore of the 2000 m. isobath, i.e., overlying the continental slope.

Short-term direct measurements of near-bottom current speeds in water depths of 725 m to 1700 m off central Oregon range from 5-20 cm/sec with maxima from 20 to 40 cm/sec (Korgen et al., 1970). The speed shows a systematic and significant increase with decreasing depth. However, neither the current directions nor the time of this study are given by Korgen et al. (1970). Measurements on the Oregon and Washington slope have been interpreted as indicating the presence of a relatively high-speed core within the undercurrent from May through September (Huyer and Smith, 1976), with a maximum speed of 16 cm/sec. (averaged over six weeks). Data on the lateral and vertical extent of the flow are limited, but the core appears to migrate seasonally, shoaling from deeper than 400 m in May to the shelf edge (200 m) by June (Huyer and Smith, 1976). However, more recent direct current measurements from the Oregon and Washington continental slope (A. Huyer, 1982, personal communication) show weak mean southward flow along the bottom at water depths below 700 m during the period 1 February to 31 March 1978. During the interval from 25 May to 10 July 1978, mean currents along the bottom were to the north, with speeds of >5 cm/sec. above 500 m, 2-5 cm/sec between 500 m and 700 m, and <2 cm/sec. below 700 m water depth. In summer, northward subsurface flow on the continental slope is well-documented for the spring and summer seasons, but available data indicate weak subsurface flow over the slope during the winter. Inter-annual variability in the winter flow regime, however, is unknown.

In light of these most recent current measurements, the role of the poleward undercurrent in the northward transport of material

derived from the southern source areas (Klamath Mountains and California Coast Range) during their peak winter discharge appears open to question. If the deep-water flow is indeed southward at this time, then northward dispersal of material is not occurring within the poleward undercurrent because the poleward undercurrent does not exist! The wind-driven surface currents and associated turbid layers proposed by Spigai (1971) must then dominate the transport activity. Such turbid layers and fine-grained suspensates may act as the near-shore and shelf-break sources for horizontally-advected, intermediate-depth nepheloid layers observed off Oregon and Washington in October and November (Pak et al., 1980). Because wind-driven northerly surface currents exist over the entire length of the Oregon-Washington shelf during the winter (Hickey, 1979), their activity could influence material derived from all source areas. In addition, any relatively coarse-grained components brought out of the Columbia during its summer discharge and temporarily deposited near its mouth can be resuspended by the long-period winter storm waves and transported north-northwesterly across the margin (Sternberg and McManus, 1972). Such a sequence of episodic transport events would produce the pattern exhibited by the feldspar abundance of the 2-20 μm fraction (Figure 4a).

Inter-annual variability in the deep water flow over the slope is unknown. If the flow is actually northward during most winters, then these data do not allow distinction between transport within the undercurrent and transport across the shelf in turbid layers followed by downslope processes. Under these conditions, some combination of the two transport mechanisms may cause sediment dispersal to the north-

northwest, as exhibited by the chlorite and hornblende abundance patterns (Figures 3b, 4c, and 4d). Karlin (1980) does not discuss how the poleward undercurrent obtains its sediment load; the model proposed by Spigai (1971) provides a mechanism for the introduction of such material to the undercurrent which is consistent with both the winter current pattern and the bottom sediment data.

During the late spring and early summer, circulation is southward across the entire shelf (Huyer et al., 1975). As a result, the Columbia River effluent at its time of peak discharge forms a plume in the surface waters which has been traced using temperature, salinity, and light scattering (Pak et al., 1970). This plume moves to the south-southwest, so that at 44°40'N. its axis lies 80 km off the coast (40 km seaward of the shelf break). The axis can be traced for 100 km by its particle content (McCave, 1979).

Since the Columbia River is the only source with a spring/summer discharge peak, only material derived from the Columbia should show the effect of southward transport within the surface waters. In this case, the strength and location of the poleward undercurrent has limited influence on sediment dispersal because the Columbia River effluent generally remains confined to the wind-driven upper 20-30 m of the water column (Pak et al., 1970). The zone of high (>90%) smectite abundance along the Oregon upper continental slope (Figure 3a) lies beneath the summer position of the Columbia River plume; however, our data do not eliminate the Oregon Coast Range as a source of these smectites, implying winter discharge and subsequent northwesterly transport by wind-driven surface currents. On the basis of his

suspended sediment budget calculations, Karlin (1980) estimated that the Columbia River contributes three times as much material as the Oregon Coast Range, but he was also unable to distinguish the source of these smectites. If these smectites are derived from the Columbia River, the poleward undercurrent may limit their southern-most occurrence by acting on particles settling from the surface waters to the sediment-water interface. In such a case, particles with the lowest settling velocities would be transported furthest back to the north during their transit time through the water column, allowing the poleward undercurrent to exert a secondary control on the southern limit of Columbia River sediment distribution.

Relative Importance of Eastern and Western Boundary Undercurrents on Sediment Dispersal

Investigations of the sediments beneath western boundary undercurrents (WBUC), especially those of the eastern United States continental slope and rise, have identified mineralogic (Heezen et al., 1966; Hollister and Heezen, 1972; Zimmerman, 1972; Klasik and Pilkey, 1975; Tucholke, 1975), palynmorphic (Needham, 1969; Habib, 1972), and textural (Ledbetter, 1979; Ledbetter and Ellwood, 1980; Ledbetter et al., 1981; Bulfinch and Ledbetter, 1981) characteristics which reflect the predominant role of the WBUC in sediment dispersal and deposition. Low fluvial suspended sediment discharge, trapping of fine-grained sediments within the coastal estuaries, and the location of the strong Gulf Stream current between the coast and the continental slope/rise limit the amount of terrigenous material which moves

directly downslope from the continental source areas (Heezen et al., 1966; Zimmerman, 1972). This effectively reduces the number of sources which contribute to the slope/rise deposits, making it easier to preserve and recognize distinctive mineral signatures in the sediments. The major sources of material for sediments beneath the WBUC in the last glacial period were the Triassic and Paleozoic redbeds of the Gulf of St. Lawrence (Heezen et al., 1966), while Holocene deposits appear to be derived from Labrador Sea sediments (Zimmerman, 1972). These sediments can be traced for distances of 1000-3000 km by their mineralogy alone. In addition, the WBUC itself is a strong and persistent feature (Zimmerman, 1971, 1972; Hollister and Heezen, 1972; Stanley et al., 1981), with average velocities from long-term near-bottom current meter moorings of 10-20 cm/sec. and maximum values of 40 cm/sec. or greater (Stanley et al., 1981). This vigorous circulation winnows the underlying sediments, so that coarsening of the mean silt grain size in a transect of samples across the WBUC has been used to locate its high velocity core (Bulfinch and Ledbetter, 1981).

If the poleward undercurrent is the dominant process in the northward transport of material along the Oregon-Washington slope, it should also leave a distinctive signature in the underlying sediments. The mineral data presented above do not provide such a distinctive signature because of the presence of several large sediment sources within the study area and their apparent influence on adjacent slope deposits. Pacific Northwest estuaries do not trap fine-grained fluvial sediments (Peterson et al., 1982), and winter circulation on the shelf (during peak fluvial discharge) may transport the resultant turbid layers and

fine-grained suspensates to the shelf break (Spigai, 1971). As a result, the slope is not isolated from proximal source areas, and distinctive mineral signatures can only be traced for several hundred kilometers along the margin. The undercurrent itself is also relatively weak, with average velocities of approximately 2-7 cm/sec. and maximum of 16 cm/sec. (Huyer and Smith, 1976; A. Huyer, 1982, unpublished data). Because of both the weak circulation and grain size variability between sources (Krissek, 1982b), mean silt grain size shows no pattern along the Oregon continental slope which indicates the position of the undercurrent or any high velocity "core" (Figure 6). The location of the poleward undercurrent, if it is indeed the major transport mechanism for the northward dispersal of material, is therefore not recorded either texturally or mineralogically in the underlying sediments.

Although the sediment mineralogy indicates that northward transport influences the entire slope, our data do not allow distinction between material transported by the poleward undercurrent and that carried across the shelf and downslope in turbid layers and fine-grained suspensate. The lack of a distinct record of along-margin flow beneath the eastern boundary undercurrent, however, implies that it plays a less dominant role in sediment dispersal than a western boundary undercurrent. Further fieldwork is needed to more clearly outline the processes involved in sediment transport within our study area. The behavior of the poleward undercurrent during the winter must be studied more extensively, and suspended particulate and sediment trap samples from the continental shelf and slope waters must be obtained and analyzed. Only such process-oriented studies will allow the relative

Figure II-6. Mean silt grain size plotted against water depth for six transects (two each from the northern, central, and southern Oregon slope) across the slope. No recognizable pattern of sediment coarsening occurs at depth on the slope to indicate the location of a high-speed "core" of the eastern boundary undercurrent.

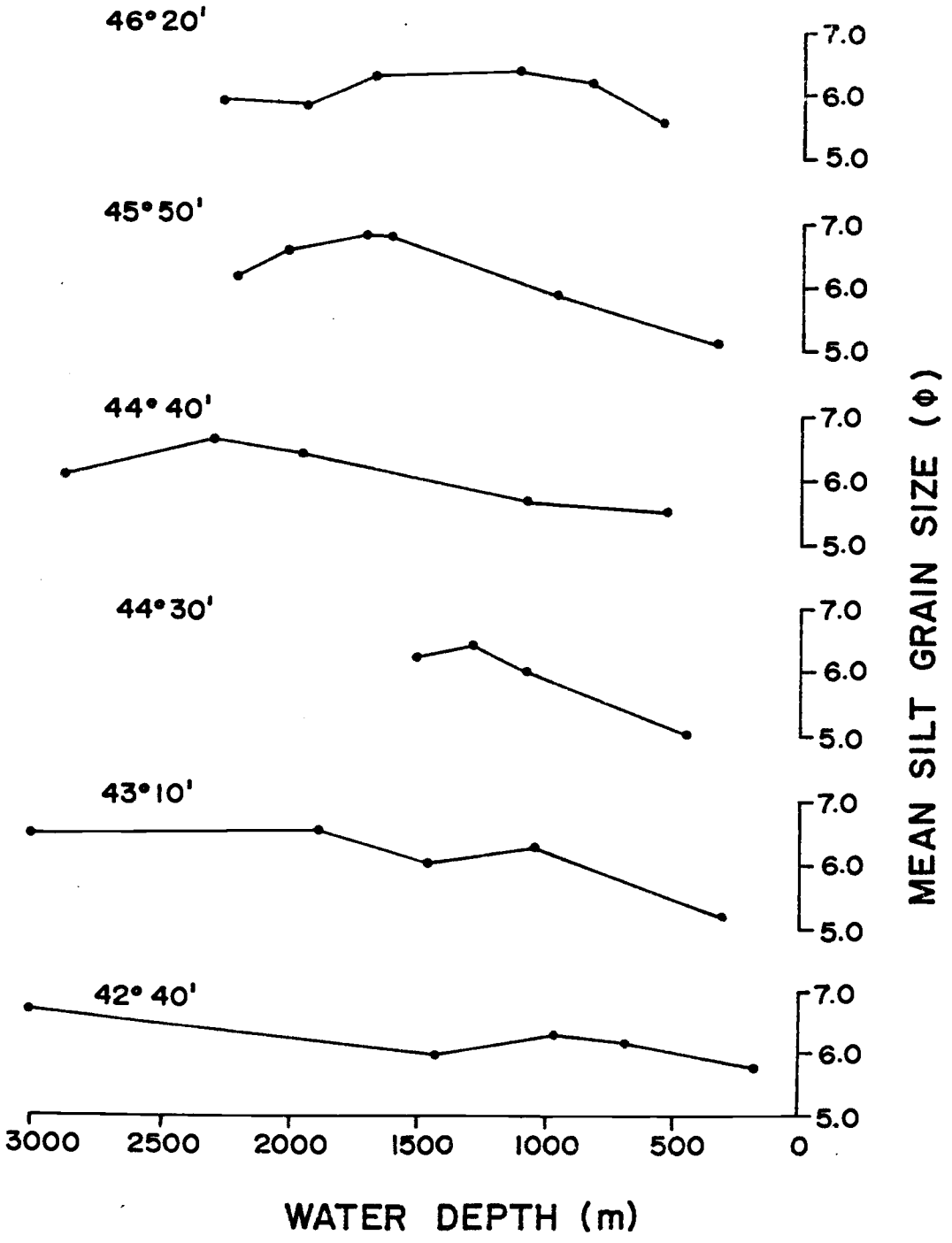
46°20'
45°50'
44°40'
44°30'
43°10'
42°40'
7.0
6.0
5.0
MEAN SILT GRAIN SIZE (φ)
3000
2500
2000
1500
1000
500
0
WATER DEPTH (m)

Figure II-6.

and seasonal importance of along-margin vs. down-slope sediment transport to be determined within an eastern boundary undercurrent system.

PROJECT ACKNOWLEDGEMENTS

The authors wish to thank Mark E. Hower for assistance in sample collection and analysis. The officers and crew of the R/V WECOMA, students from the marine technician program at Clatsop (OR.) Community College, Alan Federman, and Peter Kalk provided able assistance during the collection of the cores used in this study. Vern Kulm and Ross Heath provided thoughtful reviews of the manuscript. This study was funded by the National Science Foundation under grant OCE-7819825 and by the NSF/Ocean Margin Drilling Program under JOI Subcontract 26-81.

CHAPTER III

CONTINENTAL SOURCE AREA CONTRIBUTIONS TO FINE-GRAINED SEDIMENTS ON THE OREGON AND WASHINGTON CONTINENTAL SLOPE AS CALCULATED BY LINEAR PROGRAMMING

ABSTRACT

Chemical and quantitative mineral abundance data for the 2-20 μm and the <2 μm fractions of 78 samples from the Oregon-Washington continental slope have been modelled using linear programming to estimate sediment contributions from continental source areas. In the 2-20 μm fraction, the mineral data distinguish three source areas while the chemical data define only two. Results from the two data sets indicate similar patterns and magnitudes of source area influence on the continental margin. In the <2 μm fraction, the mineral results indicate very high Columbia River influence on the entire margin and the chemical results do not agree with single mineral abundance patterns. The difficulties with the calculation in the <2 μm fraction may be caused by the uniform nature of the <2 μm data. Both sets of results for the <2 μm fraction are therefore considered of limited usefulness.

The contributions are used to construct a sediment budget for 2-20 μm-sized sediments on the continental slope. The slope sediments contain approximately 47% Columbia River, 32% Klamath Mountain, and 21% California Coast Range material. Approximately 25-50% of the Columbia River, 29-46% of the Klamath Mountain, and 7-12% of the California Coast Range annual suspended sediment input is retained on the slope, indicating that the slope acts as a more effective trap of 2-20 μm material from proximal than distal source areas. This study also demonstrates the importance of multiple sediment sources and sediment mixing in the formation of hemipelagic sediments on a continental margin.

INTRODUCTION

Past studies of fine-grained sediment dispersal in marine environments have benerally inferred the relative importance of multiple source areas on the basis of the abundance of single minerals (especially the clay minerals smectite, chlorite, illite, and kaolinite; Biscaye, 1965; Griffin et al., 1968; Kolla and Biscaye, 1973; Kolla et al., 1976; Pinet and Morgan, 1979; Griggs and Hein, 1980; Karlin, 1980). However, the proposed contributions cannot be quantified by such a univariate approach, particularly if a sedimentary deposit receives contributions from two or more sources. Heath and Dymond (1977) applied normative analysis to a data set of elemental abundances from deep-sea sediment samples in order to describe the sediments as mixtures of hydrothermal, detrital, hydrogenous, and biogenous material end-members. Dymond and Eklund (1978) used a linear programming solution of elemental abundances to estimate constituent abundances in metalliferous sediments. Heath and Pisias (1979) also used linear programming to convert X-ray diffraction analysis results to mineral abundances using talc as an internal standard. Cobler and Dymond (1980), Dymond et al. (1980), Dymond (1981), and Heath and Dymond (1981) have continued to expand the application of linear programming to deep-sea chemical data, and Heath and Dymond (1981) and Leinen and Pisias (1982) have incorporated Q-mode factor analysis as an objective technique for the determination of end-member compositions from the data set.

The dispersal of hemipelagic sediments on the Oregon and Washington continental slope has been discussed previously in a qualitative manner by Russell (1967), Duncan et al. (1970), Spigai (1971),

Olmstead (1972), Baker (1973), Karlin (1980), and Krissek and Scheidegger (1982b). Only the work by Krissek and Scheidegger (1982b), however, has involved both analyses of material coarser than 2 μm and the use of quantitative X-ray diffraction techniques (Gibbs, 1967b). The first point is important because particles in the 2-20 μm size range form approximately 40% of the hemipelagic surface sediments on the continental slope; the second is important because only quantitative mineral abundances can be compared with other absolute (e.g., geochemical) data from the same samples (Heath and Pisias, 1979; Krissek and Scheidegger, 1982a).

On the basis of their recent work, Karlin (1980) and Krissek and Scheidegger (1982b) concluded that the major continental sources of sediments found on the Oregon-Washington continental slope are the California Coast Range, Klamath Mountains, and the Columbia River (Figure 1). Both studies indicated that material derived from the southerly sources is transported northward on the margin for distances of hundreds of kilometers. While Karlin (1980) emphasized the role of a poleward undercurrent, Krissek and Scheidegger (1982b) concluded that the transport could be attributed to either the poleward undercurrent, wind-driven winter circulation on the continental shelf and subsequent downslope transport of turbid layers (Spigai, 1971), or a combination of the two. In addition, it is known that Columbia River sediments in the <2 μm fraction are transported southward along the margin by surface water flow during spring and early summer (Pak et al., 1970; Karlin, 1980; Krissek and Scheidegger, 1982b). Krissek (1982b) demonstrated that fluvial sediments derived from each of these source areas have recognizable mineral signatures in the 2-20 μm size

Figure III-1. Bathymetry of the Oregon-Washington continental slope and location of the samples used in this study. Contours are in meters. The location of the major continental source areas of the Pacific Northwest is shown.

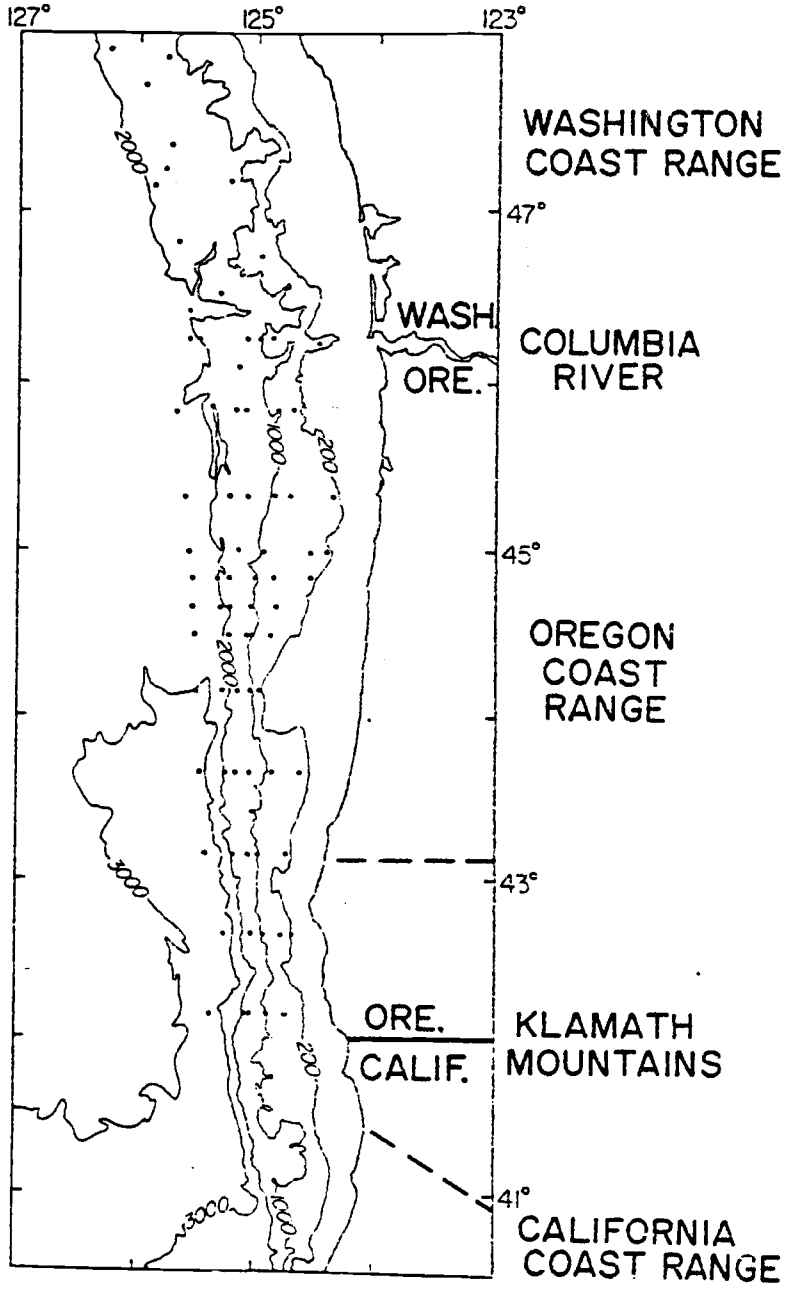
127°
125°
123°
WASHINGTON
COAST RANGE
47°
WASH.
ORE.
COLUMBIA
RIVER
45°
OREGON
COAST
RANGE
43°
ORE.
CALIF.
KLAMATH
MOUNTAINS
41°
CALIFORNIA
COAST RANGE
2000
3000
200

Figure III-1

fraction, but a distinction in the <2 μm fraction can only be made between the northern (Columbia River) and the southern (Klamath Mountain + California Coast Range) sources. The quantitative mineral data used by Krissek (1982b) and Krissek and Scheidegger (1982b) present an excellent opportunity for the application of the linear programming technique to continental margin sediments.

The application of linear programming to quantitative mineral and elemental abundances from each sample makes it possible to uniquely address several basic questions related to fine-grained sedimentation in the marine environment. First, the effects of mixing sediment derived from several source areas on the formation of hemipelagic sediments are investigated and found to be especially important in regions of the slope away from a major source. Second, the mineral and chemical data are modelled independently, and their results indicate that the mineral data set provides more distinctive sediment tracers. Because of the relatively uniform composition of the <2 μm fraction, this study also provides a test of the response of the technique to subtle compositional differences, and suggests that such modelling has limited usefulness under these constraints. Finally, the source area contributions calculated during the modelling are used to construct a sediment budget for the slope. This budget indicates that proximal sources contribute more sediment to the slope than distal sources, and that the slope traps a higher proportion of the material discharged each year from proximal than from distal sources.

SAMPLING AND ANALYTICAL METHODS

Surface sediment samples from 78 cores taken on the Oregon and Washington continental slope were used in this study (Figure 1). Samples from 14 streams entering the Pacific Ocean were used to characterize the mineral composition of material derived from the three major continental source areas. Because of the greater time involved in chemical analyses, only six of these stream samples were used to characterize the chemical composition of the fluvial sediments. Because these six streams (Eel and Mad Rivers, Redwood Creek, Klamath, Rogue, and Columbia Rivers) carry approximately 88% of the total annual suspended sediment discharged from the three major source areas and approximately 80% of the total annual sediment discharged from the entire Pacific Northwest (Karlin, 1980), I am confident that these samples are representative of the material entering the Pacific Ocean within the study area.

Samples were disaggregated and size-separated into >63, 20-63, 2-20, and <2 μm fractions using standard techniques (Krissek, 1982b; Krissek and Scheidegger, 1982b). The 2-20 μm and < 2 μm size fractions were freeze-dried, and sub-samples of each were analyzed using a quantitative X-ray diffraction technique (Gibbs, 1967b). Results were presented by Krissek (1982b) for the fluvial samples and by Krissek and Scheidegger (1982b) for the marine samples. Elemental abundances of Si, Al, Fe, Ca, Na, K, Mg, Ti, Ba, Sr, Cu, and Mn were determined by atomic absorption spectrophotometry and colorimetric techniques (Krissek et al., 1980).

End-member compositions, representing the material derived from

each source area for the four data sets (2-20 μm mineral, 2-20 μm chemical, <2 μm mineral, <2 μm chemical), were calculated using a discharge-weighted approach (Krissek, 1982b). Mineral data from 14 streams and chemical data from six streams were used in constructing the end-members. Annual suspended sediment discharge values were taken from Karlin (1980).

The end-member compositions were then used in linear mixing equations which include the weight fractions of each end-member as unknowns. Linear programming was used to calculate the weight fractions, which estimate source area contributions to the slope sediments. This technique is applicable when the system can be expressed as an overdetermined series of simultaneous equations (i.e., the number of individual mineral or chemical abundances is equal to or greater than the number of source areas). The general form for each equation is:

$$\%M_S = \%M_{CR}(X_{CR}) + \%M_{KM}(X_{KM}) + \%M_{CCR}(X_{CCR})$$

where $\%M_S$ is the mineral or element abundance in the slope sample,

$\%M_{CR}$, $\%M_{KM}$, $\%M_{CCR}$ are the mineral or element abundance in the Columbia River, Klamath Mountain, and California Coast Range end-members, respectively.

and X_{CR}, X_{KM}, X_{CCR} are the weight fraction of the sediment contributed by the respective source areas.

Five such equations were used for the mineral calculations and six equations were used for the chemical data because Q mode factor analysis of the mineral and chemical abundances indicated that five

minerals and six elements accounted for most of the variance in the data sets.

In a three end-member system, each combination of three equations from the five or six that are available provides a unique solution. Therefore, criteria must be provided for the selection of a "best" solution. In the present study, two criteria were established: 1) all contributions must be non-negative, since negative contributions have no physical interpretation; and 2) the "best" solution is the one which minimizes the residual (i.e., the sum, for all minerals or elements, of the absolute value of the difference between the calculated and the known abundance).

As discussed by Heath and Pisias (1979), a major unknown in linear programming is the "stability" of the calculated contributions, i.e., how the contributions respond to changes in the initial abundance data. If the contributions change rapidly with small variations in the initial data, then the modelling results must be viewed with caution. If the contributions change only slightly with small fluctuations in the initial data, then the results can be viewed with greater confidence. Because linear programming is a modelling and not a truly statistical technique, confidence intervals commonly are not assigned to the calculated contributions. The residual for these calculations (i.e., the portion of the initial data unaccounted for by the modelled composition) ranges from 10% to 15%. Therefore, I roughly estimate that the uncertainty associated with the calculated contributions is ±15% (absolute). The uniformity of the chemical data

may cause larger uncertainties for those results, especially in the <2 μm fraction. Changes in end-member compositions away from each source area due to size-selective transport (Gibbs, 1967a; Arcaro, 1978) may also be a major source of error in the calculated contributions.

DATA AND RESULTS

THE 2-20 μm FRACTION

Mineral end-members (Columbia River, Klamath Mountains, and California Coast Range) for the 2-20 μm fraction are presented in Figure 2 (Krissek, 1982b). Material derived from the Columbia is rich in plagioclase feldspar, illite, and quartz, while California Coast Range sediments also contain chlorite; Klamath Mountain detritus includes a distinctive hornblende component.

The calculated contributions are mapped in Figure 3. The Columbia River contribution (Figure 3a) is largest (>75%) to the north-northwest away from its mouth, with a weaker contribution southward on the Oregon margin. The southward influence has its maximum extent along the uppermost slope. The Klamath Mountain contribution (Figure 3b) is strongest (>75%) immediately offshore from this source region (compare with Figure 1), and decreases both downslope and alongslope. The California Coast Range contribution (Figure 3c) is strongest (generally 25-50%) in a lobe-like feature extending northward along the middle to lower slope as far as 46.5° N., with slightly lower contributions outside this feature.

The abundance patterns of plagioclase and hornblende in the 2-20 μm fraction are shown in Figure 4 (Krissek and Scheidegger, 1982b) for comparison with the linear programming results. The Columbia River is the major plagioclase source (Figure 4a) and plagioclase shows a large-scale dispersal pattern to the northwest similar to that exhibited in Figure 3a. South of 46° N., however, the linear programming results provide a clearer and more detailed picture of

Figure III-2. Mineral composition of the discharge-weighted end-members in the 2-20 μm size fraction (from Krissek, 1982b). The California Coast Range material is chlorite-rich, and the Klamath Mountain sediments contain a distinctive hornblende signal.

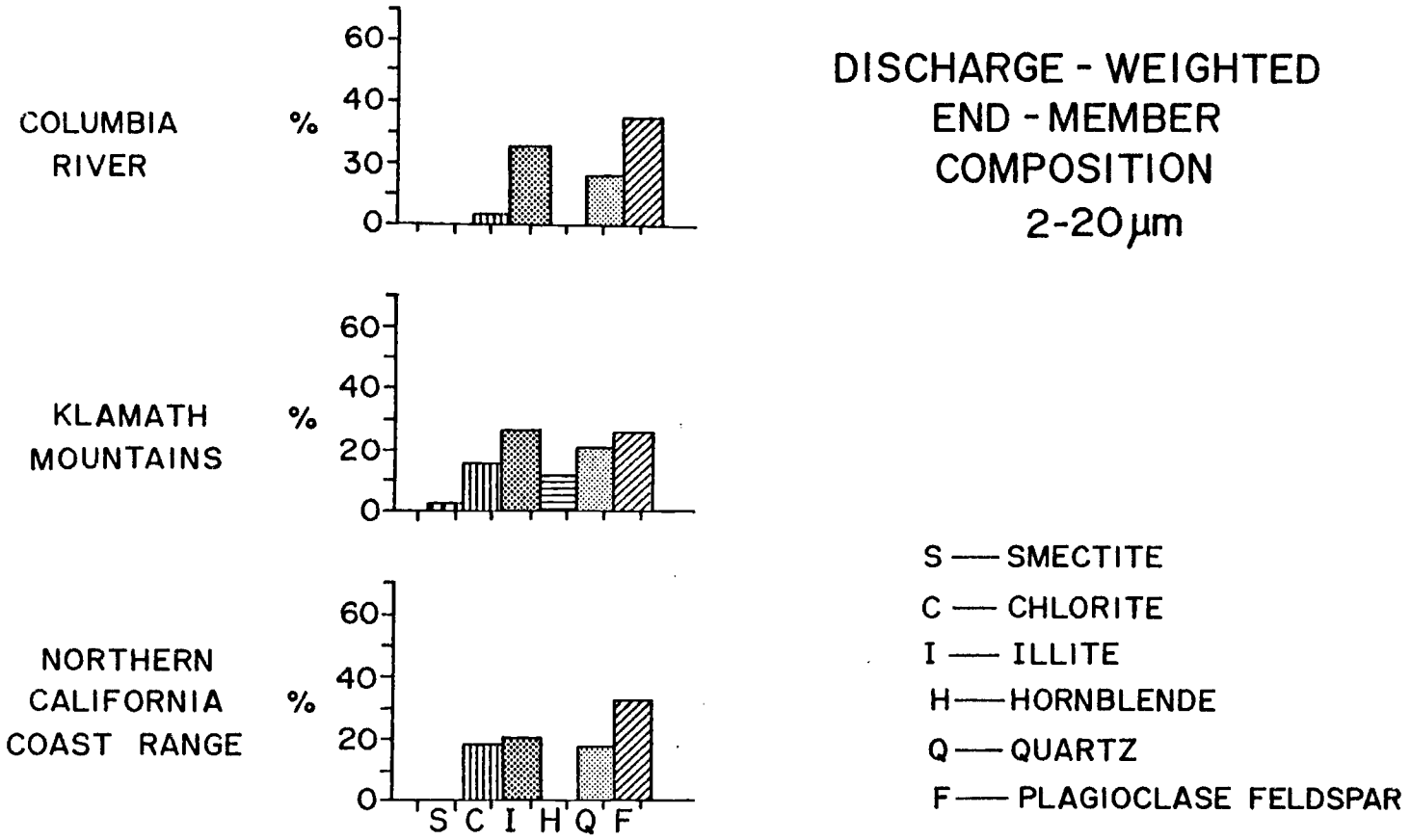
COLUMBIA RIVER
%
60
40
30
0
KLAMATH MOUNTAINS
%
60
40
20
0
NORTHERN CALIFORNIA COAST RANGE
%
60
40
20
0
S C I H Q F
DISCHARGE - WEIGHTED END - MEMBER COMPOSITION 2-20 μm
S — SMECTITE
C — CHLORITE
I — ILLITE
H — HORNBLENDE
Q — QUARTZ
F — PLAGIOCLASE FELDSPAR

Figure III-2

Figure III-3. Linear programming-calculated source area contributions to the 2-20 μm fraction of the slope sediments based in mineralogy.

a.) Columbia River contribution.

b.) Klamath Mountain contribution.

c.) California Coast Range contribution.

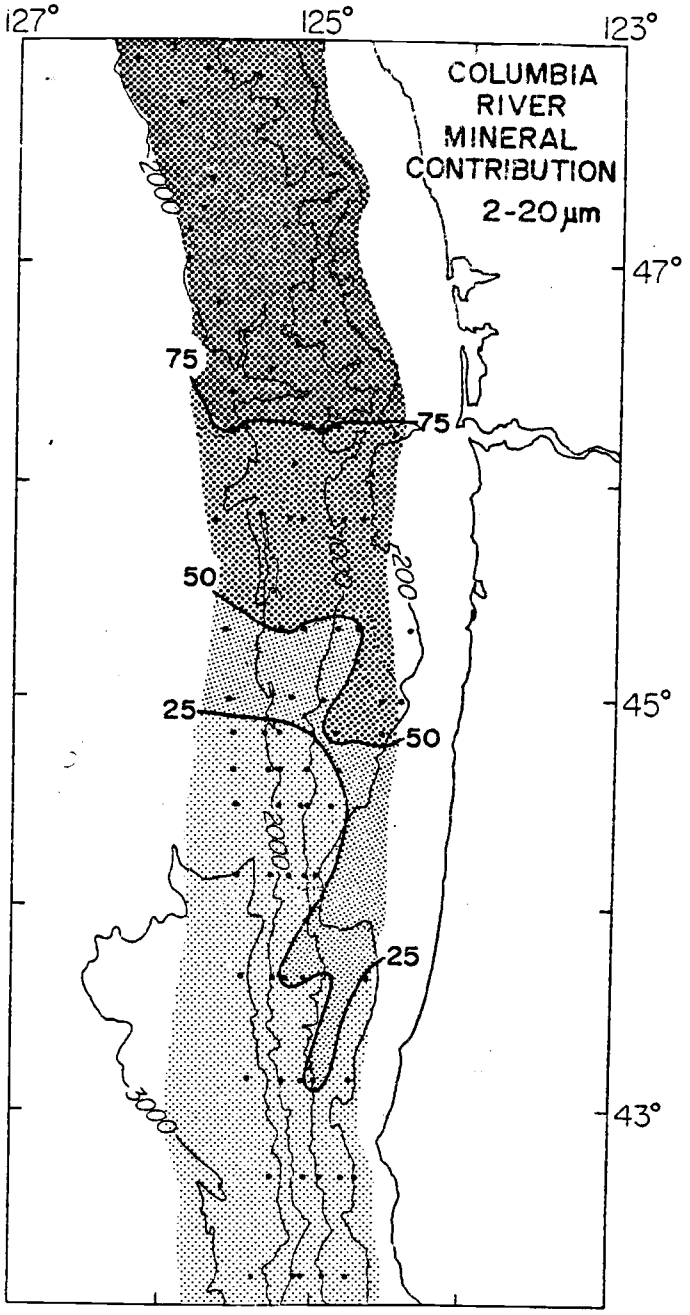

Figure III-3a

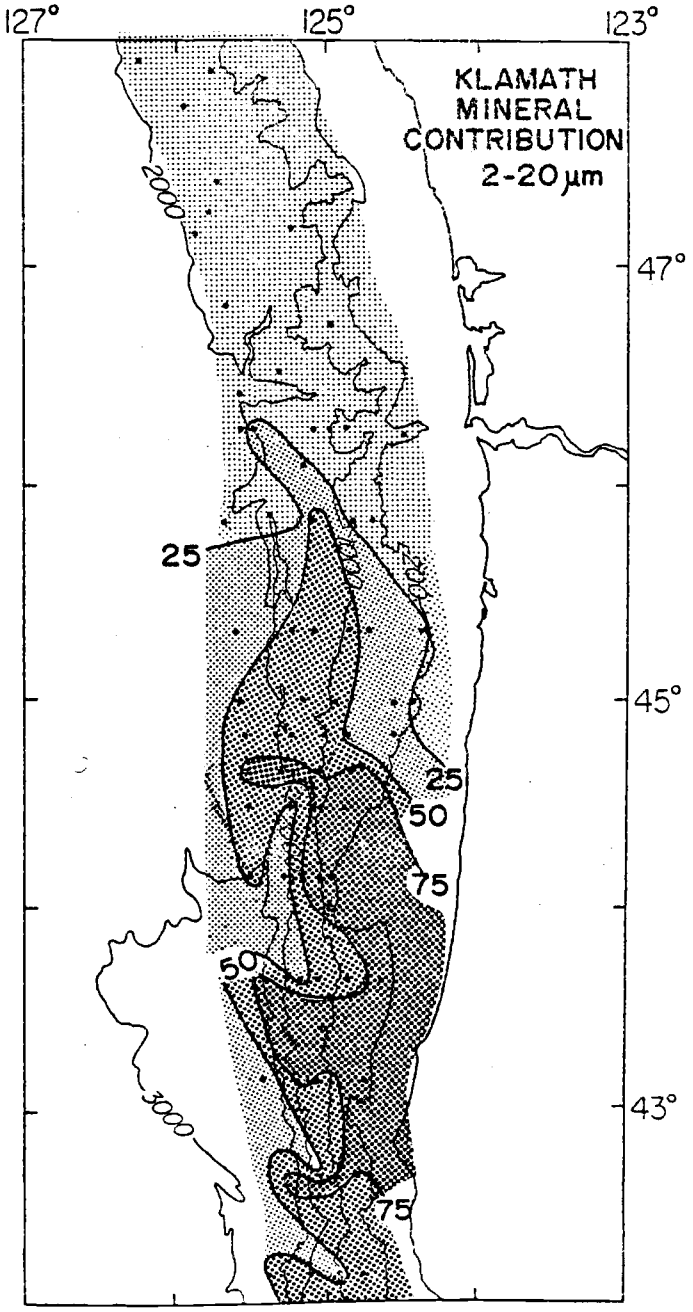

Figure III-3b

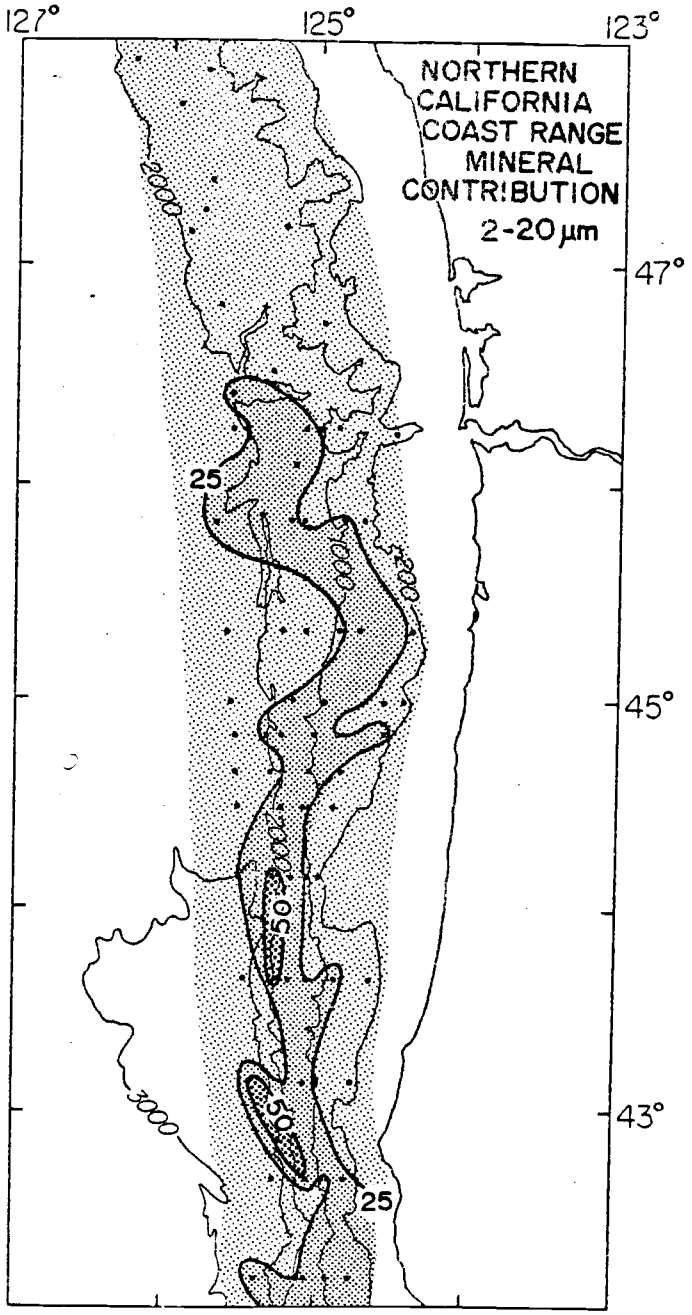

Figure III-3c

Figure III-4. Mineral abundances in the 2-20 μm fraction of the slope sediments (from Krissek and Scheidegger, 1982b).

a.) Feldspar abundances. Note similar pattern for the modelled Columbia River contributions (Figure 3a).

b.) Hornblende abundances. Note similar pattern for Klamath Mountain contributions (Figure 3b).

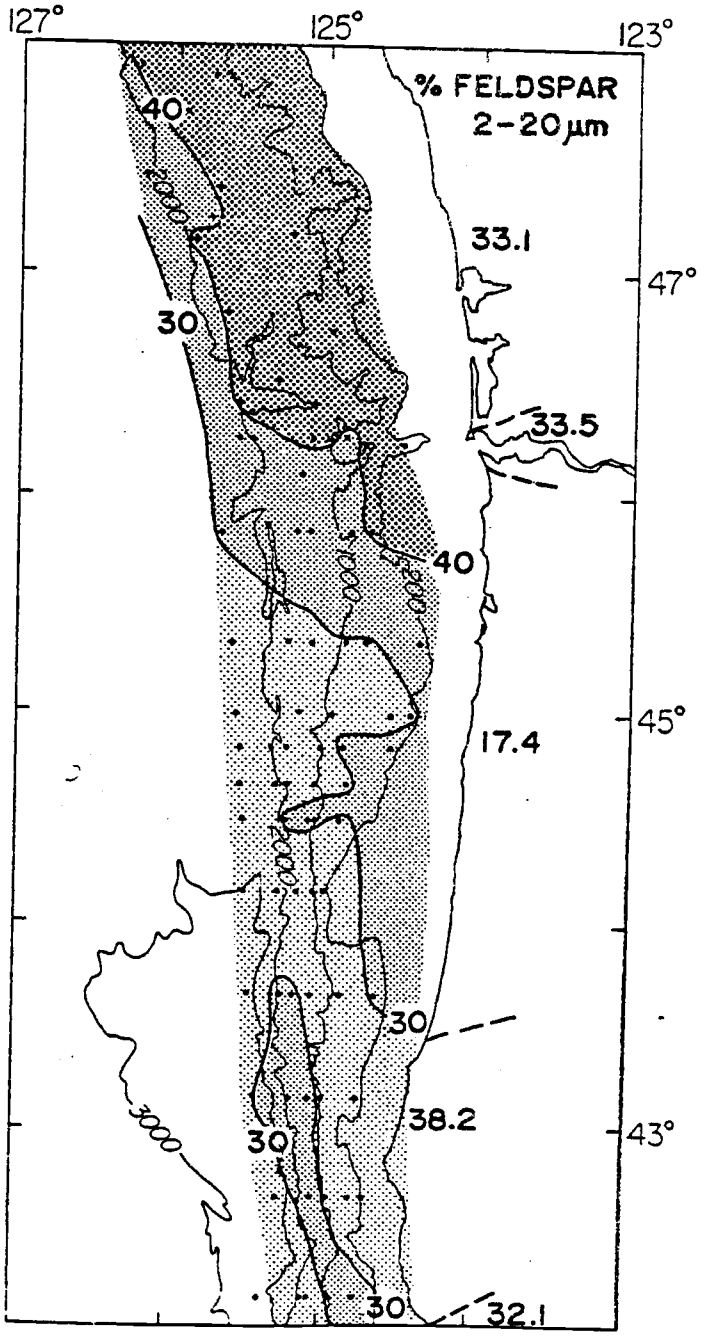

Figure III-4a

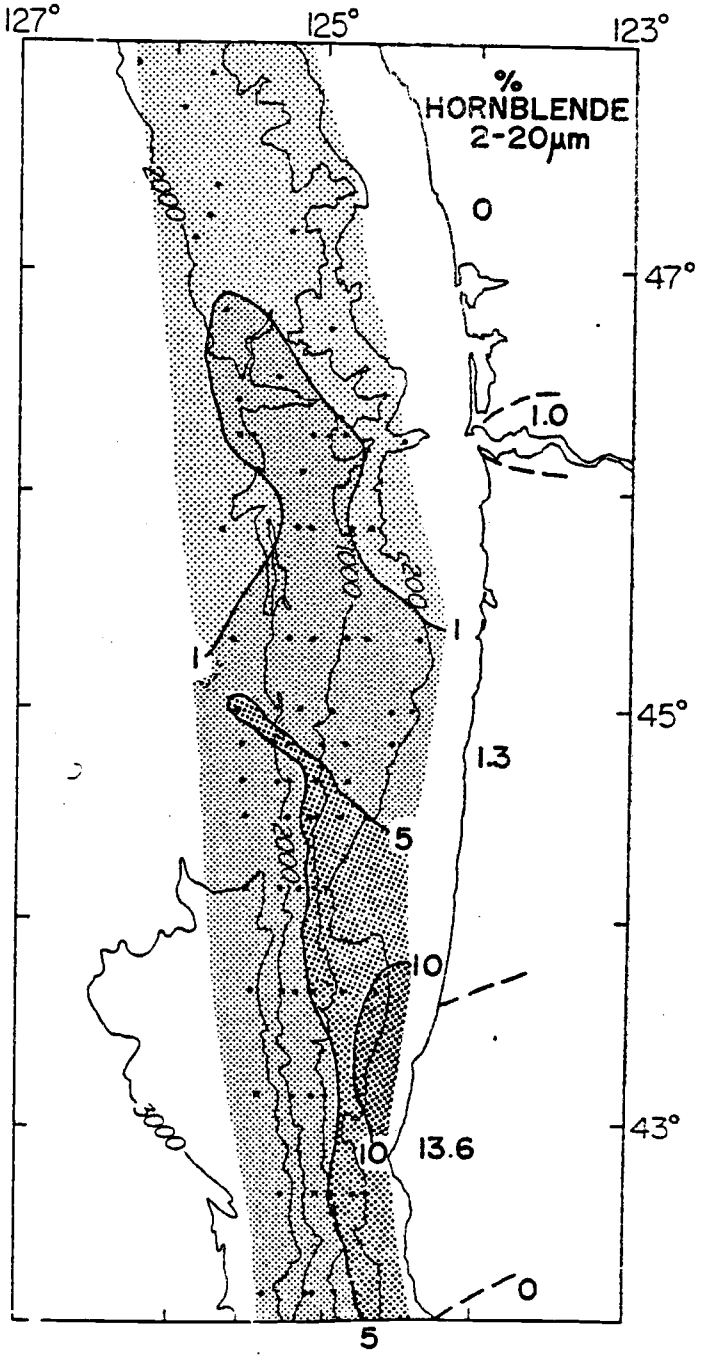

Figure III-4b

Columbia River influence than the single mineral abundance pattern because equivalent feldspar concentrations can be contributed to this region from other source areas. Hornblende (Figure 4b) is a distinctive tracer of the Klamath Mountain material, and provides an excellent indicator of Klamath Mountain influence on the upper slope close to the source (compare to Figure 3b). Because hornblende is unique to the Klamath Mountains, its abundance provides a relatively detailed and sensitive indicator of the Klamath Mountain influence even at greater distances from the source. These two examples indicate that single mineral abundance patterns can provide relatively good indicators of source area influence when a single source dominates the sediment. In distal environments material from several sources is mixed, and only unique mineral tracers (e.g., hornblende for the Klamath Mountains) can indicate source area contributions. Non-unique tracers (e.g., feldspar) are poor indicators of source area influence in distal environments. In areas where sediment is supplied by several sources (as on the central Oregon slope), the multivariate approach of linear programming provides better indicators of source area contributions than the univariate approach of mineral abundance patterns.

The chemical compositions of the three major end-members in the 2-20 μm fraction are listed in Table 1, and abundances for the Klamath Mountain and California Coast Range sources are normalized to the Columbia River source and plotted in Figure 5. The two southerly sources show similar patterns relative to the Columbia River abundances with enrichment in Mg and Fe and depletion in Ca, Ti, and Sr. Mean

Table III-1. Discharge-weighted source area chemical compositions.

	ELEMENTAL ABUNDANCES (weight % of the oxides)											
AREA	Si	Al	Fe	Ca	Na	K	Mg	Ti	Ba	Sr	Cu	Mn
Columbia River 2-20 μm	58.76	14.75	6.76	2.71	2.14	1.79	2.30	1.45	0.079	0.030	0.004	0.109
Klamath Mountains 2-20 μm	55.59	15.65	8.55	2.40	2.08	1.48	6.02	0.84	0.071	0.015	0.005	0.113
California Coast Range, 2-20 μm	56.26	16.65	8.24	1.06	2.10	1.89	4.61	0.90	0.065	0.010	0.004	0.108
Columbia River <2 μm	50.40	12.88	8.48	1.24	0.52	1.40	2.14	0.92	0.064	0.015	0.010	0.218
Klamath Mountains <2 μm	44.32	17.25	10.39	1.54	1.16	1.93	7.08	0.99	0.080	0.012	0.016	0.177
California Coast Range, <2 μm	45.36	19.80	10.19	0.69	0.82	3.02	6.29	0.82	0.090	0.006	0.010	0.142

Figure III-5. Chemical composition of the discharge-weighted end-members in the 2-20 μm size fraction normalized to the Columbia River source. Fe, Ca, K, Mg, Ti, and Sr were used in the linear programming modelling.

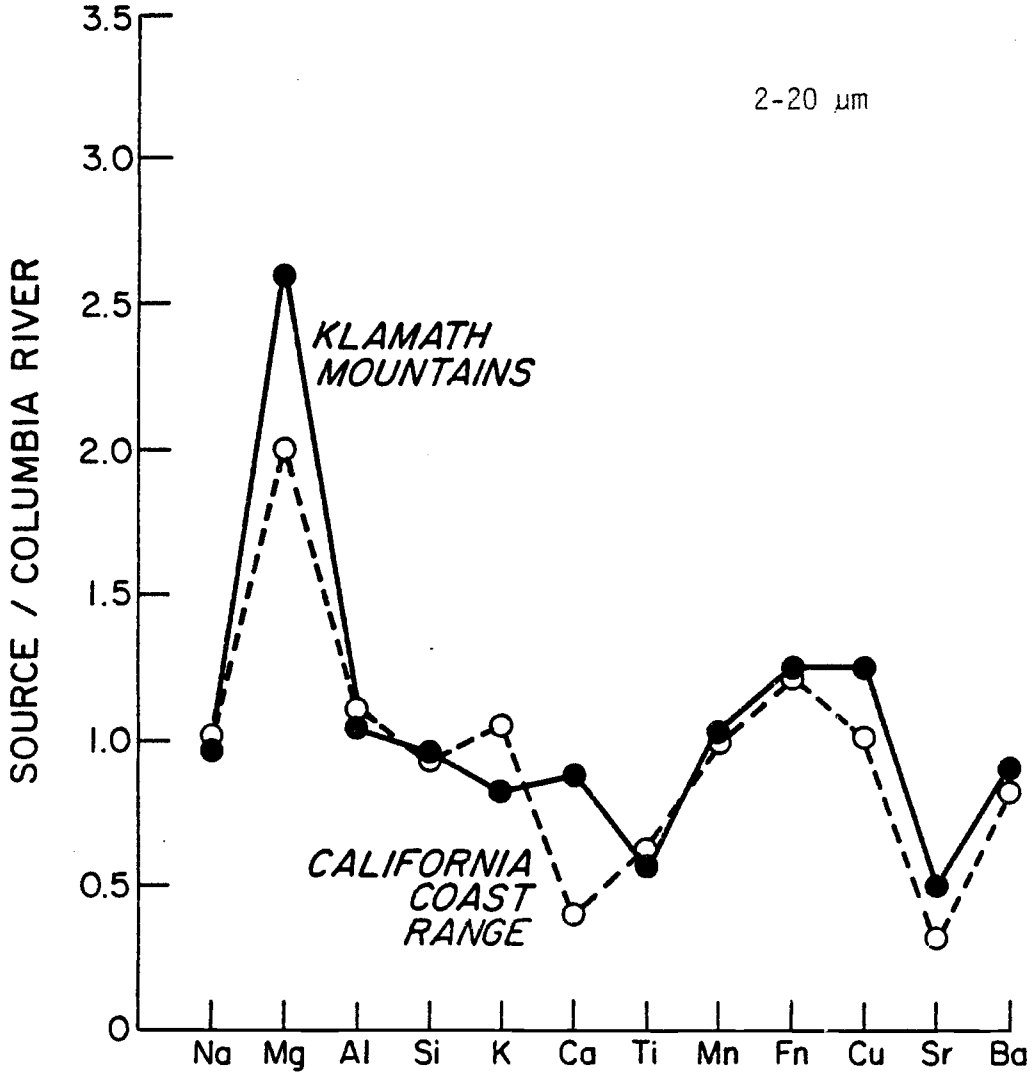
2-20 µm
SOURCE / COLUMBIA RIVER
3.5
3.0
2.5
2.0
1.5
1.0
0.5
0
KLAMATH MOUNTAINS
CALIFORNIA COAST RANGE
Na
Mg
Al
Si
K
Ca
Ti
Mn
Fn
Cu
Sr
Ba

Figure III-5

elemental abundances for the 2-20 μm fraction of the marine samples are given in Table 2, and the small standard deviations about these mean values indicate that the slope sediments have relatively uniform compositions throughout the study area. Results of a Q-MODE factor analysis with elements normalized to equal means but before varimax rotation (Leinen and Pisias, 1982) support this conclusion. The first principal factor identified by the analysis indicates that 96.6% of the data variance is explained by the mean chemical composition. Only 3.4% of the variance is associated with changes from that mean value.

As a result of subsequent varimax rotation in the Q-MODE factor analysis, six elements were identified as best explaining the variability in the data set (Leinen and Pisias, 1982). These elements were Fe, Ca, K, Mg, Ti, and Sr. The factor analysis also identified only two terrigenous-related factors in the data set. The first, which accounted for 44.5% of the data variance, was dominated by Fe and Mg and corresponded to the general composition of material derived from the southern source areas (Klamath Mountains + California Coast Range). The second factor, which accounted for 36.5% of the data variance, was dominated by Ca and Sr (probably associated with anorthite-rich plagioclase (Krissek and Scheidegger, 1982b)), and corresponded to the general composition of material derived from the Columbia River. The third factor, which accounted for 17.9% of the data variance and was dominated by K, had highest loadings offshore and could not be related to any continental source area.

Because of the results of the factor analysis and the data presented in Figure 5, the 2-20 μm fraction was modelled by linear

Table III-2. Chemical composition of Oregon-Washington slope sediments.

SIZE FRACTION	MEAN ELEMENTAL ABUNDANCE ± 1 STANDARD DEVIATION (weight % of the oxide)											
	Si	Al	Fe	Ca	Na	K	Mg	Ti	Ba	Sr	Cu	Mn
2-20 μm	60.67	14.51	6.50	1.98	2.35	1.96	3.93	0.98	0.084	0.021	0.004	0.070
	±3.27	±0.89	±0.80	±0.53	±0.25	±0.59	±0.78	±0.09	±0.026	±0.008	±0.001	±0.010
<2 μm	48.16	16.56	8.91	1.15	0.88	2.08	4.88	0.88	0.081	0.014	0.011	0.087
	±2.34	±0.65	±0.52	±0.33	±0.33	±0.26	±0.67	±0.06	±0.020	±0.004	±0.003	±0.030

programming using only six elements (Fe, Ca, K, Mg, Ti, and Sr) and two end-members (a northern [Columbia River] and a southern [Klamath Mountains + California Coast Range] source). However, the analysis was performed twice, using different weighting schemes for the elemental abundances in each case. In the first analysis, all elements were given a weight of 1.0, so that the most abundant elements have the greatest influence on the model. In the second analysis, elements were assigned unequal weights such that all elements had equal means and therefore all had an equal influence on the model. Mean residual for the calculation with equal weights was 6.5% and K consistently had the maximum residual. This reflects the importance of K in explaining the variance within the slope data set while K contents of the end-members are relatively uniform (Figure 5). Mean residual for the calculation with equal elemental means was 11.0%. Iron consistently showed the maximum residual, reflecting the decreased influence of the most abundant element when non-constant weighting factors are used to produce equal elemental means. Results of the two analyses generally agree within ±15% (absolute), but because the model with equal elemental weights gave a better agreement of the calculated and measured abundances, its results are presented here.

The calculated contributions show areal patterns similar to those from the mineral-calculated contributions. The Columbia River end-member is shown as an example (compare Figure 3a and 6). Highest Columbia River influence again occurs to the northwest of its mouth, with lower contributions extending southward on the slope. The zone of relatively low (<25%) contributions on the middle slope at

Figure III-6. Columbia River contribution calculated by linear programming of the chemical data. Note similarity of the pattern to Figures 3A and 4A.

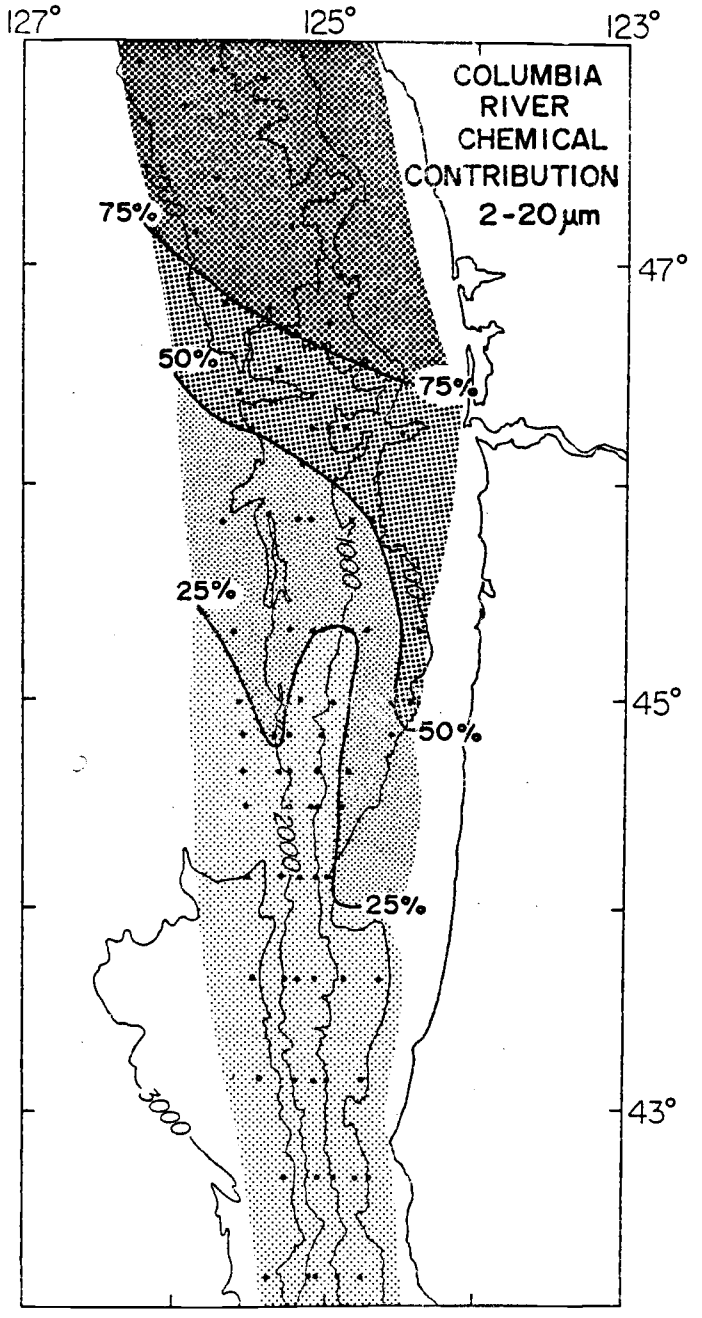
127°
125°
123°
COLUMBIA
RIVER
CHEMICAL
CONTRIBUTION
2-20μm
47°
45°
43°
75%
50%
75%
25%
50%
25%
3000
3000
3000

Figure III-6

approximately 45°N. in the chemical results may reflect a change in the stability of the calculated contributions between the two data sets (Table 3). Small changes in the chemical data produce a large change in the calculated contributions, while the mineral results change only slightly with larger data fluctuations. The relatively uniform chemical data appear to produce more unstable results than the mineral modelling.

The magnitudes of the Columbia contributions calculated from the two data sets also agree reasonably well (Figure 7). Mineral contributions tend to be higher than the chemical results, especially on the central and southern Oregon slope, but the reason for this is unknown. I speculate that this difference arises because a Columbia-type mineralogy can be obtained by diluting the southern source mineralogies with some non-quantified component (opal, carbonate, or locally-important Oregon Coast Range material). The Columbia contribution may therefore be exaggerated whenever a non-quantified mineral component is present. Alternately, the uniformity of the chemical data may cause those results to respond much more quickly and unstably to compositional changes, decreasing the calculated Columbia contribution. Such explanations, however, are purely speculative.

THE <2 μm FRACTION

The <2 μm mineral end-members (Krissek, 1982b) are shown in Figure 8. Columbia River material is dominated by smectites. Klamath Mountain and California Coast Range sediments have a more diverse

Table III-3. Mineral and chemical composition of the 2-20 μm fraction of adjacent samples used for the linear programming modelling, listed with the modelling results.

Sample	Mineral Abundance (wt.%)					Source Area Contributions (%)		
	Chlorite	Illite	Hornblende	Quartz	Feldspar	Columbia R.	Klamath Mtns.	Calif. Coast Range
122	11	25	3	21	26	32.6	67.4	0
123	9	30	4	19	26	44.7	55.3	0

Sample	Elemental Abundance (%)						Source Area Contributions (%)		
	Fe	Ca	K	Mg	Ti	Sr	Columbia R.	Klamath Mtns.	Calif. Coast Range
120	6.26	1.76	1.94	3.76	1.06	0.02	25.8	57.7	16.5
121	6.22	1.59	1.94	4.08	1.00	0.02	6.3	72.9	20.8

Figure III-7. Comparison of the Columbia River contributions calculated using mineral and chemical data. Line shown has slope = 1 with uncertainty estimates of ±15%. Equation of the regression line is given.

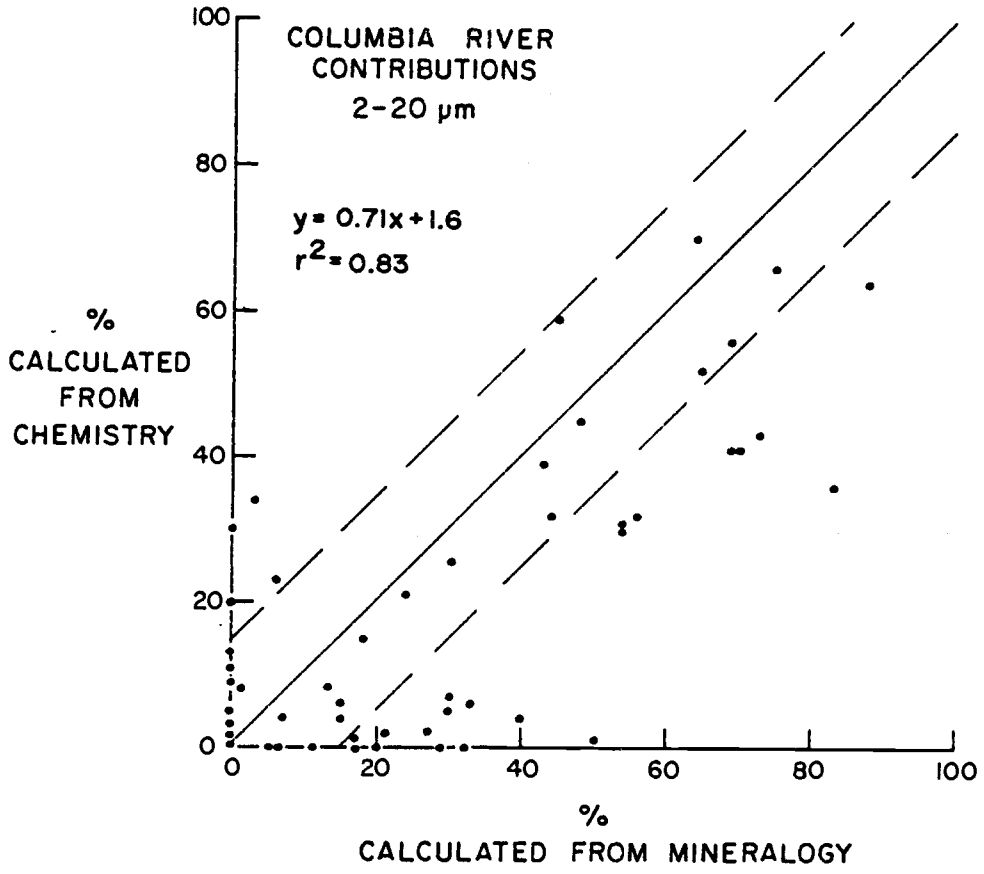
COLUMBIA RIVER
CONTRIBUTIONS
2-20 μm
y = 0.71x + 1.6
r² = 0.83
% CALCULATED FROM CHEMISTRY
% CALCULATED FROM MINERALOGY
0
20
40
60
80
100

Figure III-7

Figure III-8. Mineral composition of the discharge-weighted end-members in the <2 μm size fraction (Krissek, 1982b). Columbia River material is smectite-rich, while the southerly sources have more diverse mineralogies.

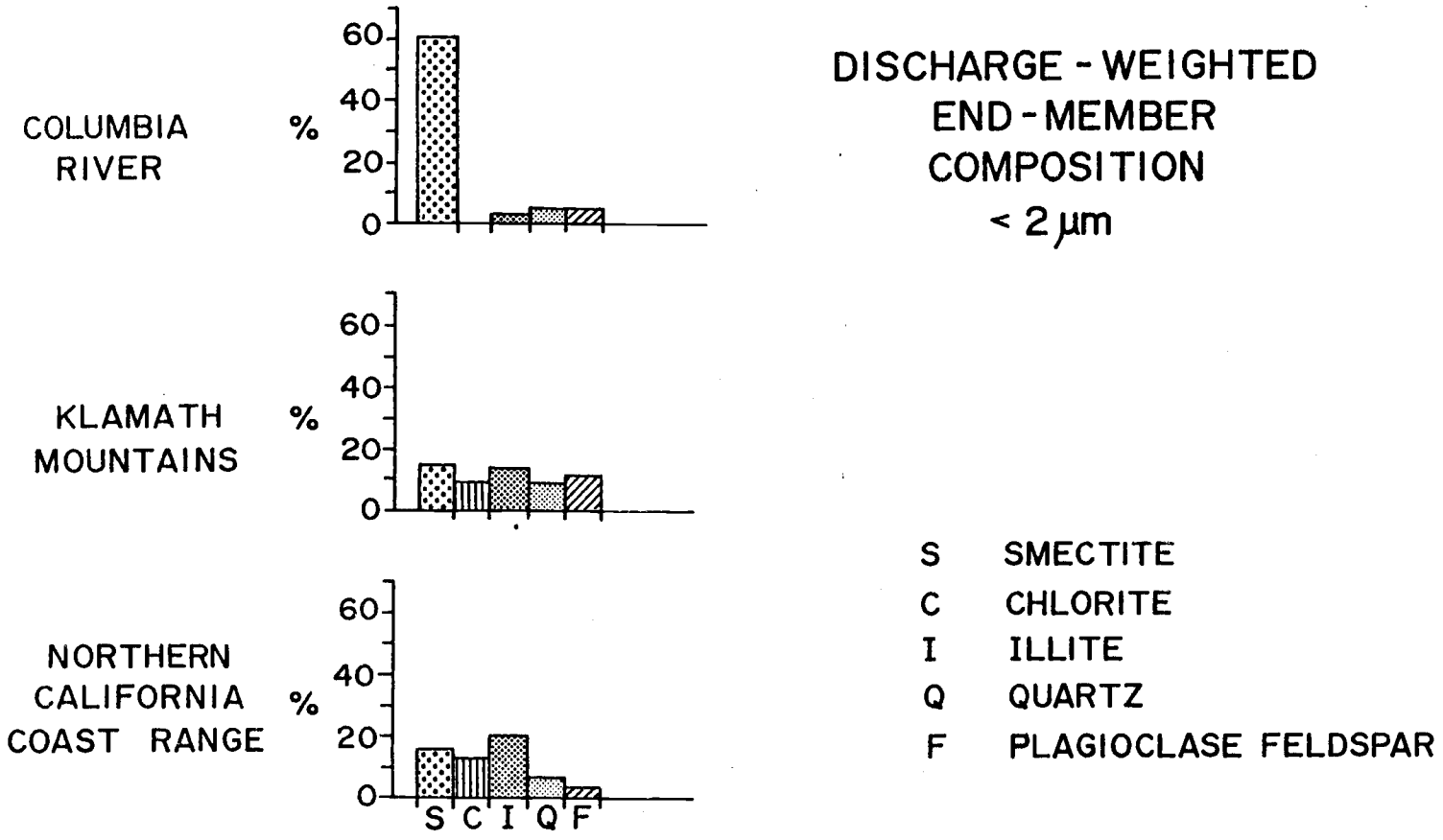
COLUMBIA RIVER
%
60
40
20
0
KLAMATH MOUNTAINS
%
60
40
20
0
NORTHERN CALIFORNIA COAST RANGE
%
60
40
20
0
S C I Q F
DISCHARGE - WEIGHTED END - MEMBER COMPOSITION
< 2 μm
S SMECTITE
C CHLORITE
I ILLITE
Q QUARTZ
F PLAGIOCLASE FELDSPAR

Figure III-8

mineralogy, containing equal to subequal amounts of all five measured minerals. A Q-mode factor analysis of the mineral data identified only two distinguishable sources. The first source, indicated by a factor rich in illite and chlorite which accounted for 47.4% of the data variance, was a combined Klamath Mountain-California Coast Range source; the second, indicated by factors rich in feldspar and smectite which accounted for 38.5% and 12.7% of the data variance respectively, was the Columbia River. Therefore, the <2 μm mineral data were modelled using only two end-members (Columbia River and Klamath Mountain + California Coast Range).

Results of this calculation are shown in Figure 9. These data suggest that the contribution of fine-grained Columbia River material is extremely high (>90%) off its mouth and southward on the slope, especially the uppermost slope (Figure 9a). The Columbia River influence is estimated to be greater than 50% over the entire study area. This value seems quite high in view of the available sediment source data which indicate that both the California Coast Range and the Klamath Mountains discharge more suspended sediment annually than the Columbia (Karlin, 1980). In addition, the fine-grained silt data indicate a predominant northerly transport, contrasting strongly with the pattern shown for the <2 μm fraction (Figure 9a). The contribution from the southern source (Figure 9b) is the inverse of the Columbia River pattern, with decreasing influence from south to north but an isolated zone of contributions greater than 25% on the Washington slope. This zone of increased influence on the Washington slope may be caused either by the local input of Washington Coast Range material, with a

Figure III-9. Linear programming-calculated source area contributions to the <2 μm fraction of the slope sediments.

a.) Columbia River contribution.

b.) Southern source (Klamath Mountain + California Coast Range) contribution.

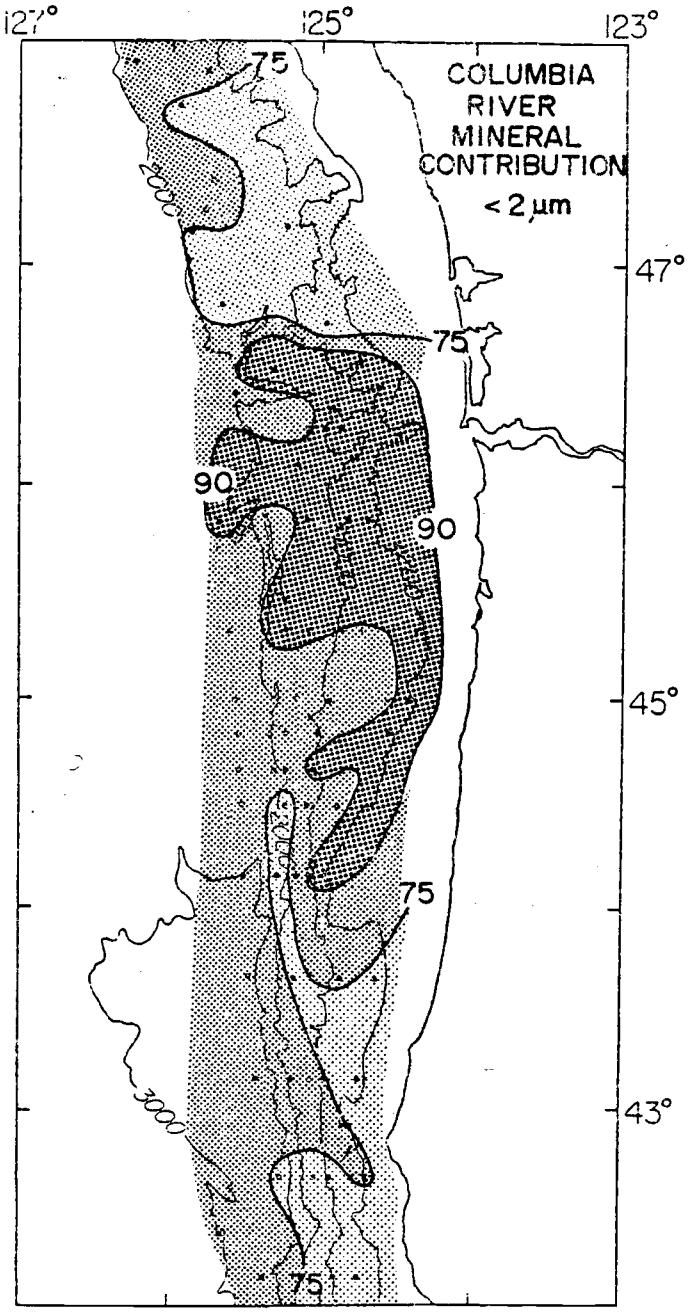

Figure III-9a

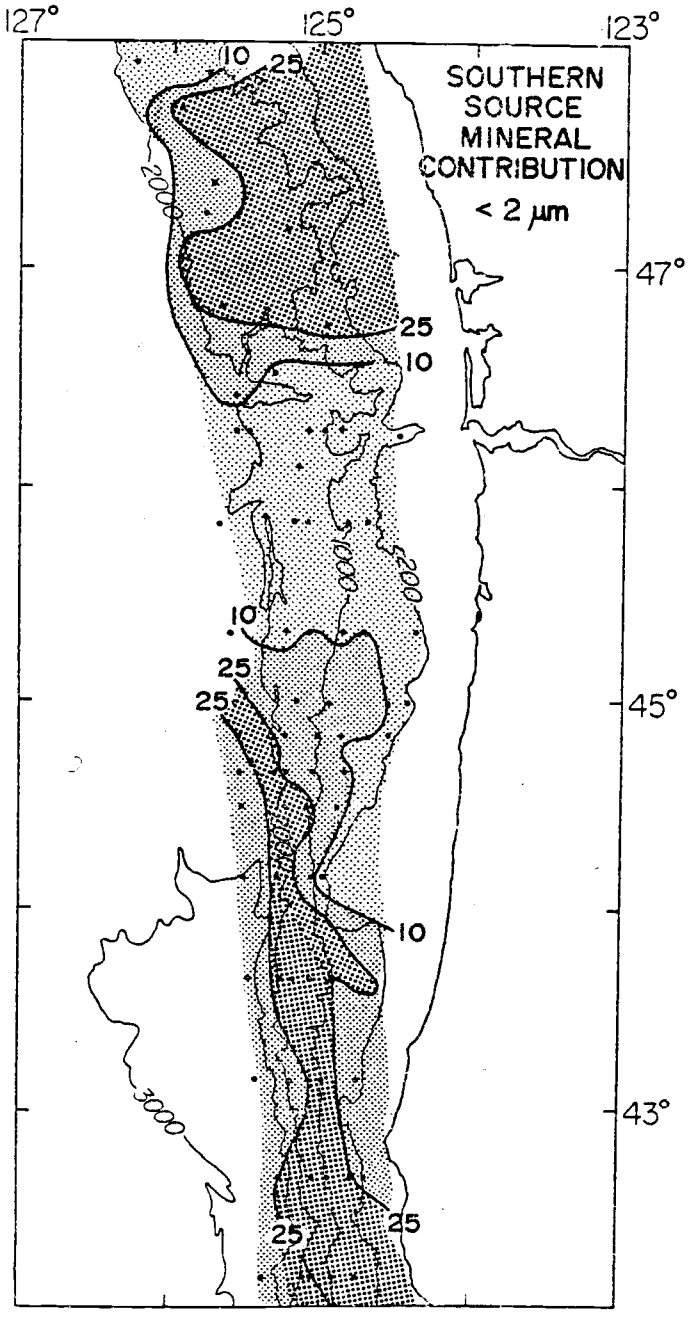

Figure III-9b

mineralogy similar to that from the southern source (Krissek, 1982b), or by dilution of the southern influence on the northern Oregon slope. If southern source material is transported northward along the entire Oregon-Washington slope (Karlin, 1980; Krissek and Scheidegger, 1982b; Figure 10a), but the Columbia River influence is strongest on the northern Oregon slope, then the relative influence of the southern source will be reduced on the northern Oregon slope. North of the mouth of the Columbia, where the input of Columbia-derived sediments is low, the relative influence of southern source components will again increase.

Because of the predominance of smectite in the <2 μm fraction of the marine sediments and of the Columbia River end-member (Figure 8), the offshore smectite abundance pattern closely resembles the Columbia River contribution map on the northern and central Oregon margin (compare Figures 9a and 10b). On the Washington and southern Oregon margin, however, where the sediments appear to be a mixture of material from the two sources, the magnitude of the Columbia River contributions appears quite high in light of the regional suspended sediment discharge data of Karlin (1980). The essentially monominerallic nature of the Columbia River source (Figure 8) allows its contribution to be adjusted to fit the smectite abundance quite well without influencing the modelled abundance of the other minerals. Thus, any factor which increases the smectite abundance (localized Oregon Coast Range input, size-selective transport on the Oregon slope; Krissek and Scheidegger, 1982b) will cause a concomitant increase in the calculated Columbia River contribution. As a result, the Columbia River results may

Figure III-10. Mineral abundances in the <2 μm fraction of the slope sediments (after Krissek and Scheidegger, 1982b).

a.) Chlorite abundance. Note weak similarity with Figure 9b.

b.) Smectite abundance. Note weak similarity with Figure 9a.

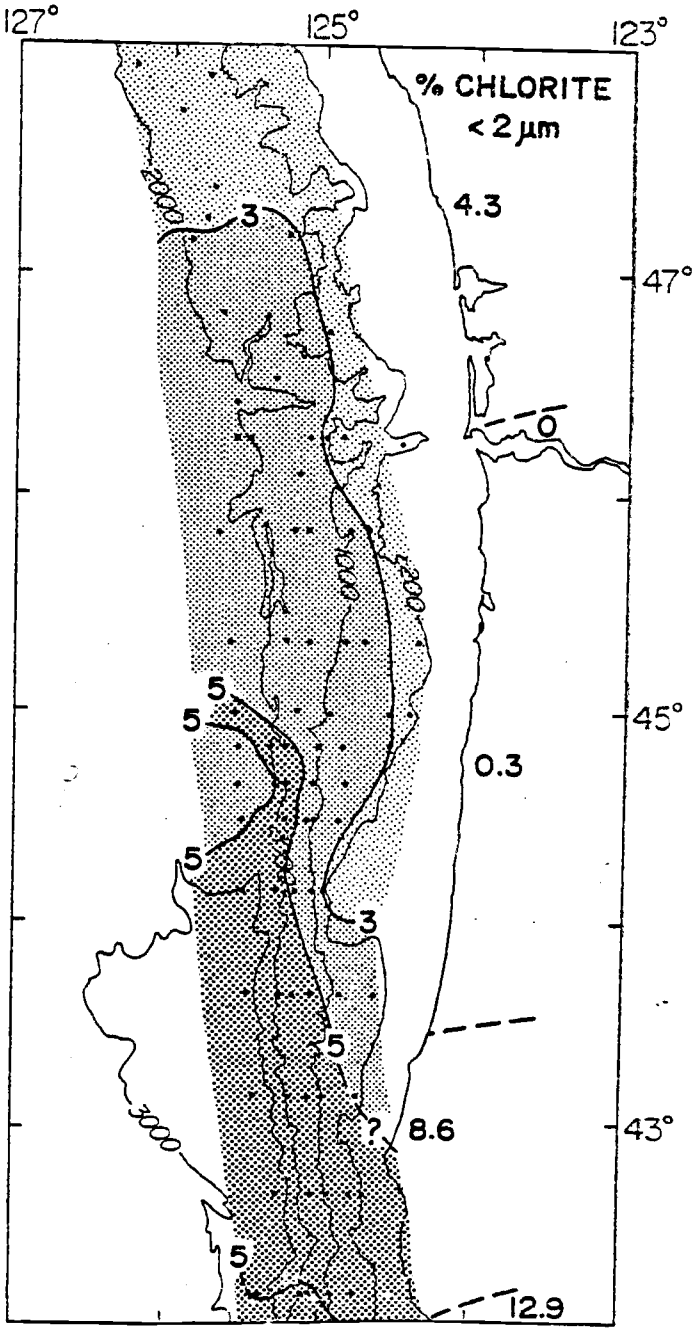

Figure III-10a

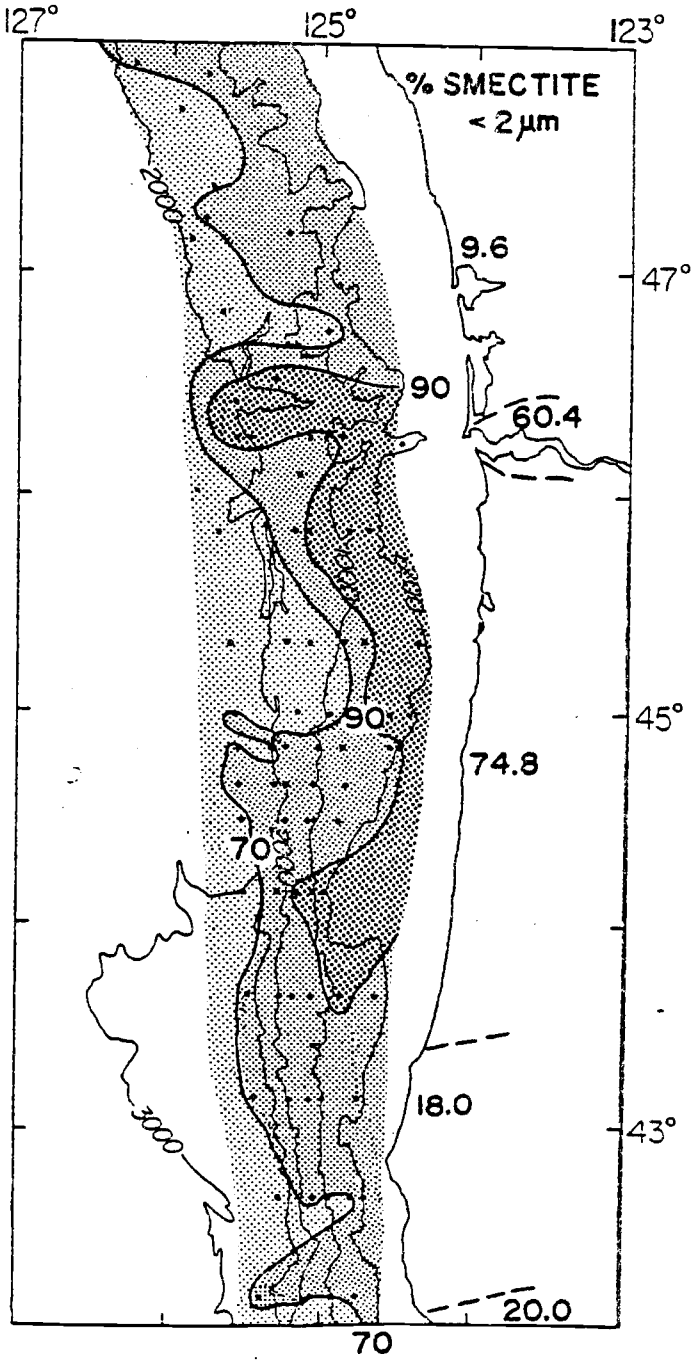

Figure III-10b

reflect transport and depositional processes rather than source area effects and these results should be viewed with caution.

The chemical compositions of the three major end-members in the <2 μm fraction are listed in Table 1, and abundances for the southern two sources are normalized to the Columbia River source and plotted in Figure 11. The two southern sources show similar patterns relative to the Columbia River abundances except for Ca and Cu, but both are enriched in Na, Mg, Al, K, and Ba and mildly depleted in Mn and Sr. Mean elemental abundances for the <2 μm fraction of the slope sediments are listed in Table 2, and the small standard deviations about these mean values again indicate compositional uniformity throughout the study area. The first principal factor extracted by Q-mode factor analyses of the <2 μm chemical data, weighted to equal means and prior to varimax rotation (Leinen and Pisias, 1982), accounts for 96.5% of the data variance. Thus, most of the data variance can be explained by the mean elemental abundances, and only a small portion (3.5%) is associated with variations about the mean. The <2 μm fraction of the slope sediments is enriched in Al, Fe, and Mg and depleted in Si, Ca, and Na relative to the 2-20 μm fraction, reflecting the increased importance of phyllosilicate and amorphous phases in the finer material (Krissek and Scheidegger, 1982b).

Results of a subsequent varimax rotation in the factor analysis identified two distinguishable sources, with Ca, Na, Mg, Ba, Sr, Cu, and Mn as the important elements. The first source, indicated by a factor rich in Mg, Cu, and Mn which accounted for 43.2% of the data variance, was the combined Klamath Mountain-California Coast Range source. The second, indicated by a factor rich in Ca, Na, and Sr

Figure III-11. Chemical composition of the discharge-weighted end-members in the <2 μm size fraction normalized to the Columbia River source. Ca, Na, K, Mg, Sr, and Mn were used in the linear programming modelling.

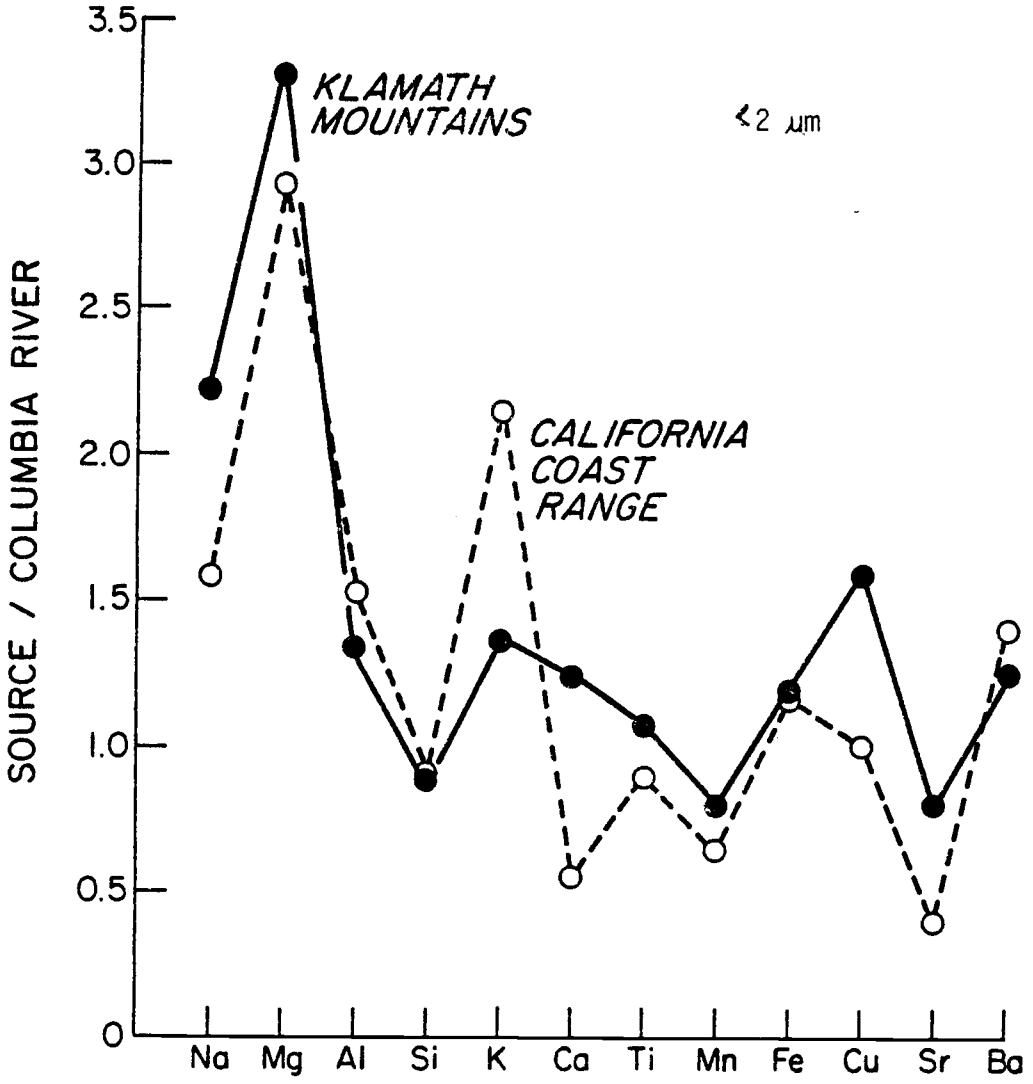

Figure III-11

which accounted for 38.1% of the data variance, represented the Columbia River source.

Because of the results of the factor analysis and the data presented in Figure 11, the <2 μm fraction was modelled using only six elements and two end-members. The analysis was performed using both equal weights and unequal weights (equal means) for all elements. The calculated contributions generally agree within ±15%, except for samples from the Washington slope which the unequal weight (equal mean) analysis classifies as 100% southern source material. The mean residual is 2.3% for the equal weight model and 4.2% for unequal weight (equal mean) calculation. Because the equal weight model has a lower mean residual and gives more reasonable contribution estimates for the Washington slope, its results are presented here.

The Columbia River contributions are shown in Figure 12 as an example of these results. While the chemical and mineral results have similar patterns on the northern and central Oregon slope (compare Figure 12 and Figure 9a), the patterns on the Washington slope and the magnitudes over the entire slope are quite different. The chemical results show strongest Columbia River influence on the Washington slope, while most of the Oregon slope contains less than 50% Columbia River material. The lack of agreement in the magnitude of the Columbia River contributions is clearly indicated in Figure 13. The chemical results also show little agreement with the smectite abundance pattern (Figure 10b). Since the 2-20 μm fraction data showed good agreement between single mineral abundances and calculated contributions close to each source, the lack of agreement in the <2 μm fraction may indicate that the end-members are not consistently able to evaluate contributions

Figure III-12. The Columbia River contribution to the slope sediments in the <2 μm fraction calculated by linear programming modelling of the chemical data. Note lack of similarity with Figures 9a and 10b.

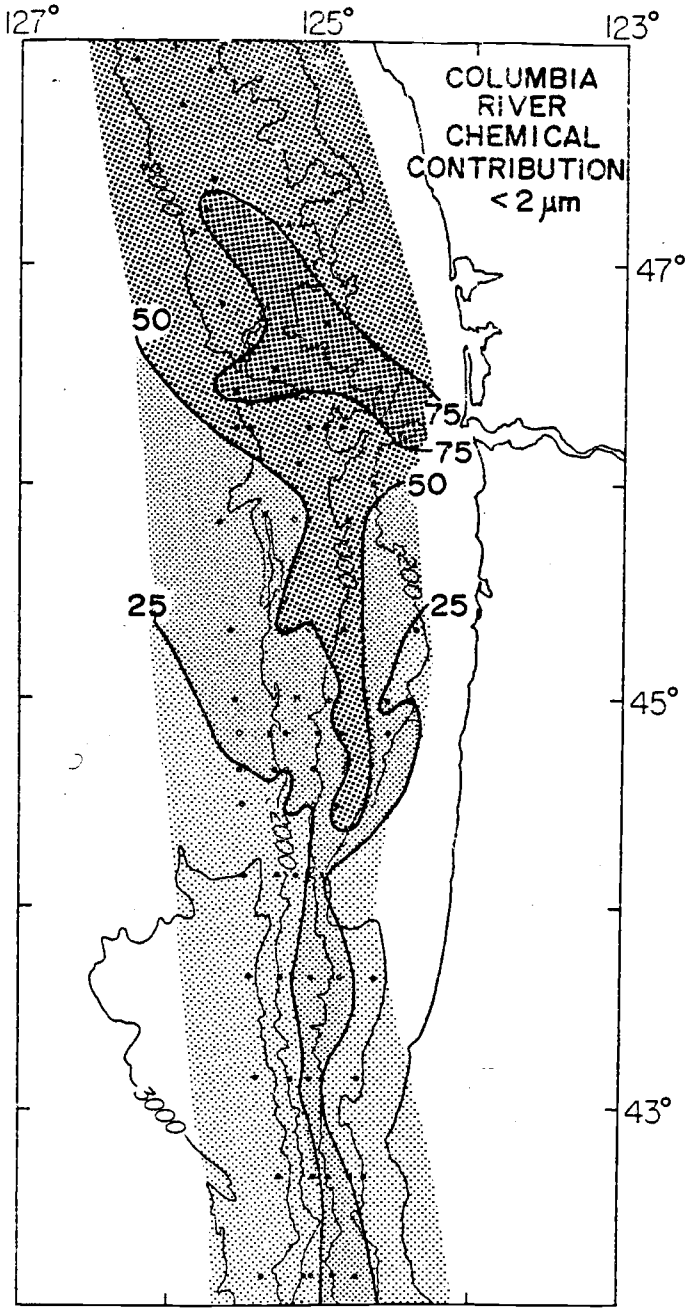

Figure III-12

Figure III-13. Comparison of the Columbia River contributions calculated using mineral and chemical data. Line shown has slope = 1. Equation of the regression line is given.

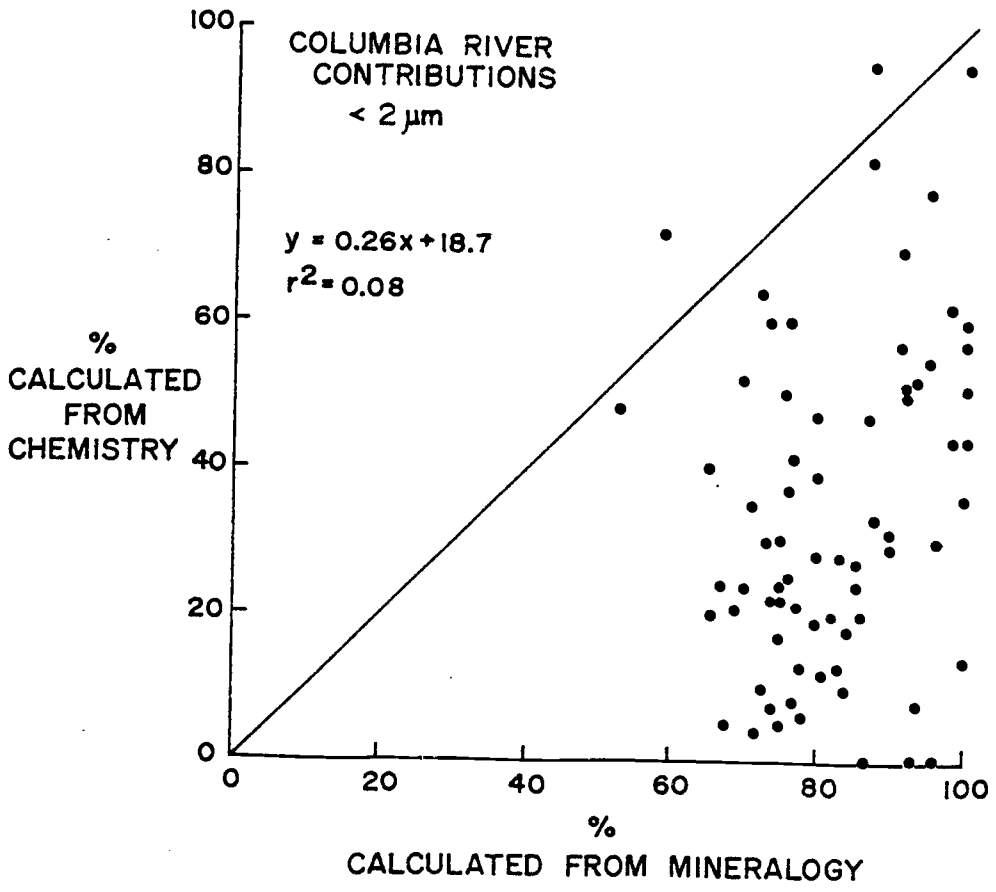

Figure III-13

to the compositionally-uniform slope sediments. An alternate explanation is that the chemical results provided better sediment tracers than the mineralogy.

While the chemical contributions appear more reasonable than the mineral results in view of Karlin's (1980) sediment discharge data, the chemical results are extremely unstable (Table 4). Therefore, one set of the <2 μm results contains stable but very high values, while the second contains reasonable but unstable coefficients. For these reasons, any sediment budget for the <2 μm fraction must be viewed as tentative.

Table III-4. Mineral and chemical composition of the <2 μm fraction of adjacent samples used for the linear programming modelling, listed with the modelling results.

Sample	Mineral Abundance (wt.%)					Source Area Contribution (%)	
	Smectite	Chlorite	Illite	Quartz	Feldspar	Columbia River	Southern Source
163	82	6	9	5	3	78.2	21.8
164	98	6	8	3	1	86.7	13.3

Sample	Elemental Abundances (%)						Source Area Contributions (%)	
	Ca	Na	K	Mg	Sr	Mn	Columbia River	Southern Source
164	1.00	0.64	2.19	6.19	0.01	0.08	0.0	100.0
165	1.14	0.61	2.34	5.84	0.01	0.08	21.0	79.0

DISCUSSION

The processes controlling the dispersal of hemipelagic sediments on the Oregon-Washington continental margin have been discussed in detail by Krissek and Scheidegger (1982b). Agreement between the mineral abundance and mineral contribution patterns (Figures 3 and 4, 9 and 10), especially near each source, indicate that the linear programming results are consistent with the dispersal processes proposed in that work and will not be discussed further here.

RELATIONSHIPS BETWEEN CHEMICAL AND MINERAL COMPOSITION

The data set presented here is one of the first to contain both elemental and quantitative mineral abundances for hemipelagic sediments. As such, it provides an excellent opportunity to examine the relationships between the chemical and mineral composition of fine-grained marine sediments, and the variation of those relationships with sediment grain size.

The relationship between contributions calculated using chemical data and those calculated using mineral data in the 2-20 μm fraction appears reasonable (Figure 7), indicating that the elemental abundances are dominated by mineral components which have been quantified. Non-quantified components may include carbonates, opal, non-diffracting or poorly crystalline detrital or authigenic phyllosilicates, or non-diffracting or poorly crystalline hydrogenous iron oxides and hydroxy-oxides (Lisitzin, 1972; Cronan, 1974). In the 2-20 μm fraction, the mineral data account for an average of 84.3% of the sediment (Krissek

and Scheidegger, 1982b), further supporting the conclusion that other components exert only a minor influence.

Contributions calculated using the two <2 μm data sets (Figure 13) show no agreement. Two possible explanations for this lack of agreement are: 1) sediment phases which were not quantified in the mineral data may exert a strong influence on the sediment chemistry, and 2) the linear programming technique may not consistently estimate source area compositions when the end-members and slope sediments are relatively uniform. In order to determine the possible influence of non-diffracting or poorly-crystalline phases (especially aluminosilicates and iron oxyhydroxides) on the sediment chemistry, eight samples were analyzed with a selective acid ammonium oxalate leach (Wang, 1978). Of the eight samples, four had relatively good agreement for the mineral and chemical results; it was hypothesized that these four samples contained little or no non-diffracting or poorly-crystalline material. The other four samples showed very poor agreement between the calculated contributions; it was hypothesized that these four samples contained much non-diffracting and/or poorly-crystalline material.

The acid ammonium oxalate leach is a standard soil analysis technique (Wang, 1978) which dissolves amorphous inorganic Fe and Al and organic-complexed Fe and Al. The leach solutions were analyzed by atomic absorption spectrophotometry for the extracted Fe and Al, and results (mean ±1 standard deviation) are summarized in Table 5. The results indicate that no difference exists in the extractable Si, Al, and Fe contents of the <2 μm fraction of these two groups. Therefore, I conclude that the abundance of non-diffracting material is

Table III-5. Chemical composition of acid ammonium oxalate leach from samples initially believed to contain little (Group 1) and much (Group 2) non-diffracting material in the <2 μm size fraction.

Sample group	Elemental Abundances (%)		
	SiO_2	Fe_2O_3	Al_2O_3
Good agreement between calculated contributions (?little non-diffracting material?)	0.71 ± 0.06	1.51 ± 0.34	1.22 ± 0.16
Poor agreement between calculated contributions (?much non-diffracting material?)	0.69 ± 0.03	1.42 ± 0.14	1.26 ± 0.07

similar for the two sample groups and does not cause the differences observed in the mineral and chemical results.

The second possibility is that limitations within the modelling technique cause the observed differences. The data shown in Tables 3 and 4 indicate that the calculated contributions are very sensitive to small changes in the original data. As a result, the compositional uniformity of the <2 μm chemical data set and the relative uniformity of its end-members may have a major influence on the modelling results. Because of these uncertainties, the <2 μm linear programming results appear to be of limited value. The qualitative indicators (single mineral abundances) provide a reasonable picture of sediment dispersal on the margin, but the uncertainties associated with the source area contributions limit their usefulness in further calculations for the <2 μm fraction.

SEDIMENT BUDGETS

The source area contributions calculated above can be used to construct a sediment budget for the slope within our study area. The 2-20 μm budget can be presented in detail because the 2-20 μm source area contributions appear to be reasonable, but the uncertainties associated with the <2 μm modelling results limit consideration of that fraction. Other uncertainties also affect the parameters used in the sediment budget calculation, and will be discussed here. Sedimentation rates were obtained from an assortment of radiocarbon, biostratigraphic, and tephra-chronologic data, in some cases with only one age control

point per core. Although the range of values is reasonable when compared to examples from other continental slopes (Doyle et al., 1979; Garrison, 1981; Reimers, 1981; DeMaster, 1981), these rate estimates bring their own uncertainty into the calculation. The discontinuous and nonuniform nature of sedimentation on the slope in both space and time (Kulm and Scheidegger, 1979; Krissek and Scheidegger, 1982b), also introduces uncertainties into the budget results. From several 3.5 kHz lines, I estimate that as little as 50% of the upper slope and 30% of the lower slope may be subject to deposition. If these estimates are valid for the entire slope, the results of the budget calculation will overestimate the true total sediment accumulation by a factor of 2 to 3. The unit mass accumulation rate ($g/cm^2/yr$) used in the calculation may also vary both spatially and temporally with sediment grain size and depositional process. Finally, the fluvial suspended sediment discharge data (Karlin, 1980) used to estimate the effectiveness of the slope as a trap for fine-grained sediments are also subject to some question. These values are based on discharge records from two to nineteen years long, and may not include either geologically-significant large-discharge events (i.e., 100 year, 500 year, etc. floods) or anthropogenic effects. As a result of all these uncertainties, the 2-20 μm sediment budget presented here represents the best effort possible with the present data, but must be recognized as only an initial attempt.

Available sedimentation rates were compiled from Barnard (1978) and Kulm and Scheidegger (1979). Rates for the northern Oregon upper and central Oregon upper and lower slopes were estimated by considering the rates known for adjacent environments at similar water depths and

the location of each region relative to the major sediment sources. The rates are listed in Table 6. Mean wet bulk density of the surface sediments was 1.52 g/cm^3, and mean water content (weight of water/ weight of solids) was 114% (G.H. Keller, unpublished data, 1982). These values yield a mean dry bulk density of the surface sediments of 0.78 g/cm^3. The accumulation of material from each source on the slope was then calculated by:

$$M_i = \sum_{\substack{\text{area} \\ \text{of} \\ \text{slope}}} S \cdot \rho_d \cdot (D) \cdot X_i \cdot A$$

where M_i = total mass accumulating on the slope per year from source area i,

S = sedimentation rate on the slope,

ρ_d = dry bulk density,

D = weight fraction of the sediment in the size range of interest,

X_i = contribution (weight fraction) from the source area i,

and A = area of the slope with sedimentation rate S and source area contribution X_i.

The slope sediments contain an average of 40.5% 2-20 μm material and 40.9% <2 μm material.

The results of the budget calculation are given in Table 7. For the 2-20 μm fraction, contributions from only two sources can be calculated with the chemical data. These results show good agreement of the total mass contributed in the 2-20 μm fraction as calculated

Table III-6. Sedimentation rates on the Oregon and Washington continental slope.

Province	Sedimentation Rate ($cm/10^3$ yr)	Number of rates available	Reference
Washington Upper Slope	10-44	5	Barnard (1978)
Washington Lower Slope	17-43	5	Barnard (1978)
Northern Oregon Upper Slope	30-40	0	Estimated
Northern Oregon Lower Slope	53	1	Kulm and Scheidegger (1979)
Central Oregon Upper Slope	20-30	0	Estimated
Central Oregon Lower Slope	25-50	0	Estimated
Southern Oregon Upper Slope	10	3	Kulm and Scheidegger (1979)
Southern Oregon Lower Slope	20-65	3	Kulm and Scheidegger (1979)

Table III-7. Source area contributions to slope sediments, estimated discharge of suspended sediment from each source area, and estimated effectiveness of the continental slope as a trap for fine-grained sediments derived from each source area. Results for the <2 μm fraction are speculative.

Source Area	Contributions (10^{12} g/yr.) to the slope sediments: Mineral Results	Chemical Results	Estimated Fluvial Input	% Retained on the slope: Mineral Results	Chemical Results
2-20 μm Fraction					
Columbia River	1.53-3.05	1.52-2.69	6.01	25.4-50.7	25.3-44.8
Klamath Mountains	1.21-1.94	1.93-3.21	4.22	28.7-46.0	13.2-30.7
California Coast Range	0.72-1.21		10.45	6.9-11.6	
<2 μm Fraction					
Columbia River	2.49-4.22	1.12-2.96	3.40	73.2-124.1	32.9-87.0
Klamath Mountains	0.47-0.95	1.03-2.26	3.21	4.0-8.0	8.7-19.1
California Coast Range			8.61		

using the mineral and the chemical data, and suggest that the source areas decrease in importance from north to south (i.e., in the order Columbia River, Klamath Mountains, California Coast Range). When grouped as a southern vs. northern source, the combined influence of the Klamath Mountain and California Coast Range material is slightly greater than that of the Columbia River. The centralized location of the Columbia River within the study area and the dispersal mechanisms which control the transport of Columbia River sediments (Krissek and Scheidegger, 1982b) combine to produce a strong Columbia River influence on the Washington and the central and northern Oregon continental slopes. Material from the southern sources must be transported further to be included within the study area boundaries, thereby limiting the Klamath Mountain and California Coast Range influence on the Oregon-Washington continental slope.

The estimates of fluvial input within the 2-20 μm and the <2 μm size fractions (Table 7) were calculated using the annual suspended sediment discharge data of Karlin (1980) and the suspended sediment grain size data compiled by Krissek (1982b). Approximately 50% of the 2-20 μm fluvial material discharged annually into the Pacific Ocean from streams within the study area is derived from the California Coast Range; only 7-12% of the California Coast Range input can be accounted for in the slope sediments. The remainder evidently either never enters the Oregon-Washington slope system or bypasses the system and is deposited in other areas (e.g., the Delgada Fan; Hein, 1973). The Klamath Mountains contribute approximately 20% of the annual input of 2-20 μm material, and 28-46% of the Klamath material is deposited

on the slope. The Columbia River contributes approximately 30% of the regional input, and 25-50% of this material remains within the system. It is interesting that both the Columbia River and the Klamath Mountains have between 25% and 50% of their 2-20 μm material trapped on the slope, since these two source areas lie predominantly or wholly within the boundaries of the study area. The California Coast Range is a more distant source, and its resultant influence on the slope (relative to its potential contribution) is smaller.

Because of the uncertainties associated with the <2 μm contribution calculations, the budget values listed in Table 7 for the <2 μm fraction are speculative. The Columbia River results estimate that 33-124% of the <2 μm material derived from that source area are trapped on the slope. However, large areas of the northeast Pacific Ocean are known to be dominated by fine-grained, Columbia-derived sediments (Griggs and Kulm, 1970; Duncan et al., 1970) of both Holocene and Pleistocene age. The abundant abyssal Pleistocene material may indicate that the trapping efficiency of the slope is significantly reduced during low stands of sea level. If the trapping efficiency of the slope is as high as indicated here, however, it is difficult to envision sufficient Columbia-derived material bypassing the slope to exert a strong influence on the abyssal deposits at the present time. In addition, the <2 μm material may remain in suspension longer than the 2-20 μm sediments and be transported further away from the source. Therefore, it is unlikely that <2 μm material should be trapped more efficiently on the slope than the 2-20 μm fraction. As a result, this budget does not allay our suspicions that the Columbia contributions

are erroneously high, and little significance can be placed on the budget for the <2 μm fraction.

The results of the 2-20 μm source area contribution and sediment budget calculations provide excellent examples of the formation of hemipelagic sediments from multiple sources. Fine-grained sediment studies in the past (Biscaye, 1965; Griffin et al., 1968; Kolla and Biscaye, 1973; Kolla et al., 1976) have emphasized the compositional changes which occur away from a single source without providing information on the material which acts to dilute that signal. In the case of the Washington and Oregon continental slope, multiple sources are identifiable in the chemical and mineral data, and the terrigenous components dominate the sediments. Therefore it is possible to describe the slope sediments as mixtures of material from the various source areas. In areas where a single source dominates the sediments (e.g., Columbia River influence on the Washington margin in the 2-20 μm fraction) the consideration of abundance changes away from the source are probably sufficient to describe the processes of sediment formation. In cases where several sources contribute equally to the sediment (e.g., central Oregon slope in the 2-20 μm fraction), the consideration of single mineral abundance changes away from a source provide a limited picture of the processes of sediment formation. That picture may be determined by the mineral which is considered, and may describe only a small portion of the resultant sediments. Therefore, whenever possible, the supply of sediment from several source areas should be investigated, especially in continental margin environments. Such investigations demand multivariate data sets and source area samples whenever possible,

but describe the processes of sediment formation much more fully than the single source approach.

PROJECT ACKNOWLEDGEMENTS

The author wishes to thank Mark E. Hower for assistance with the mineral and chemical analyses used in this study. Chi Meredith and Nicklas Pisias provided patient and valuable introductions to the world of linear programming and factor analysis. Ken Scheidegger, Ross Heath, and Jack Dymond reviewed the manuscript and provided constructive critiques throughout its many stages. This work was funded by the National Science Foundation under grant OCE-7819825 and by the NSF/Ocean Margin Drilling Program under JOI Subcontract 26-81.

BIBLIOGRAPHY

Arcaro, N.P., 1978. The control of lutite mineralogy by selective transport, Late Pleistocene and Holocene sediments of northern Cascadia Basin-Juan de Fuca abyssal plain (northeastern Pacific Ocean): A test of clay mineral size dependency. Unpubl. M.S. thesis, Lehigh Univ., Bethlehem, PA., 91 pp.

Baker, E.T., 1973. Distribution and composition of suspended sediment in the bottom waters of the Washington continental shelf and slope. J. Sed. Petrology, 43, 812-821.

Baldwin, E.M., 1964. Geology of Oregon. University of Oregon Cooperative Bookstore, Eugene, 2nd edition, 165 pp.

Barnard, W.D., 1978. The Washington continental slope: Quaternary tectonics and sedimentation. Mar. Geol., 27, 79-114.

Biscaye, P.E., 1965. Mineralogy and sedimentation of recent deep-sea clay in the Atlantic Ocean and adjacent seas and oceans. Geol. Soc. Am. Bull., 76, 803-832.

Brindley, G.W., 1961. Chlorite minerals. In Brown, G. (ed.), The X-ray Identification and Crystal Structures of Clay Minerals. Mineralogical Society, London, 242-296.

Bulfinch, D.L., and M.T. Ledbetter, 1981. Western boundary undercurrent delineated by fine-fraction particle-size analysis in HEBBLE area. EOS: Trans. Am. Geophys. Union, 62, 892.

Camden-Smith, F., L.A. Perrins, R.V. Dingle, and G.B. Brundrit, 1981. A preliminary report on long-term bottom-current measurements and sediment transport/erosion in the Agulhas Passage, southwest Indian Ocean. Mar. Geol., 39, M81-M88.

Carlson, P.R., 1968. Marine geology of Astoria submarine canyon. Unpubl. Ph.D. thesis, Oregon State Univ., Corvallis, 259 pp.

Carroll, D., 1970. Clay Minerals: A Guide to their X-ray Identification. Geol. Soc. Am. Special Paper 126, Boulder, CO., 80 pp.

Chambers, D.M., 1968. Holocene sedimentation and potential placer deposits on the continental shelf off the Rogue River, Oregon. Unpubl. M.S. thesis, Oregon State Univ., Corvallis, 102 pp.

Cobler, R., and J. Dymond, 1980. Sediment trap experiment on the Galapagos spreading center, equatorial Pacific. Science, 209, 801-803.

Cronan, D.S., 1974. Authigenic minerals in deep-sea sediments. In Goldberg, E.D. (ed.), The Sea, Vol. 5, Wiley-Interscience, New York, 491-525.

DeMaster, D.J., 1981. The supply and accumulation of silica in the marine environment. Geochem. Cosmochem. Acta, 45, 1715-1732.

Doyle, L.J., O.H. Pilkey, and C.C. Woo, 1979. Sedimentation on the eastern United States continental slope. In Doyle, L.J., and O.H. Pilkey (eds.), Geology of Continental Slopes, Society Economic Paleontologists Mineralogists Special Publication 27, Tulsa, OK., 119-129.

Duncan, J.R., 1968. Late Pleistocene and postglacial sedimentation and stratigraphy of deep-sea environments off Oregon. Unpubl. Ph.D. thesis, Oregon State Univ., Corvallis, 222 pp.

Duncan, J.R., and L.D. Kulm, 1970. Mineralogy, provenance, and dispersal history of late Quaternary deep-sea sands in Cascadia Basin and Blanco Fracture Zone off Oregon. J. Sed. Petrology, 40, 874-887.

Duncan, J.R., L.D. Kulm, and G.B. Griggs, 1970. Clay mineral composition of Late Pleistocene and Holocene sediments of Cascadia Basin, northeastern Pacific Ocean. J. Geol., 78, 213-221.

Dymond, J., and W. Eklund, 1978. A microprobe study of metalliferous sediment components. Earth Planet. Sci. Letters, 40, 243-251.

Dymond, J., J. B. Corliss, R. Cobler, C. M. Muratli, C. Chou, and R. Conard, 1980. Composition and origin of sediments recovered by deep drilling of sediment mounds, Galapagos spreading center. In Rosendahl, B. R., R. Hekinian, et al., Initial Reports of the Deep Sea Drilling Project, Volume 54, Washington (U. S. Government Printing Office), 377-385.

Dymond, J., 1981. The geochemistry of Nazca Plate surface sediments: an evaluation of hydrothermal, biogenic, detrital and hydrogenous sources. In Kulm, L.D., and others (eds.), Nazca Plate: Crustal Formation and Andean Convergence, Geol. Soc. Am. Memoir 154, Boulder, CO., 175-198.

Folk, R.L., 1980. Petrology of Sedimentary Rocks. Hemphill Publishing Co., Austin, TX., 182 pp.

Garrison, R.E., 1981. Pelagic and hemipelagic sedimentation in active margin basins. In Douglas, R.E., I.P. Colburn, and D.S. Gorsline (eds.), Depositional Systems of Active Continental Margin Basins (Short Course notes), Pacific Section, Society Economic Paleontologists Mineralogists, Los Angeles, CA., 15-38.

Gibbs, R.J., 1976a. The geochemistry of the Amazon River system: Part I. The factors that control the salinity and the composition and concentration of the suspended solids. Geol. Soc. Am. Bull., 78, 1203-1232.

Gibbs, R.J., 1967b. Quantitative X-ray diffraction analysis using clay mineral standards extracted from the samples to be analyzed. Clay Minerals, 7, 79-90.

Glenn, J.L., 1973. Relations among radionuclide content and physical, chemical, and mineral characteristics of Columbia River sediments. U.S. Geological Survey Professional Paper 433-M, U.S. Government Printing Office, Washington, D.C., 52 pp.

Griffin, J., and E.D. Goldberg, 1963. Clay mineral distribution in the Pacific Ocean. In Hill, M.N. (ed.), The Sea, vol. 3, Wiley-Interscience, New York, 728-741.

Griffin, J., H. Windom, and E.D. Goldberg, 1968. The distribution of clay minerals in the world ocean. Deep-Sea Res., 15, 433-459.

Griggs, G.B., and L.D. Kulm, 1970. Sedimentation in Cascadia deep-sea channel. Geol. Soc. Am. Bull., 81, 1361-1384.

Griggs, G.B., and J.R. Hein, 1980. Sources, dispersal, and clay mineral composition of fine-grained sediment off central and northern California. J. Geol., 88, 541-566.

Habib, D., 1972. Dinoflagellate stratigraphy, Leg 11, Deep-Sea Drilling Project. In Initial Reports of the Deep-Sea Drilling Project, U.S. Government Printing Office, Washington, D.C., vol. 11, 367-425.

Halpern, D., R.L. Smith, and R.K. Reed, 1978. On the California Undercurrent over the continental slope off Oregon. J. Geophys. Res., 83, 1366-1372.

Harlett, J.C., 1972. Sediment transport on the northern Oregon continental shelf. Unpubl. Ph.D. thesis, Oregon State Univ., Corvallis, 120 pp.

Harward, M.E., 1969. Methods and criteria for clay mineral identification. Unpubl. laboratory manual, Oregon State Univ., Department of Soils, Corvallis, 7 pp.

Hays, J. B., 1973. Clay petrology of mudstones, Leg 18, Deep Sea Drilling Project. In Kulm, L. D., Von Huene, R., et al., Initial Reports of the Deep Sea Drilling Project, Volume 18, Washington (U. S. Government Printing Office), 903-914.

Heath, G.R., and J. Dymond, 1977. Genesis and transformation of metalliferous sediments from the East Pacific Rise, Bauer Deep, and Central Basin, northwest Nazca plate. Geol. Soc. Am. Bull., 88, 723-733.

Heath, G.R., and J. Dymond, 1981. Metalliferous sediment deposition in time and space: East Pacific Rise and Bauer Basin, northern Nazca Plate. In Kulm, L.D., and others (eds.), Nazca Plate: Crustal Formation and Andean Convergence, Geol. Soc. Am. Memoir 154, Boulder, CO., 175-198.

Heath, G.R., and N.G. Pisias, 1979. A method for the quantitative estimation of clay minerals in North Pacific deep-sea sediments. Clays Clay Minerals, 27, 175-184.

Heezen, B.C., C.D. Hollister, and W.F. Ruddiman, 1966. Shaping of the continental rise by deep geostrophic contour currents. Science, 152, 502-508.

Hein, J.R., 1973. Increasing rate of movement with time between California and the Pacific Plate: From Delgada submarine fan source areas. J. Geophys. Res., 78, 7752-7762.

Hickey, B.M., 1979. The California Current System--hypotheses and facts. Progress in Oceanography, 8, 191-279.

Hollister, C.D., and B.C. Heezen, 1972. Geologic effects of ocean bottom currents: western North Atlantic. In Gordon, A.L. (ed.), Studies in Physical Oceanography, Gordon and Breach, London, 37-66.

Huyer, A., R.D. Pillsbury, and R.L. Smith, 1975. Seasonal variations in the alongshore velocity field over the continental shelf off Oregon. Limnol. Oceanogr., 20, 90-95.

Huyer, A., and R.L. Smith, 1976. Observations of a poleward undercurrent over the continental slope off Oregon, May-June 1975. EOS: Trans. Am. Geophys. Union, 57, 263.

Ingraham, W.J., 1967. The geostrophic circulation and distribution of water properties off the coasts of Vancouver Island and Washington, spring and fall, 1963. Fisheries Bull., 66, 223-250.

Johnson, D.A., and J.E. Damuth, 1979. Deep thermohaline flow and current-controlled sedimentation in the Amirante Passage: Western Indian Ocean. Mar. Geol., 33, 1-44.

Karlin, R., 1980. Sediment sources and clay mineral abundances off the Oregon coast. J. Sed. Petrology, 50, 543-560.

Klasik, J.A., and O.H. Pilkey, 1975. Processes of sedimentation on the Atlantic continental rise off the southeastern U.S. Mar. Geol., 19, 69-89.

Knebel, H.J., J.C. Kelly, and J.T. Whetten, 1968. Clay minerals of the Columbia River: A qualitative, quantitative, and statistical evaluation. J. Sed. Petrology, 38, 600-611.

Kolla, V., and P.E. Biscaye, 1973. Clay mineralogy and sedimentation in the East Indian Ocean. Deep-Sea Res., 20, 727-738.

Kolla, V., L. Henderson, and P.E. Biscaye, 1976. Clay mineralogy and sedimentation in the west Indian Ocean. Deep-Sea Res., 23, 949-962.

Korgen, B. J., G. Bodvarsson, and L. D. Kulm, 1970. Current speeds near the ocean floor west of Oregon. Deep-Sea Res., 17, 353-357.

Krissek, L.A., 1982a. Continental source area contributions to fine-grained sediments on the Oregon and Washington continental slope as calculated by linear programming. 27 manuscript pages, 7 tables, 13 illustrations.

Krissek, L.A., 1982b. The composition of fine-grained fluvial sediments of the Pacific Northwest. 25 manuscript pages, 8 tables, 8 illustrations.

Krissek, L.A., and K.F. Scheidegger, 1982a. A comparison of clay mineral abundances calculated by semiquantitative and quantitative methods. Submitted to J. Sed. Petrology, 7 manuscript pages, 1 table, 2 illustrations.

Krissek, L. A., and K. F. Scheidegger, 1982b. The sedimentological significance of an eastern boundary undercurrent and its role in continental margin sedimentation. 25 manuscript pages, 6 illustrations.

Krissek, L.A., K.F. Scheidegger, and L.D. Kulm, 1980. Surface sediments of the Peru-Chile continental margin and the Nazca Plate. Geol. Soc. Am. Bull., Part I, 91, 321-331.

Kulm, L.D., K.F. Scheidegger, J.V. Byrne, and J.J. Spigai, 1968. A preliminary investigation of the heavy mineral suites of the coastal rivers and beaches of Oregon and northern California. The Ore Bin, 30, 165-180.

Kulm, L.D., R.C. Roush, J.C. Harlett, R.H. Neudeck, D.M. Chambers, and E.J. Runge, 1975. Oregon continental shelf sedimentation: Interrelationships of facies distribution and sedimentary processes. J. Geol., 83, 145-175.

Kulm, L.D., and K.F. Scheidegger, 1979. Quaternary sedimentation on the tectonically active Oregon continental slope. In Doyle, L.J., and O.H. Pilkey (eds.), Geology of Continental Slopes, Society Economic Paleontologists Mineralogists Special Publication 27, Tulsa, OK., 247-263.

Ledbetter, M.T., 1979. Fluctuations of Antarctic bottom water velocity in the Vema Channel during the last 160,000 years. Mar. Geol., 33, 71-89.

Ledbetter, M.T., and B.B. Ellwood, 1980. Spatial and temporal changes in bottom-water velocity and direction from analysis of particle size and alignment in deep-sea sediment. Mar. Geol., 38, 245-261.

Ledbetter, M.T., C.R. Blaeser, and B.B. Ellwood, 1981. Bottom-current hydrodynamics in the Vema Channel based on particle-size and alignment parameters. EOS: Trans. Am. Geophys. Union, 62, 904.

Leeper, G.W., 1962. Introduction to Soil Science. 2nd edition, Melbourne University Press, Carlton, Victoria, Australia, 222 pp.

Leinen, M., and N. Pisias, 1982. An objective technique for determining end-member compositions and for partitioning sediments according to their sources. Submitted to Geochem. Cosmochem. Acta, 30 manuscript pages, 4 tables, 11 illustrations.

Lisitzin, A.P., 1972. Sedimentation in the world ocean. Society Economic Paleontologists Mineralogists Special Publication 17, Tulsa, OK., 218 pp.

Maloney, N.J., 1965. Geology of the continental terrace off the central coast of Oregon. Unpubl. Ph.D. thesis, Oregon State Univ., Corvallis, 233 pp.

McCave, I.N., 1979. Suspended material over the central Oregon continental shelf in May, 1974: I, Concentrations of organic and inorganic components. J. Sed. Petrology, 49, 1181-1194.

Needham, H.D., D. Habib, and B.C. Heezen, 1969. Upper Carboniferous palynomorphs as a tracer of red sediment dispersal patterns in the northwest Atlantic. J. Geol., 77, 113-120.

Olmstead, D.L., 1972. Clay mineralogy of the Washington continental slope. Unpubl. M.S. thesis, Univ. of Washington, Seattle, 43 pp.

Ongley, E.D., M.C. Bynoe, and J.B. Percival, 1981. Physical and geochemical characteristics of suspended solids, Witon Creek, Ontario. Can. J. Earth Sci., 18, 1365-1379.

Pak, H., G.F. Beardsley, Jr., and P.K. Park, 1970. The Columbia River as a source of light-scattering particles. J. Geophys. Res., 75, 4570-4578.

Pak, H., J.R.V. Zaneveld, and J. Kitchen, 1980. Intermediate nepheloid layers observed off Oregon and Washington. J. Geophys. Res., 85, 6697-6708.

Peterson, C., K. Scheidegger, and P. Komar, 1982. Sand dispersal patterns in an active margin estuary of the Pacific Northwest as indicated by sand composition, texture, and bedforms. Submitted to Mar. Geol., 21 manuscript pages, 3 tables, 8 illustrations.

Pinet, P.R., and W.P. Morgan, Jr., 1979. Implications of clay-provenance studies in two Georgia estuaries. J. Sed. Petrology, 49, 575-580.

Reed, R.K., and D. Halpern, 1976. Observations of the California Undercurrent off Washington and Vancouver Island. Limnol. Oceanogr., 21, 389-398.

Reimers, C.E., 1981. Sedimentary organic matter: Distribution and alteration processes in the coastal upwelling region off Peru. Unpubl. Ph.D. thesis, Oregon State Univ., Corvallis, 219 pp.

Rosato, V.J., and L.D. Kulm, 1981. Clay mineralogy of the Peru continental margin and adjacent Nazca Plate: Implications for provenance, sea level changes, and continental accretion. In Kulm, L.D., and others (eds.), Nazca Plate: Crustal Formation and Andean Convergence, Geol. Soc. Am. Memoir 154, Boulder, CO., 545-568.

Royse, C. F., 1964. Sediments of Willapa Submarine Canyon. Technical Report No. 111, Department of Oceanography, University of Washington, Seattle, 62 pp.

Russell, K.L., 1967. Clay mineral origin and distribution on Astoria Fan. Unpubl. M.S. thesis, Oregon State Univ., Corvallis, 40 pp.

Scheidegger, K.F., L.D. Kulm, and E.J. Runge, 1971. Sediment sources and dispersal patterns of Oregon continental shelf sands. J. Sed. Petrology, 41, 1112-1120.

Scheidegger, K.F., and L.A. Krissek, 1982. Dispersal and deposition of eolian and fluvial sediments off Peru and northern Chile. Geol. Soc. Am. Bull., 93, 150-162.

Schneider, H.I., and E.E. Angino, 1980. Trace element, mineral, and size analyses of suspended flood materials from selected eastern Kansas rivers. J. Sed. Petrology, 50, 1271-1278.

Smith, J.V., 1956. The powder patterns and lattice parameters of plagioclase feldspars. I. The soda-rich plagioclases. Mineralogist Magazine, 31, 47-68.

Spigai, J.J., 1971. Marine geology of the continental margin off southern Oregon. Unpubl. Ph.D. thesis, Oregon State Univ., Corvallis, 214 pp.

Stanley, D.J.P., H. Sheng, D.N. Lambert, P.A. Rona, D.W. McGrail, and J.S. Jenkyns, 1981. Current-influenced depositional provinces, continental margin off Cape Hatteras, identified by petrologic method. Mar. Geol., 40, 215-235.

Sternberg, R.W., and D.A. McManus, 1972. Implications of sediment dispersal from long-term, bottom-current measurements on the continental shelf of Washington. In Swift, D.J.P., D.B. Duane, and O.H. Pilkey (eds.), Shelf Sediment Transport, Dowden, Hutchinson, and Ross, New York, 181-194.

Stokke, P.R., B. Carson, and E.T. Baker, 1977. Comparison of the bottom nepheloid layer and late Holocene deposition on Nitinat Fan: implications for lutite dispersal and deposition. Geol. Soc. Am. Bull., 88, 1586-1592.

Tucholke, B.E., W.R. Wright, and C.D. Hollister, 1973. Abyssal circulation over the Greater Antilles Outer Ridge. Deep-Sea Res., 20, 973-995.

Tucholke, B.E., 1975. Sediment distribution and deposition by the Western Boundary Undercurrent: the Great Antilles Outer Ridge. J. Geol., 83, 177-207.

U.S. Geological Survey Water Data Reports, 1977-1980 (published annually). Water resources data for California, Oregon, and Washington.

Wang, C., 1978. Extractable Al, Fe, and Mn (and Si). In McKeague, J.A. (ed.), Manual on soil sampling and methods of analysis, 2nd edition, Canadian Society of Soil Science, 98-108.

Walker, G.W., and P.B. King, 1969. Geologic map of Oregon. U.S. Geological Survey, Washington, D.C., map number G69158.

Weissenborn, A.E., 1969. Geologic map of Washington. U.S. Geological Survey, Washington, D.C., map number G 68452.

Whetten, J.T., J.C. Kelley, and L.G. Hanson, 1969. Characteristics of Columbia River sediment and sediment transport. J. Sed. Petrology, 39, 1149-1166.

White, S.M., 1970. Mineralogy and geochemistry of continental shelf sediments off the Oregon-Washington coast. J. Sed. Petrology, 40, 38-54.

Zimmerman, H.B., 1971. Bottom currents on the New England continental rise. J. Geophys. Res., 76, 5865-5876.

Zimmerman, H.B., 1972. Sediments of the New England continental rise. Geol. Soc. Am. Bull., 83, 3709-3724.

APPENDICES

Appendix 1

Sample Locations and Water Depths

Sample Identification and Locations

Sample Number	Latitude	Longitude	Water Depth (m)
W7905A-106	46°13.75'N	124°39.50'W	522
107	46°17.60'N	124°48.89'W	817
108	46°17.99'N	124°58.44'W	1091
109	46°18.00'N	125°06.85'W	1650
110	46°18.21'N	125°26.18'W	1925
111	46°17.67'N	125°36.82'W	2256
112	45°50.25'N	125°36.04'W	2208
113	45°49.95'N	125°24.20'W	2010
115	45°50.20'N	125°10.02'W	1697
116	45°49.86'N	124°58.06'W	1594
117	45°49.95'N	124°50.00'W	950
118	45°49.96'N	124°43.02'W	321
119	45°21.66'N	124°23.04'W	265
120	45°21.02'N	124°45.14'W	585
121	45°21.03'N	124°53.10'W	909
122	45°21.00'N	125°03.93'W	1651
123	45°20.74'N	125°19.01'W	1711
125	45°00.10'N	125°31.42'W	2775
126	45°00.01'N	125°17.08'W	1979
127	45°00.04'N	125°01.06'W	944
128	45°00.10'N	124°42.94'W	480
129	45°00.23'N	124°25.03'W	280
130	44°50.13'N	124°34.98'W	298
131	44°49.99'N	124°52.23'W	504
132	44°50.03'N	125°00.15'W	1104
135	44°49.68'N	125°19.50'W	2027
136	44°49.99'N	125°32.14'W	2840
137	44°39.97'N	125°30.91'W	2880
138	44°39.79'N	125°14.35'W	2310

Continued

Appendix 1, continued

Sample	Latitude	Longitude	Water Depth (m)
W7905A-139	44°39.98'N	125°09.83'W	951
140	44°40.11'N	125°02.24'W	1082
141	44°39.93'N	124°54.01'W	524
142	44°29.95'N	124°53.92'W	456
143	44°29.97'N	125°02.03'W	1085
144	44°30.10'N	125°06.55'W	1275
145	44°30.24'N	125°12.94'W	1503
148	44°09.84'N	125°30.14'W	3054
149	44°10.34'N	125°16.61'W	2532
150	44°09.97'N	125°08.20'W	1560
151	44°10.00'N	124°01.68'W	1099
152	44°09.99'N	124°58.08'W	271
153	43°40.10'N	125°51.17'W	871
154	43°39.93'N	125°01.12'W	1224
155	43°40.04'N	125°09.27'W	1588
156	43°40.05'N	125°19.22'W	1962
157	43°39.99'N	125°28.29'W	3118
158	43°10.12'N	125°24.18'W	3120
159	43°09.86'N	125°13.02'W	1885
160	43°09.85'N	125°05.16'W	1459
161	43°09.98'N	124°58.04'W	1036
163	43°09.98'N	124°45.14'W	308
164	42°40.11'N	124°41.81'W	177
165	42°40.04'N	124°49.00'W	682
166	42°39.67'N	124°55.82'W	947
167	42°39.67'N	124°59.00'W	1410
169	42°39.94'N	125°15.99'W	3132
170	42°09.98'N	125°21.54'W	3150
171	42°10.01'N	125°06.91'W	1917
172	42°09.89'N	125°02.16'W	1670
173	42°09.99'N	125°54.00'W	998
174	42°09.90'N	125°44.82'W	616

Continued

Appendix 1, continued

Sample	Latitude	Longitude	Water Depth (m)
TT53-14	47°12.4'N	125°10.0'W	1700
53-17	46°51.5'N	125°42.0'W	1900
63-08	46°25.3'N	125°36.3'W	2312
63-10	46°34.2'N	125°17.4'W	1821
63-12	46°44.2'N	124°59.7'W	666
63-13	47°08.5'N	125°16.8'W	1489
63-16	47°36.8'N	125°24.3'W	992
63-17	47°22.3'N	125°44.5'W	1697
63-18	47°45.7'N	125°56.8'W	1591
63-19	47°54.6'N	125°54.1'W	1520
63-20	47°58.9'N	126°30.3'W	1811
68-26	47°07.6'N	125°57.1'W	2111

Appendix 2

Sediment Texture

Appendix 2

Fine Fraction (<63μm) Size Distribution: Wt. % in the Size Interval

Sample	% Sand	% Silt	% Clay	4.0-4.50	4.5-5.00	5.0-5.50	5.5-6.00	6.0-6.50	6.5-7.00	7.0-7.50	7.5-8.00	8.0-8.50	8.5-9.00	9.0-9.50	9.5-10.00	10.0-10.50	10.5-11.00	>11.0
W7905A-106G	84.8	5.6	9.7	0.0	6.4	12.8	8.7	7.4	1.3	0.0	0.0	4.5	6.4	7.0	3.2	1.9	1.9	38.5
-107G	3.0	39.4	57.5	2.7	5.3	5.0	3.9	7.0	2.6	5.1	10.6	4.3	4.3	3.0	4.9	5.1	5.1	30.9
-108G	0.7	38.9	60.4	2.0	2.3	4.6	3.8	6.4	6.4	4.6	7.5	4.5	4.7	5.7	4.4	3.1	1.7	37.4
-109G	0.7	34.8	64.4	2.6	0.8	3.8	2.5	4.2	4.5	4.4	10.7	5.7	2.9	1.7	4.2	5.7	5.7	38.9
-110G	16.2	30.7	53.1	4.8	7.2	2.8	1.2	3.1	5.4	6.8	5.5	4.5	5.7	6.7	6.2	5.7	4.8	29.2
-111G	2.2	45.4	52.4	4.0	4.0	4.2	6.1	8.3	9.4	3.8	9.2	6.2	5.3	2.6	3.2	4.8	4.6	23.2
-112G	10.4	41.4	48.2	4.6	3.4	6.1	7.9	4.3	3.2	5.4	10.2	4.6	4.5	4.3	5.4	9.5	13.3	11.8
-113G	0.3	34.1	65.6	2.8	1.4	0.3	6.0	5.4	4.0	6.1	8.7	5.7	6.0	4.8	4.4	4.6	4.7	34.2
-115G	0.5	35.8	63.6	0.5	2.4	1.8	4.0	5.6	6.7	5.8	9.4	5.8	6.3	7.0	6.9	5.4	3.2	28.8
-116G	0.4	33.8	65.7	0.6	0.9	0.9	3.5	7.4	6.6	8.6	7.7	7.2	7.5	5.4	5.9	5.4	5.0	27.2
-117G	1.7	40.4	57.9	4.7	1.4	5.0	7.0	6.1	4.5	5.4	6.8	4.0	8.1	6.1	5.8	1.1	0.7	31.4
-118G	69.4	19.7	10.8	24.5	11.2	4.9	4.9	3.6	1.5	1.9	3.2	1.8	1.4	1.4	0.8	1.0	1.0	28.1
-119G	48.3	31.9	19.8	3.1	16.1	15.5	9.8	8.5	2.6	2.8	2.2	1.3	2.9	3.8	4.0	2.2	1.4	22.8
-120G	21.1	36.2	42.7	4.0	5.6	5.3	3.1	6.5	9.5	6.7	6.2	3.4	5.3	2.7	4.4	3.8	5.3	26.8
-121G	0.9	40.6	58.4	0.3	2.1	3.4	6.6	5.4	6.6	5.6	10.2	5.8	5.5	3.4	5.3	3.6	4.1	31.8
-122G	1.0	32.1	66.9	0.0	0.4	1.5	3.0	6.4	7.4	6.1	7.7	6.2	8.1	7.6	7.8	5.0	3.3	28.3
-123G	2.4	36.3	61.3	2.6	1.7	1.8	4.2	5.6	6.5	8.2	6.9	6.1	7.8	7.2	7.1	6.6	5.8	19.5
-125G	2.0	33.6	64.4	0.8	2.8	3.7	2.0	4.8	6.8	5.5	9.1	5.5	6.5	5.1	4.4	4.0	4.6	34.3
-127G	0.9	51.8	47.3	1.8	4.0	6.9	7.0	11.0	9.9	4.0	9.4	5.6	5.2	2.7	4.0	5.1	5.7	16.7
-128G	86.8	3.9	9.2	10.9	0.7	0.3	3.4	5.4	2.4	0.9	1.0	3.8	4.3	4.8	1.4	3.4	5.4	47.0
-129G	43.1	39.5	17.4	19.8	17.1	6.6	2.1	8.1	5.4	2.0	0.8	0.6	1.5	2.6	2.6	2.6	2.4	18.1
-130G	23.0	53.7	23.2	18.0	12.0	10.9	6.1	4.4	4.1	3.4	3.2	0.7	1.0	1.8	2.1	1.9	1.8	21.3
-131G	2.8	42.9	54.3	0.6	5.8	6.6	6.2	7.2	9.1	6.0	4.2	3.6	3.3	2.9	5.1	5.6	3.5	29.2
-132G	5.3	47.3	47.3	4.3	3.6	6.0	7.2	8.3	5.4	4.8	10.5	5.1	3.8	3.4	3.4	3.0	1.5	29.5
-135G	8.6	49.3	42.1	7.4	8.0	6.3	5.8	6.5	8.0	6.4	5.2	5.2	5.4	6.1	3.9	2.8	0.0	21.6
-136G	1.0	49.2	49.8	2.6	7.9	6.2	5.9	4.8	6.9	9.0	8.3	4.2	4.6	3.2	3.7	4.4	4.6	23.3
-137G	1.3	42.0	56.7	3.7	4.6	4.2	2.3	6.6	7.0	7.6	8.2	7.4	7.3	4.7	4.1	4.3	4.4	22.7
-138G	0.8	52.6	46.5	1.9	3.1	2.9	3.8	10.9	15.1	7.1	8.2	4.3	4.1	3.8	4.7	3.6	2.2	23.7
-139G	60.4	14.3	25.2	0.0	0.7	2.6	5.0	5.2	8.7	10.0	3.9	1.2	1.2	2.6	3.8	6.6	8.0	40.4
-140G	23.1	38.4	38.4	8.5	4.8	8.0	6.2	5.2	7.6	3.7	2.0	2.6	6.4	6.7	6.7	3.6	4.0	19.8

Continued

Appendix 2, continued

Sample	% Sand	% Silt	% Clay	4.0-4.50	4.5-5.00	5.0-5.50	5.5-6.00	6.0-6.50	6.5-7.00	7.0-7.50	7.5-8.00	8.0-8.50	8.5-9.00	9.0-9.50	9.5-10.00	10.0-10.50	10.5-11.00	>11
W/905A-141G	56.3	19.1	24.6	6.5	9.2	5.7	4.1	3.5	7.5	4.7	1.1	0.7	0.5	1.7	2.9	4.8	5.3	40.1
-142G	20.0	52.9	27.2	23.6	11.0	6.1	4.5	6.8	3.4	1.8	0.9	2.5	4.9	4.7	4.1	2.5	3.5	11.4
-143G	16.1	37.5	46.4	4.8	2.1	5.0	8.1	6.4	6.0	4.4	5.6	4.5	3.5	7.6	6.7	7.7	3.9	21.6
-144G	0.6	51.8	47.6	0.0	0.0	3.4	8.5	12.2	10.9	8.7	6.9	1.6	3.0	6.4	9.4	6.9	3.9	18.1
-145G	1.5	45.0	53.5	0.6	3.3	6.3	4.8	7.7	9.7	8.0	7.1	5.5	5.9	4.3	4.1	3.4	2.8	26.4
-148G	0.6	31.9	67.5	0.0	1.2	3.0	2.2	4.2	8.6	6.9	8.6	5.7	6.5	8.0	6.8	5.6	1.0	31.8
-149G	0.4	42.7	56.9	0.6	2.0	2.3	5.3	7.5	8.3	10.2	8.1	6.0	6.9	6.5	6.2	5.0	3.9	21.2
-150G	0.3	51.6	48.1	0.8	3.0	5.7	5.9	8.6	7.6	8.6	10.6	5.4	4.6	4.4	4.7	3.9	3.0	22.8
-151G	0.8	68.4	30.9	7.0	6.4	9.6	8.9	7.2	10.4	9.8	8.7	4.2	4.6	2.9	1.6	0.2	0.1	16.7
-152G	84.0	7.7	8.3	11.4	6.6	11.6	2.4	0.6	1.3	4.6	3.3	3.3	2.9	4.9	2.9	2.3	0.3	36.3
-153G	0.6	61.6	37.8	5.6	6.5	5.6	9.2	10.9	8.4	8.1	7.2	2.4	3.9	4.2	5.0	4.5	3.5	12.7
-154G	4.0	40.9	55.1	2.6	3.0	5.6	6.6	12.7	2.2	4.2	6.7	4.6	5.0	4.1	5.6	6.3	6.1	23.5
-155G	2.0	42.3	55.7	0.0	1.6	3.8	4.7	8.6	9.6	8.4	7.9	7.9	7.8	6.2	2.6	2.8	3.0	24.8
-156G	6.4	44.2	49.4	1.6	2.2	5.6	4.9	7.1	6.1	9.4	10.0	3.7	3.8	5.2	7.4	7.6	6.4	18.5
-157G	0.4	38.4	61.2	0.3	1.4	2.0	3.7	6.5	5.7	7.6	10.2	7.3	7.3	7.6	7.0	7.2	7.8	18.1
-158G	1.3	38.2	60.5	0.6	1.6	4.2	3.0	4.9	7.4	8.0	10.2	5.7	5.2	7.3	6.5	5.7	1.0	28.5
-159G	4.3	41.8	53.8	1.2	1.9	3.9	6.6	5.4	8.2	8.5	9.7	4.6	4.6	5.7	5.3	4.8	1.2	27.9
-160G	23.2	40.2	36.6	3.3	5.2	5.0	9.0	9.1	8.6	8.1	5.4	4.5	5.0	5.5	3.8	3.1	0.2	23.2
-161G	1.4	53.8	44.8	1.8	3.6	5.0	7.8	10.8	10.1	9.9	7.7	4.5	5.3	3.5	3.5	3.4	3.2	19.4
-163G	35.7	47.0	17.3	21.3	12.2	9.5	7.5	5.1	4.1	3.5	3.5	1.9	3.1	2.0	2.4	1.9	2.4	11.7
-164G	81.0	11.1	7.9	7.1	6.1	6.5	8.1	10.4	5.0	6.8	6.6	2.9	3.2	2.7	2.7	2.7	2.3	24.0
-165G	2.2	58.6	39.2	1.6	5.6	8.3	9.0	11.6	9.8	7.5	8.6	5.9	6.0	3.9	3.7	3.0	2.2	13.1
-166G	1.1	55.5	43.4	2.2	3.5	6.5	9.5	8.9	10.1	8.6	7.9	7.1	7.0	4.8	2.5	3.4	4.3	12.7
-167G	5.4	51.8	42.8	3.7	5.5	6.7	8.3	9.0	9.1	7.4	5.6	4.0	5.5	4.3	4.2	2.3	1.8	21.8
-169G	0.4	41.3	58.2	1.6	2.4	1.2	4.2	7.7	7.6	9.7	9.8	8.0	7.9	5.9	5.8	5.4	3.7	18.8
-170G	1.1	35.4	63.5	0.5	1.1	1.8	3.7	5.6	8.0	8.4	9.1	6.0	7.3	6.8	7.7	6.3	4.2	23.3
-171G	8.9	37.9	53.2	0.8	1.9	2.0	4.8	6.9	8.4	8.0	9.1	5.9	7.5	6.9	6.8	5.4	4.7	19.5
-172G	64.9	16.9	18.2	3.9	3.5	3.2	4.6	5.3	10.5	10.5	5.3	4.2	5.6	6.0	3.7	1.6	0.7	30.1
-173G	1.6	57.9	40.5	3.8	4.2	7.8	9.8	10.4	9.0	6.8	7.3	4.0	4.7	3.0	3.2	2.5	3.5	19.5
-174G	3.4	65.7	30.9	4.3	7.7	10.4	9.7	11.7	9.6	7.5	6.2	3.4	3.4	3.4	3.0	3.6	3.8	10.8
-175G	35.3	46.7	18.0	18.7	21.2	12.0	4.3	6.1	4.7	2.5	0.6	0.0	0.0	1.7	2.1	3.6	3.4	17.0

Continued

Appendix 2, continued

Sample	% Sand	% Silt	% Clay	4.0-4.50	4.5-5.00	5.0-5.50	5.5-6.00	6.0-6.50	6.5-7.00	7.0-7.50	7.5-8.00	8.0-8.50	8.5-9.00	9.0-9.50	9.5-10.00	10.0-10.50	10.5-11.00	>11
TT53-14	4.2	73.6	20.8	15.6	15.3	13.8	6.8	6.1	4.8	1.2	5.0	4.9	4.9	2.4	1.5	1.3	1.3	16.0
TT53-17	1.4	47.8	50.8	3.2	3.2	3.4	6.4	6.6	8.8	6.5	8.5	8.1	5.5	5.0	1.0	1.0	8.8	23.8
TT63-08	34.1	36.0	29.9	1.1	4.5	4.2	7.1	9.6	9.8	7.8	7.5	7.5	7.2	5.0	3.0	3.0	3.0	21.5
TT63-10	1.5	40.6	57.8	1.2	1.8	1.5	5.3	5.5	7.1	4.6	9.3	7.8	7.8	2.5	2.5	2.5	10.9	29.8
TT63-12	1.2	36.9	61.9	1.2	1.2	1.2	3.5	8.2	4.7	4.5	7.2	12.6	3.1	7.0	5.8	5.8	5.8	32.2
TT63-13	1.6	55.7	42.8	2.4	2.1	2.7	3.6	9.5	5.9	4.4	11.5	5.6	2.1	6.5	4.7	1.2	1.2	36.7
TT63-16	11.6	42.8	45.6	5.0	3.0	3.2	7.6	7.0	6.6	1.1	7.0	6.1	6.1	7.2	7.0	3.0	3.0	27.5
TT63-17	12.6	39.7	47.7	0.7	0.7	0.7	2.7	4.7	8.5	4.1	10.2	9.2	9.5	3.4	6.1	1.7	2.0	35.9
TT63-18	2.2	45.1	52.6	1.3	1.2	3.6	3.8	10.4	2.0	7.3	9.9	6.8	4.1	6.8	3.1	3.1	3.1	33.4
TT63-19	1.8	44.5	53.6	2.3	2.1	2.1	2.3	7.2	7.2	5.6	5.1	6.2	6.4	6.4	5.6	5.4	5.4	30.8
TT63-20	3.1	46.1	50.8	2.2	4.0	3.5	2.7	9.5	2.2	6.2	7.1	8.9	5.3	6.0	3.1	3.1	2.9	33.3
TT68-26	3.6	41.3	55.1	0.9	4.1	4.6	0.3	5.8	4.1	4.1	7.0	8.7	9.3	5.8	5.5	5.2	5.2	29.6

Appendix 3

Quantitative River Mineral 2-20 μm Data

Appendix 3 — 2 - 20μm River Samples, Quantitative Mineral Abundances

Sample	% Smectite	% Chlorite	% Illite	% Hornblende	% Quartz	% Feldspar
Bank Samples						
Soleduck	15.3	9.6	15.8	0.0	17.6	20.8
Bogachiel	8.1	7.1	13.1	0.0	16.1	17.8
Hoh	0.0	11.4	14.1	0.0	35.6	47.4
Queets	0.0	13.2	37.7	0.0	28.7	26.7
Quinault	0.0	14.6	42.1	0.0	34.6	32.1
Humptulips	25.9	5.6	5.3	0.0	23.0	33.2
North	57.2	1.3	26.9	0.0	9.6	25.2
Willapa	0.0	2.3	23.3	0.0	18.4	33.2
Columbia M-7	0.0	1.6	25.3	1.3	15.0	36.5
Columbia M-9	0.0	2.2	23.1	0.7	16.8	31.1
Necanicum	86.2	0.0	8.8	0.0	18.6	12.3
Nehalem	97.3	0.0	0.0	0.0	6.0	13.0
Miami	63.6	0.4	0.0	0.0	6.9	28.2
Kilchis	81.8	0.0	0.0	0.0	5.6	17.0
Wilson	101.4	0.0	0.0	0.0	8.4	16.5
Trask	94.8	0.0	0.0	0.0	9.4	12.0
Tillamook	137.0	0.0	1.5	0.0	13.7	9.9
Nestucca	108.1	0.0	2.0	0.7	10.2	8.6
Little Nestucca	68.6	0.5	16.4	1.3	16.0	9.4

Continued

Appendix 3, continued

Sample	% Smectite	% Chlorite	% Illite	% Hornblende	% Quartz	% Feldspar
Neskowin Creek	79.8	0.0	5.6	0.0	10.9	10.8
Salmon	97.4	1.0	6.3	0.0	15.8	7.7
Siletz	66.9	0.0	8.5	0.7	12.7	8.3
Yaquina	55.3	1.7	26.0	0.0	26.0	17.1
Alsea	60.6	0.0	13.6	0.0	16.7	11.9
Yachats	75.1	0.5	5.7	0.0	10.0	20.1
Big Creek	63.7	0.0	0.0	0.0	8.4	23.1
Cape Creek	82.9	0.0	0.0	0.0	5.8	23.9
Siuslaw	54.9	0.0	18.5	0.0	20.7	15.9
Siltcoos	18.8	0.6	1.8	0.0	21.5	20.5
Smith (Oregon)	32.1	0.6	10.2	0.0	19.5	24.8
Umpqua	37.6	2.5	8.5	0.7	18.3	14.5
Coos	87.8	0.0	0.0	0.0	7.6	27.6
Millicome	46.6	2.5	14.2	0.0	19.9	14.1
Coquille	42.6	5.2	6.4	0.1	20.2	20.1
Fourmile Creek	54.0	4.1	3.9	0.0	20.8	14.6
Floras Creek	0.0	7.5	5.3	0.0	44.6	23.9
Sixes	84.2	6.3	0.4	0.0	19.4	15.4
Elk	44.3	9.1	7.0	4.5	18.8	18.8
Brush Creek	0.0	17.9	29.9	0.9	11.2	11.2
Euchre Creek	0.0	21.6	31.4	0.0	19.3	15.4

Continued

Appendix 3, continued

Sample	% Smectite	% Chlorite	% Illite	% Hornblende	% Quartz	% Feldspar
Rogue	0.0	19.7	34.1	14.1	12.8	16.4
Hunter Creek	78.3	13.8	3.0	0.0	20.6	16.5
Pistol	46.4	15.4	9.4	0.0	19.0	13.9
Chetco	0.0	13.8	20.2	0.0	31.3	37.0
Winchuck	3.5	6.4	11.4	0.0	14.4	17.6
Smith (California)	0.0	34.9	26.2	18.5	15.2	16.8
Klamath	0.0	41.2	69.8	15.6	10.7	14.0
Redwood Creek	0.0	32.0	58.2	0.0	11.7	12.8
Little	0.0	20.9	25.6	0.0	21.7	17.0
Mad	0.0	17.5	24.6	0.1	19.4	20.7
Eel	0.0	9.8	10.0	0.0	20.2	25.0
Suspended Samples						
Chehalis - 1/27/78	0.0	2.8	7.3	0.0	12.9	33.8
Chehalis - 2/03/78	0.0	0.7	1.8	0.0	12.5	24.1
Chehalis - 2/10/78	0.0	2.4	7.8	0.0	9.0	21.0
Chehalis - 2/24/78	0.0	0.0	1.9	0.0	9.4	21.6
Umpqua	60.6	3.2	8.5	1.9	21.0	18.6
Rogue	0.0	11.1	12.2	10.8	16.9	21.7
Klamath	0.0	27.6	43.7	15.6	26.1	32.0
Mad	0.0	17.5	26.0	0.0	18.5	20.2
Eel	0.0	16.2	16.6	0.0	18.7	35.3

Appendix 4

Quantitative Marine Mineral 2-20 μm Data

Appendix 4

2 - 20μm Quantitative Mineral Abundances

Sample	% Smectite	% Chlorite	% Illite	% Hornblende	% Quartz	% Feldspar
TT53-14 2-20	0.0	0.5	4.8	0.0	19.4	35.8
TT53-17 2-20	0.0	7.2	11.0	2.9	24.1	52.8
TT63-08 2-20	0.0	9.4	22.6	5.1	20.4	48.9
TT63-10	0.0	6.6	14.8	2.4	24.2	39.8
TT63-12	0.0	3.1	11.9	0.8	20.9	40.0
TT63-13	0.0	5.8	14.0	0.6	23.5	65.4
TT63-16	0.0	6.2	10.6	0.0	22.0	46.6
TT63-17	0.0	6.4	14.4	0.0	22.2	49.8
TT63-18	0.0	5.2	9.1	0.0	26.8	55.1
TT63-19	0.0	4.8	6.4	0.0	21.1	82.6
TT63-20	0.0	3.9	9.1	0.0	23.7	48.8
TT68-26	0.0	7.6	12.6	0.0	26.4	51.8
107G 2-20	0.0	7.1	17.3	1.9	20.0	32.0
108G 2-20	0.0	6.2	25.3	1.3	17.0	39.0
109G	0.0	7.6	15.8	3.7	17.0	40.0
110G	0.0	8.2	34.1	3.1	25.0	37.0
111G	0.0	4.9	26.0	3.1	15.0	37.0
112G	0.0	7.0	16.6	0.7	22.0	35.0
113G	0.0	9.1	23.9	0.7	17.0	37.0

Continued

Appendix 4, continued

Sample	% Smectite	% Chlorite	% Illite	% Hornblende	% Quartz	% Feldspar
115G	0.0	8.1	20.2	1.3	18.0	30.0
116G	0.0	8.5	25.3	3.1	17.0	22.0
117G	0.0	5.8	14.4	0.1	16.0	32.0
118G	0.0	4.9	13.6	0.1	26.0	48.0
119G	0.0	7.1	12.2	1.3	19.0	36.0
120G	0.0	7.1	13.6	1.3	16.0	18.0
121G	0.0	11.1	31.9	3.7	20.0	30.0
122G	0.0	10.8	25.3	3.1	21.0	26.0
123G	0.0	9.4	29.7	4.3	19.0	26.0
125G	0.0	10.3	25.3	5.5	18.0	21.0
127G	0.0	13.6	22.4	4.3	17.0	19.0
129G	0.0	7.8	17.3	3.7	22.0	25.0
130G	0.0	8.7	10.7	1.9	27.0	29.0
131G	0.0	9.6	31.9	4.3	22.0	33.0
132G	0.0	11.1	20.2	3.1	19.0	24.0
135G	0.0	13.6	27.5	5.5	17.0	21.0
137G	0.0	12.4	28.2	3.7	19.0	24.0
138G	0.0	12.9	23.9	4.3	18.0	18.0
139G	0.0	12.2	20.9	3.10	19.0	23.0
140G	0.0	12.9	19.5	7.9	16.0	23.0

Continued

Appendix 4, continued

Sample	% Smectite	% Chlorite	% Illite	% Hornblende	% Quartz	% Feldspar
141G	0.0	10.1	16.6	4.3	19.0	16.0
142G	0.0	13.0	22.4	7.9	16.0	24.0
143G	0.0	14.5	29.7	7.9	21.0	30.0
144G	0.0	15.4	24.6	5.5	20.0	22.0
145G	0.0	12.5	19.5	3.7	21.0	32.0
148G	0.0	10.7	19.5	2.5	16.0	23.0
149G	0.0	11.3	14.4	2.5	19.0	19.0
150G	0.0	11.7	23.9	4.3	17.0	23.0
151G	0.0	12.5	23.1	7.3	16.0	19.0
152G	0.0	9.2	18.0	6.7	17.0	18.0
153G	0.0	20.0	24.6	5.5	20.0	21.0
154G	0.0	10.3	17.3	5.5	23.0	24.0
155G	0.0	9.0	15.1	1.9	19.0	33.0
156G	0.0	18.0	25.3	3.7	24.0	31.0
157G	0.0	12.3	20.9	4.3	22.0	21.0
158G	0.0	13.8	19.5	3.1	23.0	30.0
159G	0.0	10.2	20.9	3.7	19.0	22.0
160G	0.0	15.5	23.9	3.1	25.0	29.0
161G	0.0	12.2	27.5	2.51	24.0	20.0
163G	0.0	16.1	24.6	10.2	22.0	24.0

Continued

Appendix 4, continued

Sample	% Smectite	% Chlorite	% Illite	% Hornblende	% Quartz	% Feldspar
164G	0.0	12.5	21.7	8.5	21.0	20.0
165G	0.0	18.5	34.8	4.9	18.0	14.0
166G	0.0	12.3	23.1	5.5	17.0	20.0
167G	0.0	19.2	24.6	3.7	23.0	31.0
169G	0.0	13.5	21.7	6.1	13.0	17.0
170G	0.0	13.9	22.4	3.1	20.0	26.0
171G	0.0	11.8	24.6	3.7	21.0	21.0
172G	0.0	11.8	20.2	1.3	23.0	29.0
173G	0.0	12.5	16.6	4.3	26.0	37.0
174G	0.0	21.9	36.3	6.1	23.0	32.0
175G	0.0	17.1	21.7	10.8	27.0	35.0

Appendix 5

Quantitative River Mineral <2 μm Data

Appendix 5 <2μm River Samples, Quantitative Mineral Abundances

Sample	% Smectite	% Chlorite	% Illite	% Quartz	% Feldspar
Bank Samples					
Soleduck	25.3	5.2	0.0	5.5	3.6
Bogachiel	0.0	7.6	5.8	5.9	3.7
Hoh	2.7	6.2	19.6	6.7	7.6
Queets	0.0	4.1	18.2	5.2	0.9
Quinault	0.1	11.1	33.4	9.7	13.1
Humptulips	23.5	1.6	2.0	5.0	1.4
North	100.5	0.0	2.6	5.6	6.2
Willapa	87.1	0.0	2.7	5.3	5.2
Columbia M-7	52.1	0.0	4.2	4.5	4.0
Columbia M-9	68.8	0.0	0.0	3.8	3.0
Necanicum	44.2	0.0	2.7	6.2	1.8
Nehalem	73.8	0.0	0.0	2.9	2.4
Miami	46.9	0.0	0.0	3.3	2.5
Kilchis	95.9	0.0	0.0	2.6	0.9
Wilson	80.6	0.0	0.0	4.4	3.5
Trask	82.7	0.0	0.4	4.1	3.7
Tillamook	68.0	0.0	0.0	5.4	1.2
Nestucca	131.5	0.0	0.0	6.8	3.4

Continued

Appendix 5, continued

Sample	% Smectite	% Chlorite	% Illite	% Quartz	% Feldspar
Little Nestucca	71.8	0.0	1.8	5.6	0.9
Neskowin Creek	102.0	0.0	0.0	8.9	12.6
Salmon	48.3	0.0	0.0	4.6	1.3
Siletz	104.3	0.0	0.0	5.6	3.8
Yaquina	50.4	0.0	2.2	4.4	1.4
Alsea	68.1	0.0	0.0	5.3	0.6
Yachats	35.9	0.0	1.1	3.6	2.1
Big Creek	54.6	0.0	1.8	3.9	5.4
Cape Creek	52.0	0.0	0.0	3.1	1.6
Siuslaw	20.7	1.2	0.0	5.5	1.4
Siltcoos	24.0	0.0	0.0	4.9	3.0
Smith (Oregon)	28.6	0.0	0.0	4.5	2.1
Umpqua	62.5	0.0	0.0	4.2	1.4
Coos	44.1	0.0	0.0	3.5	4.3
Millicome	52.4	0.0	0.5	6.2	2.7
Coquille	106.8	5.7	0.0	4.9	2.4
Fourmile Creek	56.9	0.5	6.4	5.9	2.4
Floras Creek	43.7	2.4	7.8	5.1	0.8
Sixes	51.7	1.7	5.6	5.4	2.2
Elk	29.7	1.4	4.3	6.0	4.2

Continued

Appendix 5, continued

Sample	% Smectite	% Chlorite	% Illite	% Quartz	% Feldspar
Brush Creek	51.0	2.6	4.9	3.7	1.9
Euchre Creek	5.7	2.9	15.4	4.8	1.6
Rogue	65.1	6.4	4.2	4.3	2.1
Hunter Creek	62.5	4.0	4.6	3.8	1.3
Pistol	58.3	5.8	10.1	3.6	0.9
Chetco	0.0	8.0	33.9	3.5	0.8
Winchuck	0.0	6.4	9.5	5.9	3.8
Smith (California)	14.4	14.4	15.0	4.8	3.7
Klamath	21.1	7.7	0.0	9.8	4.3
Redwood Creek	0.0	13.8	64.1	3.3	0.0
Little	0.0	5.5	13.4	3.4	0.9
Mad	46.9	10.5	24.6	3.7	0.1
Eel	49.7	6.8	7.1	4.1	4.2
Suspended Samples					
Chehalis - 1/27/78	0.0	2.7	0.0	3.5	13.5
Chehalis - 2/03/78	0.0	1.7	2.1	6.1	17.4
Chehalis - 2/10/78	0.0	4.7	0.0	5.4	17.1
Chehalis - 2/24/78	0.0	7.2	0.0	8.0	8.9
Umpqua	76.8	0.0	0.0	3.9	2.1

Continued

Appendix 5, continued

Sample	% Smectite	% Chlorite	% Illite	% Quartz	% Feldspar
Rogue	26.8	8.2	14.4	11.7	12.2
Klamath	13.5	8.8	14.4	8.1	11.5
Mad	15.4	10.0	15.1	5.5	3.5
Eel	18.8	13.2	15.1	7.0	4.4

Appendix 6

Quantitative Marine Mineral <2 μm Data

Appendix 6 <2μm Quantitative Mineral Abundances

Sample	% Smectite	% Chlorite	% Illite	% Quartz	% Feldspar
TT53-14	84.0	0.0	8.6	4.2	4.6
TT53-17	59.2	5.5	12.1	6.6	17.7
TT63-08	98.8	3.2	18.9	6.5	15.0
TT63-10	104.0	1.5	9.4	5.4	8.0
TT63-12	58.2	1.0	18.8	7.0	13.5
TT63-13	73.4	1.3	8.6	4.3	5.2
TT63-16	77.6	0.4	9.8	4.8	7.9
TT63-17	52.2	0.0	5.3	4.0	3.8
TT63-18	68.6	0.3	7.8	4.7	7.5
TT63-19	77.8	0.0	8.5	4.1	5.1
TT63-20	122.4	0.0	6.8	5.1	7.0
TT68-26	57.2	1.1	7.2	5.5	10.0
W7905A-106G	103.9	1.8	2.0	5.7	9.8
-107G	95.1	2.3	5.6	4.4	6.5
-108G	76.6	2.3	3.4	4.6	5.4
-109G	73.7	3.4	8.5	5.0	7.2
-110G	89.5	5.3	0.0	6.1	9.2
-111G	106.1	4.0	6.4	4.2	4.9
-112G	102.4	2.5	6.4	4.0	7.1

Continued

Appendix 6, continued

Sample	% Smectite	% Chlorite	% Illite	% Quartz	% Feldspar
W7905A-113G	49.5	7.2	12.2	4.9	4.2
-115G	81.1	4.8	8.5	5.8	7.4
-116G	92.0	1.4	2.7	4.1	2.4
-117G	89.3	3.3	5.6	4.2	5.7
-118G	108.6	2.9	3.4	5.5	5.7
-119G	110.8	2.6	0.5	5.8	6.9
-120G	68.4	3.3	7.1	5.0	2.6
-121G	66.8	4.6	4.9	5.2	4.8
-122G	65.2	4.0	4.9	4.4	3.0
-123G	68.5	1.8	2.7	4.9	6.0
-125G	78.8	5.7	10.7	6.1	5.1
-127G	66.8	4.1	5.6	5.0	5.8
-128G	102.6	4.2	9.3	4.5	4.8
-129G	102.5	2.4	3.4	4.4	3.3
-130G	79.0	3.4	0.0	4.7	5.7
-131G	71.4	2.8	4.2	4.3	4.2
-132G	70.8	4.7	6.4	3.9	2.2
-135G	64.4	6.4	10.7	6.1	6.0
-136G	75.7	3.5	9.3	4.8	5.4
-137G	91.7	4.6	7.8	5.0	4.4

Continued

Appendix 6, continued

Sample	% Smectite	% Chlorite	% Illite	% Quartz	% Feldspar
W7905A-138G	69.6	4.1	9.3	4.5	3.6
-139G	83.3	8.4	7.1	4.6	6.4
-140G	110.0	4.8	7.1	4.8	4.3
-141G	70.8	3.6	6.4	5.0	3.6
-142G	69.6	4.6	8.5	5.2	3.8
-143G	73.4	4.7	10.7	4.9	2.9
-144G	74.8	2.9	4.2	4.8	1.3
-145G	70.7	5.8	10.5	5.6	4.2
-148G	66.5	5.8	7.8	5.1	4.1
-149G	72.5	5.3	10.0	4.9	3.0
-150G	90.3	4.7	9.3	4.5	1.9
-151G	84.3	3.1	4.2	4.9	1.6
-152G	91.4	3.0	4.2	3.6	0.7
-153G	105.4	4.5	9.3	5.0	4.4
-154G	73.7	5.3	9.3	4.2	1.2
-155G	65.8	6.0	14.4	6.1	4.9
-156G	79.7	6.6	10.0	4.8	3.5
-157G	93.6	6.2	9.3	4.4	2.3
-158G	83.9	6.2	9.3	5.0	2.8
-159G	103.2	5.3	5.6	4.2	1.2
-160G	68.5	4.2	7.1	6.1	2.7

Continued

Appendix 6, continued

Sample	% Smectite	% Chlorite	% Illite	% Quartz	% Feldspar
W7905A-161G	81.5	5.1	11.5	4.4	1.2
-163G	82.4	6.0	9.3	4.8	2.6
-164G	98.1	5.5	7.8	3.2	0.7
-165G	64.9	6.3	10.0	4.1	4.6
-166G	51.9	3.9	7.8	4.4	1.8
-167G	91.2	6.7	14.4	5.4	4.1
-169G	64.5	6.6	8.5	6.1	2.8
-170G	84.2	6.0	10.0	7.0	3.4
-171G	80.4	3.8	6.4	4.8	4.1
-172G	61.2	3.6	8.5	6.3	6.6
-173G	63.1	7.7	10.7	4.8	2.7
-174G	71.4	4.7	12.9	5.5	.01
-175G	68.3	4.7	9.3	4.9	0.9

Appendix 7

Semiquantitative River Mineral <2 μm Data

Appendix 7

<2μm River Samples, Semiquantitative Clay Mineral Abundances

Samples	% Smectite	% Illite	% Chlorite
River Bank Samples			
Soleduck	14.5	26.6	58.8
Bogachiel	2.5	35.6	62.0
Hoh	2.8	39.6	57.6
Queets	0.0	53.4	46.6
Quinault	1.1	47.9	51.0
Humptulips	23.9	18.1	58.0
North	88.1	6.5	5.3
Willapa	69.0	15.7	15.3
Columbia M-7	42.8	31.1	26.0
Columbia M-9	62.7	19.3	18.0
Necanicum	65.8	13.1	21.1
Nehalem	31.9	19.3	48.8
Miami	100.0	0.0	0.0
Kilchis	100.0	0.0	0.0
Wilson	85.2	6.3	8.5
Trask	82.1	5.7	12.2
Tillamook	86.8	8.2	5.0
Nestucca	91.6	2.6	5.7
Little Nestucca	59.0	15.9	25.1
Neskowin Creek	77.8	14.2	8.0
Salmon	74.2	10.6	15.2
Siletz	67.3	11.2	21.5
Yaquina	54.8	23.6	21.6
Alsea	60.2	11.6	28.2
Yachats	66.5	17.6	16.0
Big Creek	64.6	18.5	16.9
Cape Creek	100.0	0.0	0.0
Siuslaw	46.4	17.6	36.0
Siltcoos	57.6	8.2	34.2

Continued

Appendix 7, continued

Sample	% Smectite	% Illite	% Chlorite
Smith (Oregon)	51.5	20.2	28.3
Umpqua	76.8	5.3	17.9
Coos	83.9	7.8	8.2
Millicome	43.2	13.1	43.7
Coquille	46.2	17.3	36.4
Fourmile Creek	26.1	26.5	47.4
Floras Creek	24.6	32.2	43.2
Sixes	34.9	24.5	40.6
Elk	10.0	35.8	54.2
Brush Creek	34.9	28.3	26.8
Euchre Creek	5.8	47.0	47.2
Rogue	20.4	26.9	52.6
Hunter Creek	35.2	14.3	50.5
Pistol	17.7	31.9	50.3
Chetco	0.0	41.1	58.9
Winchuck	0.0	43.3	56.7
Smith (California)	7.7	27.7	64.5
Klamath	4.2	52.3	43.6
Redwood Creek	0.0	58.9	41.0
Little	8.8	42.2	48.9
Mad	4.5	38.8	57.1
Eel	12.0	38.6	49.3
River Suspended Samples			
Chehalis - 1/27/78	0.0	26.9	73.1
Chehalis - 2/03/78	0.0	24.4	75.6
Chehalis - 2/10/78	0.0	22.5	77.5
Chehalis - 2/24/78	0.0	27.0	73.0
Umpqua	35.8	25.0	39.2
Rogue	13.4	25.5	61.1
Klamath	10.8	31.4	57.8
Mad	4.8	45.7	49.4
Eel	11.1	37.8	51.1

Appendix 8

Semiquantitative Marine Mineral <2 μm Data

Appendix 8

<2μm Semiquantitative Clay Mineral Abundances

Sample	% Smectite	% Illite	% Chlorite
TT53-14	44.4	31.8	23.8
TT53-17	17.5	34.1	48.4
TT63-08	35.2	35.2	29.6
TT63-10	43.4	31.6	25.0
TT63-12	15.9	54.2	30.0
TT63-13	39.5	32.1	28.4
TT63-16	45.7	27.9	26.3
TT63-17	46.8	24.5	28.7
TT63-18	44.5	26.7	28.8
TT63-19	40.6	31.1	28.2
TT63-20	41.4	28.3	30.3
TT68-26	34.2	33.8	32.0
W7905A-106G	57.3	21.2	21.5
-107G	50.5	21.6	27.8
-108G	47.2	22.4	30.4
-109G	46.9	23.5	24.6
-110G	40.4	27.8	31.7
-111G	46.4	21.7	31.9
-112G	48.3	21.3	30.4
-113G	33.9	26.4	39.8
-115G	43.7	24.0	32.3
-116G	44.9	20.0	35.1
-117G	43.4	21.8	34.7
-118G	50.3	21.8	27.9
-119G	49.3	18.4	32.4
-120G	38.6	26.0	35.4
-121G	39.5	21.8	38.6
-122G	39.6	23.0	37.4
-123G	34.1	28.6	37.3
-125G	39.2	25.7	35.1

Continued

Appendix 8, continued

Sample	% Smectite	% Illite	% Chlorite
W7905A-127G	40.0	18.9	41.1
-128G	42.0	20.1	37.8
-129G	51.7	18.8	29.5
-130G	46.8	17.4	35.8
-131G	40.3	19.9	39.8
-132G	39.2	22.2	38.6
-135G	40.2	23.6	36.1
-136G	40.0	24.3	35.7
-137G	39.7	26.2	34.1
-138G	36.2	21.0	42.8
-139G	30.9	29.5	39.5
-140G	39.9	22.4	37.6
-141G	32.8	26.9	40.3
-142G	35.0	27.1	37.9
-143G	35.0	24.3	40.8
-144G	32.9	25.8	41.3
-145G	29.1	25.0	45.9
-148G	38.9	23.6	37.5
-149G	38.0	25.7	36.4
-150G	30.0	32.5	37.5
-151G	33.9	34.4	31.7
-152G	42.9	22.0	35.1
-153G	32.9	26.1	41.0
-154G	29.2	24.3	46.5
-155G	35.8	24.6	39.6
-156G	33.3	24.5	42.2
-157G	36.9	25.0	38.1
-158G	26.8	29.2	44.0
-159G	29.2	24.9	45.9
-160G	31.7	23.7	44.6
-161G	26.4	25.4	48.2

Continued

Appendix 8, continued

Sample	% Smectite	% Illite	% Chlorite
W7905A-163G	27.9	28.3	43.9
-164G	24.4	25.6	50.0
-165G	22.9	31.8	45.2
-166G	24.6	32.6	42.8
-167G	30.0	19.3	50.6
-169G	32.2	30.1	37.7
-170G	34.8	23.9	41.4
-171G	31.4	28.3	40.3
-172G	34.9	25.3	39.7
-173G	24.2	29.6	46.1
-174G	26.8	30.6	42.6
-175G	32.0	22.2	45.8

Appendix 9

2-20 μm Chemical Data

Appendix 9

2 - 20μm Chemical Composition

Sample	Si	Al	Fe	Ca	Na	K	Mg	Ti	Be	Sr	Cu	Mn
107G	52.45	12.53	5.34	2.07	1.88	1.73	2.51	0.94	0.061	0.022	0.003	.048
108G	62.05	14.02	6.43	2.27	2.22	2.11	3.08	1.01	0.082	0.023	.004	.054
109	68.31	15.40	6.37	2.26	2.49	2.33	3.61	1.06	0.127	0.026	.003	0.060
110	82.69	19.14	7.72	2.77	3.12	3.32	4.24	1.30	0.192	0.035	.004	.072
111	62.53	14.28	10.47	2.25	2.28	2.10	2.76	1.04	0.083	0.027	.008	.059
112	61.74	14.61	6.10	1.87	2.19	2.03	3.42	0.96	0.137	0.022	.004	.057
113	61.01	14.52	5.88	1.77	2.17	2.11	3.49	0.95	0.124	0.022	.003	.059
115	60.26	14.58	6.63	1.77	2.14	5.91	3.73	0.95	0.096	0.021	.005	.063
116	59.49	14.49	6.77	1.85	2.00	2.01	3.61	0.98	0.077	0.020	.005	.063
117	60.20	14.54	6.78	1.82	2.14	2.06	3.47	1.05	0.084	0.022	.004	.066
119	60.72	13.40	7.02	1.68	2.27	1.80	3.44	1.04	0.058	0.046	.004	.088
120	59.07	14.46	6.26	1.76	1.96	1.94	3.76	1.06	0.077	0.020	.004	.062
121	60.32	14.42	6.22	1.59	2.42	1.94	4.08	1.00	0.098	0.021	.004	.064
122	60.45	14.17	6.34	1.46	2.33	1.98	4.16	0.96	0.085	0.017	.004	.065
123	60.03	14.84	6.14	2.01	2.50	2.05	3.86	1.01	0.095	0.024	.003	.064
125	60.82	14.02	6.14	1.59	2.43	2.24	4.07	0.90	0.132	0.018	.003	.067
127	58.97	14.07	6.62	1.72	2.26	1.88	4.29	0.96	0.072	0.015	.009	.103
129	60.04	13.60	7.62	2.14	2.62	1.82	3.38	1.09	0.058	0.022	.003	.069
130	61.36	13.12	6.34	2.14	2.40	1.74	3.66	0.99	0.055	0.020	.004	.059
131	60.96	13.66	6.07	2.02	2.34	1.73	3.96	0.97	0.062	0.018	.004	.054
132	63.74	14.26	6.82	1.82	2.29	1.81	4.30	0.97	0.074	0.017	.004	.067

Continued

Appendix 9, continued

Sample	Si	Al	Fe	Ca	Na	K	Mg	Ti	Ba	Sr	Cu	Mn
135	60.50	13.97	7.06	1.98	2.37	2.24	4.10	0.92	0.104	0.018	.004	.064
136	60.80	14.32	5.72	1.83	2.50	2.23	3.88	0.97	0.118	0.021	.004	.065
137	60.65	14.33	6.16	1.69	2.69	1.84	4.11	0.94	0.093	0.017	.003	.094
138	59.78	14.54	6.74	1.63	2.37	1.81	4.35	0.94	0.086	0.016	.006	.071
139	60.26	14.53	6.69	1.68	2.45	1.97	4.41	1.00	0.079	0.016	.003	.068
140	59.20	14.36	6.73	1.73	2.27	1.90	4.36	1.00	0.068	0.016	.003	0.065
141	61.05	13.82	5.28	1.39	2.84	1.87	4.08	1.13	0.067	0.019	.003	.067
142	59.80	14.03	6.42	1.99	2.37	1.74	4.14	1.00	0.053	0.017	.005	.071
143	60.85	14.16	6.23	1.79	2.49	1.82	4.36	0.96	0.078	0.015	.003	.067
144	60.14	14.30	6.61	1.95	2.34	1.83	4.42	0.95	0.076	0.017	.004	.076
145	60.10	13.96	6.38	1.88	2.32	1.87	4.46	0.94	0.088	0.018	.003	.069
148	60.32	14.00	5.51	1.31	2.23	1.85	4.40	0.93	0.101	0.014	.004	.074
149	60.88	14.27	6.42	1.71	2.28	1.70	4.54	0.98	0.076	0.017	.005	.070
150	59.42	14.15	6.66	1.79	2.11	1.64	2.64	0.97	0.067	0.015	.004	.073
151	58.89	13.63	6.86	1.94	1.97	1.53	4.30	0.93	0.053	0.014	.006	.065
152	58.29	12.89	7.92	1.76	3.19	1.92	4.01	1.09	0.056	0.026	.005	.069
153	58.77	14.46	6.89	1.77	2.06	1.66	4.65	0.94	0.059	0.014	.005	.085
154	58.43	14.10	7.24	2.17	2.21	1.69	4.61	0.96	0.072	0.017	.004	.075
155	58.86	14.55	6.83	1.66	2.07	1.73	4.56	0.96	0.073	0.014	.004	.076
156	60.66	14.80	6.36	1.59	2.26	1.71	4.41	0.87	0.104	.016	0.003	.072
157	60.24	14.32	6.40	1.52	2.11	1.70	4.32	0.88	0.106	.015	.004	.079

Continued

Appendix 9, continued

Sample	Si	Al	Fe	Ca	Na	K	Mg	Ti	Ba	Sr	Cu	Mn
158	61.58	14.48	6.43	1.50	2.18	1.65	4.31	0.86	0.096	.015	.004	.071
159	59.78	14.95	6.85	1.58	2.14	1.72	4.58	0.89	0.078	.016	.004	.084
160	59.50	14.49	6.77	1.65	2.21	1.62	4.55	0.91	0.064	.014	.005	.079
161	58.37	15.35	7.35	1.74	2.04	1.69	4.92	0.91	0.064	.015	.006	.077
163	58.36	14.66	7.60	1.88	2.07	1.59	5.20	0.90	0.055	.016	.005	.079
164	58.09	14.89	7.73	1.98	2.10	1.63	5.51	0.92	0.054	.014	.005	.080
165	57.96	15.13	7.82	1.81	2.02	1.75	5.19	0.90	0.066	.015	.005	.081
166	57.08	16.81	7.23	1.76	2.10	1.75	4.81	0.89	0.061	.015	.004	.076
167	61.25	14.16	6.82	1.67	2.28	1.57	4.28	0.89	0.067	.015	.004	.070
169	60.55	13.98	6.31	1.47	2.33	1.76	4.26	0.89	0.068	.015	.004	.070
170	61.48	14.35	6.05	1.40	2.27	3.81	3.98	0.88	0.096	.015	.004	.071
171	61.08	14.11	5.95	1.43	2.28	1.90	3.91	0.91	0.102	.016	.003	.066
172	60.97	14.62	6.31	1.34	2.38	1.78	4.03	0.88	0.076	.013	.003	.084
173	61.96	14.04	5.95	1.52	2.41	1.76	3.95	0.89	0.067	.016	.003	.064
174	59.44	15.03	7.32	1.63	2.28	1.76	4.64	0.89	0.068	.016	.004	.078
175	60.34	13.29	6.94	1.84	2.19	1.49	4.62	0.81	0.053	.017	.003	.070
TT68-26	61.79	14.71	5.58	2.41	2.66	1.88	2.79	1.06	0.093	.028	.003	.066
TT63-20	63.31	14.68	5.23	2.49	2.47	1.86	2.58	1.01	0.141	.030	.003	.059
TT63-19	62.85	14.79	5.44	2.43	2.53	1.84	2.49	1.12	0.105	.029	.003	.058
TT53-14	58.97	14.81	6.58	3.35	2.53	2.10	2.64	1.18	0.081	.036	.003	.071
TT53-17	60.84	14.86	6.14	3.65	2.89	1.48	6.44	1.10	0.062	.035	.003	.090
TT63-08	58.46	15.75	6.26	3.96	2.66	2.29	3.00	0.99	0.101	.042	.004	.094

Continued

Appendix 9, continued

Sample	Si	Al	Fe	Ca	Na	K	Mg	Ti	Ba	Sr	Cu	Mn
TT63-10	59.36	15.28	5.95	3.02	2.40	1.98	2.83	1.08	0.119	.034	.004	.064
TT63-12	60.48	15.95	5.36	3.15	2.74	2.20	2.42	0.99	0.087	.044	.002	.068
TT63-13	62.35	15.15	5.64	2.52	2.60	1.96	2.62	1.14	0.077	.030	.003	.060
TT63-16	60.91	15.75	5.40	2.82	2.60	1.91	2.58	1.15	0.091	.034	.003	.061
TT63-17	61.07	14.96	5.81	2.28	2.55	1.82	2.73	1.06	0.079	.027	.003	.059
TT63-18	61.57	15.16	5.26	2.52	2.46	1.84	2.64	1.08	0.136	.028	.004	.058
Eel	56.11	16.63	8.35	1.06	2.06	1.90	4.72	0.91	0.063	.011	.005	.111
Mad	60.83	14.76	6.70	1.37	2.60	1.54	4.06	0.89	0.056	.011	.006	.090
Redwood	52.17	19.43	8.94	0.56	2.06	2.40	3.90	0.81	0.093	.008	.006	.099
Klamath	56.67	15.40	8.26	2.26	2.11	1.54	5.99	0.78	0.076	.015	.005	.106
Rogue	53.08	16.23	9.24	2.71	2.04	1.34	6.12	0.98	0.060	.018	.008	.130
Coquille	57.38	15.61	7.74	0.99	1.86	1.62	4.50	0.99	0.049	.013	.004	.072
Umpqua	57.77	15.86	7.69	1.58	1.94	1.43	2.76	1.17	0.052	.019	.005	.127
Nehalem	47.93	16.45	12.18	3.38	1.84	1.06	3.12	2.88	0.040	.036	.006	.142
Columbia M-9	59.70	14.66	6.58	2.64	2.10	1.80	2.17	1.19	0.078	.031	.004	.104
Columbia M-7	57.81	14.84	6.94	2.78	2.19	1.79	2.24	1.71	0.081	.030	.004	.115
Queets	59.17	17.11	6.64	0.63	2.40	1.86	1.86	1.07	0.071	.016	.006	.078
Chehalis[1]	50.32	17.55	8.51	2.36	1.64	1.24	2.48	1.70	0.049	.025	.015	.214
Chehalis[2]	47.23	16.25	10.24	2.76	1.52	0.98	2.93	1.56	0.043	.021	.018	.154
Chehalis[3]	47.25	16.38	9.45	2.46	1.38	1.02	2.45	1.47	0.046	.020	.012	.152

[1] 1/27/78; [2] 2/10/78; [3] 2/3/78

Appendix 10

<2 μm Chemical Data

Appendix 10

<2μm Chemical Composition

Sample	Si	Al	Fe	Ca	Na	K	Mg	Ti	Ba	Sr	Cu	Mn
106	45.99	16.23	36.53	2.49	1.28	2.30	3.86	0.95	0.047	0.015	0.009	0.066
107	48.78	16.77	9.08	1.33	0.87	1.88	3.86	0.93	.059	.014	.009	.058
108	46.75	16.01	8.44	1.18	0.82	1.77	4.07	0.84	.062	.015	.014	.064
109	51.00	16.36	8.02	1.18	1.04	2.04	4.55	0.92	.084	.016	.008	.064
110	49.55	16.11	8.75	1.29	1.10	2.18	4.57	0.89	.107	.018	.008	.072
111	49.96	15.26	8.26	1.07	0.83	1.72	3.94	0.88	.076	.013	.017	.076
112	50.60	16.18	8.89	0.99	0.88	1.99	4.69	0.84	.095	.014	.011	.064
113	49.72	16.39	8.29	1.18	0.96	2.17	4.72	0.82	.120	.014	.008	.072
115	49.83	17.15	9.78	1.07	1.02	2.21	4.78	0.87	.107	.015	.012	.070
116	48.60	16.93	9.67	1.20	0.83	1.95	4.43	0.89	.086	.015	.010	.069
117	48.48	17.26	8.94	1.31	0.79	1.93	4.41	0.93	.075	.014	.008	.076
118	49.56	16.24	8.56	0.89	0.82	1.85	3.88	0.91	.048	.013	.010	.054
119	46.61	16.24	9.09	0.88	0.72	1.78	4.66	0.91	.044	.011	.013	.146
120	46.19	16.97	8.57	1.26	0.78	1.93	4.69	0.90	.059	.016	.010	.061
121	47.86	17.20	8.88	0.29	0.84	2.10	4.91	0.87	.073	.014	.012	.071
122	48.41	16.59	9.28	1.08	0.71	2.11	4.98	0.84	.096	.013	.008	.072
123	46.93	17.26	8.59	1.50	0.98	2.24	4.80	0.86	.087	.018	.009	.076
125	54.65	16.00	8.54	1.02	0.86	2.02	4.83	0.84	.115	.014	.011	.122
127	45.64	16.43	8.59	1.04	0.73	2.00	5.17	0.80	.074	.011	.024	.220
128	45.35	17.47	9.49	0.80	0.64	2.10	4.75	0.99	.060	.011	.008	.078

Continued

Appendix 10, continued

Sample	Si	Al	Fe	Ca	Na	K	Mg	Ti	Ba	Sr	Cu	Mn
129	45.54	16.28	8.71	1.10	0.801	1.83	4.62	0.92	.089	0.012	.008	.085
130	47.45	16.22	8.42	1.22	0.66	1.77	4.56	0.90	.057	.013	.010	.064
131	46.43	16.24	7.78	1.31	0.91	2.07	4.82	0.87	.058	.013	.015	.069
132	46.98	16.78	8.76	1.19	0.69	2.00	5.29	0.88	.080	.013	.012	.074
135	48.00	16.02	8.56	1.20	0.80	2.02	4.93	0.81	.083	.012	.012	.072
136	49.08	15.81	8.61	1.15	0.78	2.02	4.90	0.78	.090	.013	.018	.092
137	46.66	15.56	8.89	0.95	0.73	1.99	4.83	0.75	.119	.014	.011	.311
138	46.38	15.96	9.39	1.06	0.61	1.92	4.97	0.81	.090	.012	.017	.089
139	46.29	17.02	8.82	1.01	0.79	2.09	5.43	0.90	.072	.013	.008	.076
140	45.39	16.40	8.65	1.23	0.72	2.00	5.37	0.86	.061	.012	.010	.073
141	42.36	16.68	9.07	0.97	0.61	1.90	5.18	0.90	.075	.012	.013	.068
142	44.14	16.90	8.70	1.22	0.93	2.12	4.23	0.87	.066	.011	.016	.098
143	46.52	16.74	8.76	1.13	0.67	2.03	5.32	0.88	.075	.012	.010	.075
144	45.07	16.49	8.60	1.32	0.59	1.96	5.31	0.81	.096	.013	.013	.124
145	46.56	16.79	9.03	1.13	0.64	2.06	5.36	0.85	.078	.012	.009	.074
148	48.36	15.99	8.80	1.06	0.78	2.12	5.34	0.84	.221	.014	.009	.112
149	48.76	16.66	9.33	0.95	0.67	2.10	5.38	0.83	.107	.012	.010	.083
150	47.35	16.91	9.25	1.10	0.61	2.02	5.40	0.87	.081	.012	.099	.084
151	44.23	15.88	8.39	1.17	0.54	1.81	4.94	0.81	.064	.013	.016	.070
152	46.75	15.71	9.87	0.83	0.622	1.96	5.26	0.82	.056	.012	.011	.080
153	46.52	17.36	9.31	1.25	0.60	2.13	5.62	0.86	.069	.011	.010	.093

Continued

Appendix 10, continued

Sample	Si	Al	Fe	Ca	Na	K	Mg	Ti	Ba	Sr	Cu	Mn
154	46.29	16.72	8.34	1.21	0.93	2.25	5.86	0.83	.067	.011	.010	.077
155	46.52	16.64	8.65	1.08	0.81	2.14	5.33	0.83	.092	.012	.011	.110
156	48.58	17.09	8.24	0.91	0.91	2.35	5.78	0.86	.106	.012	.009	.094
157	50.31	16.23	8.75	0.90	0.89	2.22	5.34	0.82	.130	.013	.008	.110
158	51.26	16.19	9.24	0.86	0.75	2.24	5.46	0.78	.119	.012	.010	.095
159	48.01	16.22	9.40	0.92	0.70	2.36	5.73	0.77	.090	.010	.012	.154
160	49.19	16.13	8.71	1.09	0.65	2.18	5.25	0.84	.070	.012	.014	.080
161	47.03	17.21	9.64	1.08	0.61	2.19	5.62	0.90	.072	.012	.013	.089
163	46.06	16.62	9.85	1.08	0.58	2.11	5.65	0.89	.057	.010	.012	.092
164	46.66	17.12	9.94	1.00	0.64	2.19	6.19	0.95	.059	.010	.011	.083
165	48.18	17.26	10.03	1.14	0.61	2.34	5.84	0.93	.068	.012	.009	.084
166	44.04	16.46	9.37	1.25	0.67	2.23	5.44	0.85	.080	.015	.012	.084
167	49.08	16.82	8.22	0.92	0.68	2.24	5.68	0.89	.074	.010	.011	.116
169	49.44	16.16	8.64	0.84	0.69	2.15	5.24	0.79	.109	.012	.012	.099
170	52.10	16.25	8.31	0.78	0.78	2.34	5.33	0.86	.115	.012	.008	.095
171	49.31	16.67	8.94	0.91	0.68	2.32	5.27	0.80	.094	.012	.009	.084
172	48.18	16.26	9.11	0.78	0.75	2.44	5.54	0.82	.082	.010	.011	.191
173	48.45	17.66	8.81	0.98	0.69	2.64	5.83	0.85	.078	.011	.009	.088
174	48.27	17.84	9.59	1.18	0.63	2.47	5.76	0.91	.082	.011	.010	.089
175	44.70	15.25	9.05	1.18	0.53	2.03	5.52	0.85	.055	.012	.014	.078

Continued

Appendix 10, continued

Sample	Si	Al	Fe	Ca	Na	K	Mg	Ti	Ba	Sr	Cu	Mn
TT53-14	49.17	16.16	9.16	1.54	1.49	2.03	3.71	0.98	.059	.018	.007	.071
TT53-17	49.80	17.96	9.74	2.17	1.82	2.07	4.68	1.07	.062	.024	.009	.134
TT63-08	49.21	18.13	9.54	2.16	1.52	2.50	4.08	0.97	.075	.027	.010	.130
TT63-10	50.90	16.57	9.09	1.65	1.08	2.05	4.15	0.98	.073	.019	.008	.066
TT63-12	50.44	18.08	8.58	2.24	2.40	3.01	4.13	0.93	.080	.033	.007	.112
TT63-13	51.87	16.43	8.61	0.91	1.47	1.97	3.79	0.98	.076	.013	.008	.058
TT63-16	50.62	17.47	8.74	1.18	1.27	2.05	3.95	1.04	.073	.016	.008	.058
TT63-17	50.25	15.41	9.79	0.68	1.64	1.83	3.48	0.87	.066	.011	.007	.059
TT63-18	51.56	16.16	8.34	1.10	1.26	1.98	3.89	1.00	.111	.016	.008	.057
TT63-19	48.90	15.30	8.34	0.84	1.17	1.68	3.36	0.91	.085	.013	.007	.053
TT63-20	52.32	15.56	8.20	1.06	1.28	1.88	3.75	0.90	.118	.017	.009	.058
TT68-26	52.45	15.87	8.99	0.80	1.58	2.00	3.96	0.91	.107	.013	.010	.085
Eel	45.47	19.54	10.20	0.70	0.80	2.97	6.43	0.83	.083	.006	.009	.144
Mad	46.89	19.04	10.00	0.92	1.07	2.88	6.67	0.75	.086	.007	.012	.145
Redwood	41.90	24.31	10.44	0.38	0.72	3.90	3.93	0.98	.164	.009	.016	.137
Klamath	46.52	16.75	9.85	1.72	1.45	2.05	7.54	0.96	.079	.012	.014	.149
Rogue	39.20	18.44	11.66	1.13	0.51	1.67	6.02	1.06	.082	.012	.021	.244
Coquille	48.14	19.19	11.92	0.54	0.49	1.95	6.47	1.08	.046	.009	.031	.125
Umpqua	44.67	19.20	11.22	0.34	0.41	1.11	3.02	1.17	.024	.006	.009	.183
Chehalem	39.38	17.20	12.26	1.08	0.43	0.77	2.87	1.58	.033	.014	.010	.200
Columbia M-9	51.66	12.35	8.06	1.18	0.45	1.27	1.93	0.83	.060	.014	.010	.253

Continued

Appendix 10, continued

Sample	Si	Al	Fe	Ca	Na	K	Mg	Ti	Ba	Sr	Cu	Mn
Columbia M-7	49.13	13.40	8.89	1.30	0.59	1.52	2.35	1.00	.068	.016	.009	.184
Queets	42.36	21.75	9.78	0.44	0.93	2.99	2.66	1.13	.066	.015	.016	.148